A Smart Home Medical Device for Accurate Metabolic Assessment

by

Mark Sprowls

A Dissertation Presented in Partial Fulfillment
of the Requirements for the Degree
Doctor of Philosophy

Approved May 2021 by the
Graduate Supervisory Committee:

Erica Forzani, Chair
Hugo Destaillats
Doina Kulick
Mehdi Nikkhah
Gregory Raupp

ARIZONA STATE UNIVERSITY

August 2021

ABSTRACT

Energy Expenditure (EE), a key diagnostic measurement for treatment of obesity, is measured via indirect calorimetry method through breath biomarkers of CO_2 production and/or O_2 consumption rates (VCO_2 and/or VO_2, respectively). Current technologies are limited due to prevailing designs requiring wearable facial accessories that present accuracy, precision, and usability concerns with regards to free living measurement. A novel medical device and smart home system, named Smart Pad, has been developed, with the capability of energy expenditure assessment via VCO_2 measured from a room's CO_2 concentration. The system has 3 distinct capabilities: contactless EE measurement, air quality optimization via actuation of room ventilation, and efficiency optimization via ventilation actuation of only human-occupied environments. The Smart Pad shows accuracy of 90% for 14-19 minutes of resting measurement and accuracy of 90% for 4.8-7.0 minutes of exercise measurement after calibrating for air exchange rate (λ [$hour^{-1}$]) using a reference method. Without reference instrument calibration, the Smart Pad system shows average accuracy of nearly 100% with correlations of Y=1.02X, R=0.761 for high resolution measurements and Y=1.06X, R=0.937 for averaged measurements over 50-60 minutes. In addition, the Smart Pad validation for contactless EE measurement has been performed in different environments, including a vehicle, medical office, a private office, and an ambulatory enclosure with rooms, ranging in volume from 3.1 m^3 to 18.8m^3. It was concluded that contactless EE measurements can be accurately performed in all tested scenarios with both low and high air exchange environments with λ ranging from 1.5 $Hours^{-1}$ to 10.0 $Hours^{-1}$. The system

represents a new way to assess EE of individuals under free-living conditions in an unobstructive, passive, and accurate manner, and it is comparable or better in single breath gas measurement accuracy (with comparisons sourced from FDA data) than other medical devices (e.g. Vyntus CPX™, MasterScreen CPX™, Oxycon Pro™, and MedGem™) which were 510(k) cleared by the FDA for prescription use in metabolic/cardiopulmonary diagnostics.

ACKNOWLEDGMENTS

I acknowledge first and foremost my PhD advisor Erica Forzani. Erica, this amazing project has offered me so much in so many different ways. I will never forget the invaluable lessons you taught me as your advisee and the accomplishments we've made on this project. I will always look up to you as an exemplary leader and engineer.

I would also like to graciously acknowledge my dissertation committee's support throughout these years. I am so thankful to have true experts in a range of related fields to this project to help it grow. Special thanks to Hugo, who taught me so much about the true rigor of real science and how to pursue it, as well as to Gabriel Pyznar and Francis Tsow, the guidance and mentorship in developing electrical systems you provided cannot be understated. Special thanks as well to Dr. Kulick for her unique perspective as a clinician and support throughout the Mayo Clinic study, critical to the success we saw on this project. I am so lucky to have had you all's support and mentorship.

To Arizona State University Ira A Fulton Schools of engineering for providing the funding to pursue my research for some of these years. Also, to the A.J. and Sigismunda Charitable trust, the Mayo Clinic philanthropist funds, and the Global Sport institute for generously providing resources to develop this nascent technology.

I give thanks to my parents and two sisters for their strong support during my research pursuits as a PhD student. To my lab mates as well for all the intellectual support through these long years of research and development.

TABLE OF CONTENTS

Page

LIST OF FIGURES viii

LIST OF TABLES xi

CHAPTER

1 INTRODUCTION, BACKGROUND, AND PROJECT MOTIVATION 1

1.1 Importance of Caloric Balance and Energy Expenditure to Weight Loss 1

1.2 Current Technological Challenges to Energy Expenditure Measurement 2

1.3 Research Knowledge Gap in Human Metabolism 6

1.4 Research Knowledge Gap in Physical Modeling of Indoor Air 7

2 SMART PAD: A CONTACTLESS DEVICE FOR METABOLIC MEASUREMENT 9

2.1 Smart Pad System Overview 9

2.2 Smart Pad: Target Application Environment 11

2.3 Smart Pad Sensing Module 12

2.4 Smart Pad Actuation Module and Testing Environment 14

2.5 Smart Pad Data Analysis 16

2.6 Characterization of Smart Pad Sensors in Controlled Environments 23

2.6.1 Summary 23

2.6.2 Methodology 24

CHAPTER Page

2.6.3 Results 25

2.6.4 Smart Pad Measurement Specifications 30

2.6.5 Conclusions 30

3 CLINICAL EVALUATION OF SMART PAD MEASUREMENTS 32

3.1 Abstract 32

3.2 Experimental Set Up 33

3.3 Cross Sectional Study 36

3.3.1 Cross Sectional Study Methodology 36

3.3.2 Cross Sectional Study Results (n=20) 37

3.3 Longitudinal Study 41

3.3.1 Longitudinal Study: Accuracy Across All Longitudinal Measurements 41

3.3.2 Longitudinal Study: Correlation Analysis 42

3.4 Conclusion 45

4 ENGINEERING A FASTER, FULLY AUTOMATED SMART PAD 47

4.1 Abstract 47

4.2 Smart Pad: Physical Characteristics, Design, and Testing Environment 48

4.3 Methodology: CO_2 Measurement Range Optimization for REE assessment 51

4.4 Methodology: CO_2 Measurement Range Optimization for Exercise assessment ... 54

4.5 Methodology: Effect of REE on Accuracy for Optimized Measurement Range 55

CHAPTER Page

4.6 Methodology: CO_2 Decay: Study of Unoccupied Room Air Exchange (λ) 55

4.7 Results: Measurement Range Optimization for REE assessment 56

4.8 Results: Measurement Range Optimization for Exercise assessment 62

4.9 Results: Effect of REE on Accuracy for Optimized CO_2 Measurement Range..... 66

4.10 CO_2 Concentration Decay: Evaluative Study of Room Air Exchange Rate (λ) ... 71

4.11 Discussion: Compensation for Imprecision using Repeated Measures 85

4.12 Conclusions 87

5 SMART PAD: VALIDATION IN AMBULATORY ENVIRONMENT AND DEVELOPMENT OF A CONTACTLESS EXERCISE TEST 89

5.1 Abstract 89

5.2 Methodology 90

5.3 Results 95

5.4 Conclusions 105

6 VEHICLES: A USEFUL ENVIRONMENT FOR METABOLIC ASSESSMENT ... 106

6.1-Abstract 106

6.2 Methodology 106

6.3 Results 109

6.3 Simulation of CO_2 Accumulation Patterns Within a Vehicle Cabin..... 112

7 SMART PAD AND INTEGRATION WITH MULTIPLE IOT DEVICES 116

CHAPTER Page

7.1 Abstract 116

7.2 Smart Pad Measurements 116

7.2 Smart Camera and Combined Metrics 119

7.3 Fifteen Month Follow-up for BMI Matched Young and Old Subjects 122

8 SUMMARY AND FUTURE WORK 124

8.1 Further Engineering Requirements for a Viable Product 124

8.2 U.S. Regulatory (FDA/CLIA/IBC) Clearance Pathway 125

8.3 Future Scientific and Physiological Research Focused Work 129

8.4 Conclusions 131

BIBLIOGRAPHY 133

APPENDIX

A PUBLICATION AUTHORSHIP RESULTING FROM PHD STUDIES 144

LIST OF FIGURES

Figure Page

Figure 1: Smart Pad System for Contactless Energy Expenditure (EE) Measurement. ... 10

Figure 2: Smart Pad Target Application Environment. 12

Figure 3: Smart Pad Hardware Components and Assembly Process. 13

Figure 4: Smart Pad Measurement Environment and Actuator System. 15

Figure 5: Smart Pad Data Analysis Algorithm. 17

Figure 6. Environmental Chamber Set Up..... 24

Figure 7. Environmental Chamber Study Sample Raw Data and Analysis..... 25

Figure 8. Comparison of Temperature Measured on Smart Pad and Reference Device .. 26

Figure 9. Comparison of Humidity Measured on Smart Pad and Reference Device. 27

Figure 10. Effect of Humidity on Air Exchange (λ_0) and VCO_2 Error % 28

Figure 11. Effect of Temperature on Air Exchange (λ_0) and VCO_2 Error %. 28

Figure 12. Experimental Set Up for Medical Office Validation Study. 33

Figure 13. Diagram Showing Room Geometry for Medical Office Study. 36

Figure 14: Example of Data Analysis During the 2019 Clinical Study..... 38

Figure 15: Smart Pad Accuracy During the 2019 Clinical Study for N=20 Subjects..... 40

Figure 16: Results from Longitudinal Study of Metabolism and Lifestyle Patterns. 42

Figure 17: Longitudinal Study Correlation Results for the 22 Year Old Male. 44

Figure 18. Longitudinal Study Correlation Results for the 24-Year-Old Male. 45

Figure 19: Study Design for Optimization of Smart Pad Operating Parameters. 49

Figure 20. Schematic of Testing Environment Layout for Chapter 4..... 51

Figure 21. Effect of Measurement Duration on REE Measurement Accuracy 57

Figure Page

Figure 22: Sample Raw Data for a CO_2 Threshold Range of 500-650. 60

Figure 23: Baseline Adjusted Fitting for REE using Reference Method Calibration. 61

Figure 24: Effect of CO_2 Operating Range on VCO_2 Measurement for Exercise. 63

Figure 25. CO_2 Fitting for Exercise EE using Reference Method Calibration. 66

Figure 26. Effect of BMI on Smart Pad REE Measurement Accuracy and Duration. 67

Figure 27: CO_2 Accumulation for Subject #2 using Reference Method Calibration 69

Figure 28: CO_2 Accumulation for Subject #3 using Reference Method Calibration 70

Figure 29. Results of λ_{Acc} Correlative Study and Simplified CO_2 Accumulation Model. 73

Figure 30: Sample CO_2 Accumulation/Decay Fittings for Subject #5. 77

Figure 31. Sample CO_2 Accumulation/Decay Fittings for Subject #1. 78

Figure 32. REE Measurements for Subject #1 using Simplified Accumulation Model… 80

Figure 33: REE Measurements for Subject #2 using Simplified Accumulation Model… 81

Figure 34: REE Measurements for Subject #3 using Simplified Accumulation Model… 82

Figure 35: REE Measurements for Subject #4 using Simplified Accumulation Model… 83

Figure 36: REE Measurements for Subject #5 using Simplified Accumulation Model… 84

Figure 37. Smart Pad Accuracy using Eq (9) and Extrapolating from Standard Error. 87

Figure 38. 4th Smart Pad Operating Environment During Construction. 91

Figure 39. Test Protocol for Contactless Physical Fitness Assessment. 92

Figure 40. Layout of Measurement Environment at Health Futures Center. 94

Figure 41. View from within Health Futures Center Ambulatory Testing Environment. 95

Figure 42. Pilot Data for Smart Pad CTET Test at Health Futures Center. 96

Figure 43. MGC CPX Ultima^{TM} $VO_{2,\,max}$ Test Data for CTET Pilot Testing. 98

Figure Page

Figure 44. Automated $VO_{2, max}$ Analysis Results from Developed Python Code..... 99

Figure 45. Raw Data from MGC Ultima CPX^{TM} for CTET..... 100

Figure 46. Results of Preliminary CTET Measurement. 100

Figure 47. Preliminary Smart Pad Performance at Health Futures Center. 102

Figure 48. Vehicle Used and Study Design. 107

Figure 49. CO_2 Accumulation Data from Recirculation Mode Across 0-70 MPH. 109

Figure 50. Relationship Between Effective Air Exchange Rate (λ) and Driving Speed. 110

Figure 51. Real Time Data from Contactless REE Measurements from in a Vehicle.... 111

Figure 52: Contactless REE Measurement Accuracy within a Moving Vehicle. 112

Figure 53. CO_2 Concentration Profiles for Various Occupants/Driving Speeds. 114

Figure 54. Effects of EE and Air Exchange on CO_2 Accumulation Patterns. 115

Figure 55. Aging Pilot Study Design and Sequence of Events 117

Figure 56. Tracking Age Related Metabolic Changes using Smart Pad..... 119

Figure 57. Smart Pad Integration with Contactless Human Tracking Software. 121

Figure 58. Changes in Physical Fitness and Metabolism Due to Aging and Injury. 122

LIST OF TABLES

Table Page

Table 1. Comparison of Smart Pad System Versus Current Technologies 5

Table 2. Design of Experiments for Environmental Chamber Measurements 25

Table 3. Effect of Temperature, CF, and RH on Smart Pad Measurement 29

Table 4. Smart Pad System Measurement Specifications..... 30

Table 5: Subject Physical Characteristics for Optimized Smart Pad Study..... 55

Table 6: Results from Contactless REE Measurement (for Figure 23) 62

Table 7: Results for Exercise VCO_2 Assessment (from Figure 25)..... 66

Table 8: Results for Subject #2 REE Assessment (from Figure 27)..... 70

Table 9. Results for Subject #3 REE Assessment (from Figure 28)..... 71

Table 10. Results for λ Evaluation from CO_2 Accumulation and Decay (for Figure 30) . 77

Table 11. λ_{Acc} Evaluation from CO_2 Accumulation and Decay #1 (for Figure 31) 78

Table 12. λ_{Acc} Evaluation from CO_2 Accumulation and Decay #2 (for Figure 31) 79

Table 13. Smart Pad Accuracy for Subject #1 using Simplified Accumulation Model. .. 81

Table 14. Smart Pad Accuracy for Subject #2 using Simplified Accumulation Model. .. 82

Table 15. Smart Pad Accuracy for Subject #3 using Simplified Accumulation Model. .. 83

Table 16. Smart Pad Accuracy for Subject #4 using Simplified Accumulation Model. .. 84

Table 17. Smart Pad Accuracy for Subject #5 using Simplified Accumulation Model. .. 85

Table 18. Implications of Standard Error with Regards to Equation (9) 86

Table 19. Smart Pad Comparison with FDA 510(k) Cleared Indirect Calorimeters 126

CHAPTER1

1 INTRODUCTION, BACKGROUND, AND PROJECT MOTIVATION

1.1 Importance of Caloric Balance and Energy Expenditure to Weight Loss

According to the world health organization (WHO, 2020), energy balance is at the heart of weight loss/gain and consists of 2 different parameters: “Calories in”, which is food intake in kcal/day, an excess of which results in weight gain, and “calories out”, which is calories “burned” over the course of a day in kcal/day, also known as energy expenditure (EE [kcal/day]), an excess of which results in weight loss. In common clinical practice, the energy needs of a patient are determined through estimation of various predictive equations (Mifflin et al., 1990). Althought the equations provide the predicted population’s average value for resting energy expenditure (REE), they do not accurately assess individual resting energy expenditure. Individual’s REE values can deviate positively or negatively in ±900 kcal/day, which is a significant margin when compared to total energy expenditures (TEE) within a single day (Deng & Scott, 2019; McClave et al., 2016). Theser errors can are especially problematic considering that typical caloric deficits in the range of 500 kcal/day for a successful weight loss diet (Fock & Khoo, 2013), and this is the U.S. NIH suggested caloric deficit for person suffering from class I obesity (NIH, 1998). As such, errors in measurement or estimation of REE can lead to unsuccessful weight loss.

Daily EE assessment can offer newfound accuracy in true average EE measurements over a longitudinal period, which may offer greater clinical utility for obesity treatment since EE is known to vary significantly from day to day. Even with

highly controlled dietary regiments and limited physical activity, day-to-day 24-hour EE varies by as much as 8-10% (Donahoo et al., 2004; Ravussin et al., 1986; Rumpler et al., 1990). Pooled mean of day-to-day variability (in terms of CV) for free-living EE in 21 studies has been shown to be 11.8% (Black & Cole, 2000). Specifically, in the treatment of obesity, it is common for EE to change significantly over time. This occurs when a person undertakes a caloric deficit diet, often causing the body's REE to also decrease (de Jonge, Bray, et al., 2012; A. Dulloo & Schutz, 2015; A. G. Dulloo & Jacquet, 1998; Hill et al., 2012; Jebb et al., 1996), resulting in what is referred to as a "weight loss plateau", where the rate of weight loss slows down or stops completely despite consistent dieting in terms daily caloric intake. For obese patients who often undergo deficit diets for months, accounting for changes in REE is often beneficial for continued success in a weight loss program. There is strong evidence suggesting that accounting for fluctuations in EE via repeated EE measurement improves weight loss outcomes (Bray, 2004; Campos et al., 2006; Criscione et al., 2013; Elliot et al., 1987, 1989; McDoniel et al., 2008; Seagle et al., 2009; Stump et al., 2017).

1.2 Current Technological Challenges to Energy Expenditure Measurement

Measurement of REE is not commonly adopted by clinical practices. Instead, an erroneous technique of using predictive equations for estimation of TEE is commonplace, which is a potential cause for limited success in treatment of clinical obesity. These predictive equations have low measured accuracies, based on N=337 measurements of a representative population (Frankenfield, 2013), with the best performing and most widely used, Mifflin St. Joer equation (Mifflin et al., 1990) only being observed to have an 82% accuracy for a 90% CI. Many studies have observed similar findings (Cancello et al.,

2018; Hasson et al., 2011; Purcell et al., 2019; Siervo et al., 2014). Besides application to obesity medicine, personalized metabolic assessment has invigorated a passion for personal health monitoring and calorie tracking across the world, evidenced by worldwide Smartwatch adoption, although, this technology has notably low accuracy for EE measurement (Chowdhury et al., 2017). As such, a convenient and accurate EE measurement technology could substantially benefit both obesity patients and individuals interested in their own personal health.

Given known inaccuracies of predictive equations for TEE, it is reasonable to wonder why EE measurement tools are not used extensively in clinical practice. EE measurement using current technologies is a technique affected by widely recognized issues (Simonson & DeFronzo, 1990) that are a result of a fundamental design flaw of these devices: they typically require a subject to breathe into a mouthpiece, mask, or some object worn on the subject's face. Wearing a facial accessory possible results in errors including elevated VCO_2 and VO_2 from hyperventilation occurring while wearing an object for breath gas collection on the face, or, alternatively, mistakenly breathing into an EE measurement medical device that is not fitted in an airtight manner to the subject's face. These tools have the added operational issues related to wearing an object on the subject's face, including discouraged repeated measurement due to discomfort, which is important given high day-to-day variability in TEE, 11.8% (Black & Cole, 2000). Other considerations are related to sterilization of facial accessories, an aspect which increases both device cost (purchase of additional single use accessories), procedural time requirements (sterilization of facial accessories), and inherently increases the risk of transmission of various pathogens. There is some evidence to support that these wearable

accessories may actually interfere with free-living metabolism measurement (Horner et al., 2001). In addition to usability concerns, many current FDA cleared/approved (FDA, 2003, 2006) technologies for REE measurement have reproducibility errors worse than ±10% (68% CI) by multiple definitions of reproducibility (Cooper et al., 2009).

Alternatively, there is a technique for EE measurement from ambient sensors, in what is referred to as an "indirect calorimeter room" (Grunwald et al., 2003; Rising et al., 2015; M. Sun et al., 1994). The indirect room calorimeter method is similar to the technique presented in this work, however, in principle it relies on gas composition measurements for the inlet and outlet for the ventilation system of the room and therefore at its very basis requires a great deal of installation and a specially constructed environment (T. Nguyen et al., 2003). Current methodologies for development of an indirect calorimeter room are remiss in the sense that they are not portable and require extensive installation time, and therefore, unsuitable for widespread clinical adoption. Another non-intrusive technique is referred to as doubly labeled water method. This technique requires urine collection and the usage of bulky laboratory equipment for isotope analysis (Ainslie et al., 2003) that is prohibitively expensive and not a point of care measurement. In this technique, a subject is given a dose of isotope-doped water (^{18}O and ^{2}H) and resulting isotope excretion rates over the course of several weeks are measured using a mass spectrometer. Based on this fundamental principle, the technique requires multiple lab visits for a single subject and a large amount of resources for lab equipment, isotope-doped water, and non-trivial time for execution of the isotope analysis (Schoeller & van Santen, 1982). Table 1 below summarizes many shortcomings

of current metabolic measurement technologies, and the potential advantages the Smart Pad system developed as the focus of this dissertation presents:

Table 1. Comparison of Smart Pad System Versus Current Technologies

	Doubly-labeled water method	**Hand-held breath analyzers**	**Metabolic cart**	**Metabolic rooms**	**Smart Pad (This work)**
Measurement duration	7-10 days	10 min, prior resting of 20 min	10 min, prior resting of 20 min	1-7 days	Variable: 15 minutes to full days
Sample	Urine	Breath	breath	Indoor air	Indoor air
Instruments	Mass-spectrometer and isotope doped water	Point of care device	Human-sized instrument with wheels	CO_2 + O_2 analyzers, flowmeters, computer, pumps, etc.	Ambient sensors
Procedural requirement for subject	Drink water and urinate (2 lab visits)	Breathe into accessory for 10 minutes.	Breathe into accessory for 10 minutes	Minimum 1 hour	14-19 min occupancy (contactless)
Procedural requirement for test administrator	Brief subject. Calibrate GC/LC-MS (20+ min) and perform measurement (20+ min)	Brief subject. Scan sensor QR code. Fasten facial accessory.	Brief subject. Calibrate instrument (30 min warm up). Fasten facial accessory.	Extensive weekly maintenance and ventilation modification	None. Even unconscious /sleeping/comatose/critically-ill persons can be evaluated
Consumables	$^{2}H^{18}O_2$ doped water with known concentration (100+$/test)	Single use chemical sensors ($3-5/test)	Wearable face masks (reusable, but, $30+ each)	No consumable	No consumable

To the best of the team's knowledge, this is the first systematic study of an EE measurement technique requiring no wearable equipment and relying on CO_2 measurements within the bulk of a confined environment in lieu of inlet/outlet CO_2

measurements, as is the funamental basis of the indirect calorimeter room method. Two attractive usage applications of the device are in clinician's attending room, where the Smart pad could measure the resting EE of every single patient on a given day without requiring any wearable equipment, and also in a person's personal office where it could be used to contactlessly measure that person's EE daily for months or years. This creates an unparralleled wealth of data that is of great value for EE measurement, given that parameter's high variation day-to-day (Black & Cole, 2000).

As such, it is a great benefit to medicine to develop an EE assessment tool to combat "weight loss plateaus" and identify normal daily variability in EE that 1. Enables frequent EE measurements, to identify average EE for dietary planning, 2. Performs accurate indirect calorimetry, since inaccurate EE estimation can lead to large errors in energy balance, resulting in unsuccessful weight loss, And 3. Provides true free-living EE measurements, so that clinicians can prescribe dietary regiments to their patients based on EE measurements during their true uninterrupted daily living patterns. These factors were the motivation of the dissertation research compiled within this document.

1.3 Research Knowledge Gap in Human Metabolism

Additionally, numerous factors such as acute cognitive stress (Sawai et al., 2007; Gérald Seematter et al., 2002; G. Seematter et al., 2000), sleep (Benedict et al., 2011; de Jonge, Zhao, et al., 2012; Shlisky et al., 2012), physical activity (Speakman & Selman, 2003), and exposure to environmental pollutants (Esparza et al., 2000; Manore et al., 2009) can affect our body's resting energy expenditure (REE)**.** Longitudinal EE study in humans has greatly improved the research community's understanding of slowly changing physiological parameters aging (Alfonzo-González et al., 2006; Lührmann et

al., 2009; Min Sun et al., 2001), bodyweight (de Jonge, Bray, et al., 2012; A. Dulloo & Schutz, 2015; A. G. Dulloo & Jacquet, 1998; Hill et al., 2012; Jebb et al., 1996), chronic disease progression (Gong et al., 2015; Magoffin et al., 2008; Scott et al., 2001), however, longitudinal assessment of more acute physiological factors: cognitive stress, sleep, physical activity (day-to-day effect) has been largely unstudied in the research community, and was one motivation for a portion of the research reported in this work.

1.4 Research Knowledge Gap in Physical Modeling of Indoor Air

The assessment of a room's air exchange rate, referred to as λ in this work, is a critical challenge for measurement of REE from ambient CO_2 accumulation patterns. λ, an important consideration for all occupied indoor environments, is commonly measured in hospitals striving to minimize pathogen transmission within operating rooms (Dascalaki et al., 2008), schools (Yang et al., 2009) where ventilation can influence learning performance (Bakó-Biró et al., 2012), and office buildings striving to maintain healthy levels of indoor pollutants (Bluyssen et al., 1996) to prevent incidences of sick building syndrome (Redlich et al., 1997). It has been characterized in previous scholarly works from human generated CO_2 decay data (Batterman, 2017; Ramalho et al., 2013; Turanjanin et al., 2014), and the decay modelling procedure is in good agreeance with reference methods (e.g. tracer gas with constant injection rate) for λ measurement in temporarily unoccupied indoor environments (Claude-Alain & Foradini, 2002; Cui et al., 2015). Recently, this decay λ value has been applied to CO_2 accumulation data for determination of human CO_2 emission rate in a recent study (Gall et al., 2021) to assess one physiological effect of stress. The fundamental model has been described previously in several academic works (Batterman, 2017; Haverinen-Shaughnessy et al., 2011; Ruiz

et al., 2018) and applied to CO_2 accumulation data to assess λ. However, until the publication of this dissertation, there has never been a study of the CO_2 accumulation model with a direct measurement of λ using a medical device to assess source CO_2 strength (referred to as k_{gen} [ppm/hour] or VCO_2 [ml/min], which capture essentially the same physical effect of CO_2 production with differing units). As such, the research reported here challenges a fundamental assumption of previous works, which is that the presence of a human in an indoor environment has a negligible effect on air exchange.

CHAPTER 2

2 SMART PAD: A CONTACTLESS DEVICE FOR METABOLIC MEASUREMENT

2.1 Smart Pad System Overview

The Smart Pad system (Forzani et al., 2018; Ruiz et al., 2018; Sprowls et al., 2020; Sprowls, Serhan, et al., 2021; Sprowls, Victor, Mora, et al., 2021; Sprowls, Victor, Serhan, et al., 2021) consists of a sensor array integrated into a detection module located in the rear of a seat pad, within the seat pad's back cushion (Shown in Figure 1A)**.** The array monitors carbon dioxide (CO_2) and related environmental parameters for correction to standard conditions (humidity, temperature, and barometric pressure) which are all used in the calculation of EE, the primary output measurement of the system. The data collected from the sensor array is transmitted to a user's cell phone, where CO_2 accumulation regressions (swift package for automated CO_2 analysis in iOS currently under development) and ventilation system control logic related to operation of the system are performed. During this dissertation work. CO_2 data was collected with the Smart pad system and analyzed using Origin™ or programmatically using in house developed Python code. A functional HVAC (heating, ventilation, and air conditioning) actuator control system was developed which controls the room's air ventilation via a set of inlet/outlet fans and is turned on/off when deemed necessary by the logic control unit of the system (programmed into a cell phone). The ventilation and actuator system are beneficial for the system optimization and advantageous for taking a large volume of energy expenditure measurements in a given timespan, but in principle, are not necessary for contactless EE measurement. That being said, the actuator system does have independent value in it's potential to intelligently control building ventilation (i.e. turning

off ventilation when deemed unnecessary) for energy savings and also for the purpose of preventing CO_2 accumulation beyond 1000 ppm, a level some have observed to result in negative cognitive effects (Satish et al., 2012) and potentially other health issues (Jacobson et al., 2019). A cutout showing the full integration and application of the Smart Pad system is shown below in Figure 1.

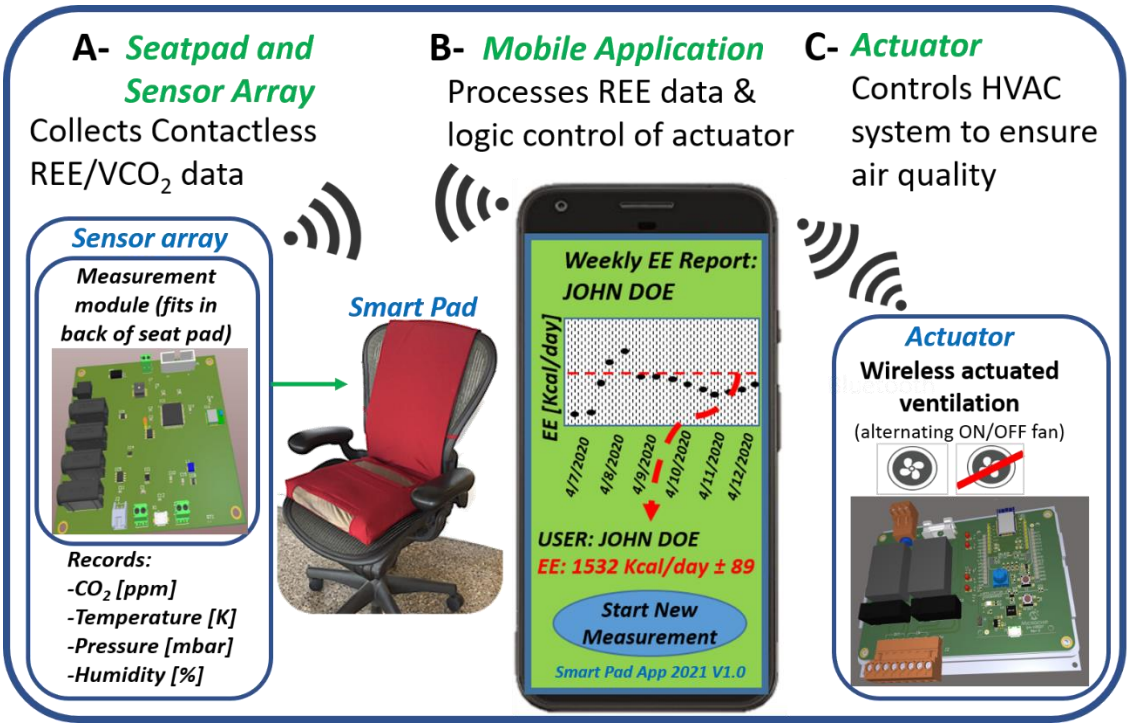

Figure 1: Smart Pad System for Contactless Energy Expenditure (EE) Measurement. Consisting of (A) a sensor array discretely packaged within a seatpad (B) automated data analysis package for EE measure from CO_2 data integrated with a user interface viewed from an application on a mobile device. (C) An actuator system which sends on/off signal to a set of inlet/outlet fans. The usage of the fan system allows for precise control of CO_2 within the target environment.

2.2 Smart Pad: Target Application Environment

The Smart Pad has great potential for measurement of human metabolism in any environment where breath gases could possibly accumulate, including measurement in any medium-sized environment of suitable volume such as a private office (Sprowls, Victor, Mora, et al., 2021), medical office (Sprowls, Victor, Serhan, et al., 2021), bedroom, vehicle (Sprowls et al., 2020), clinician's attending room, classroom (Ruiz et al., 2018), etc. Due to inherent ease of use and the completely passive nature of the proposed innovative measurement technique, the Smart pad system has enormous potential in both clinical and research settings. The system could be installed in an obesity clinician's attending room, as shown in Figure 2, where it could measure the EE of all patients seen in that room on a given day, without a time-consuming use protocol for the clinician. Additionally, the system could be installed in a person's bedroom or office where it could track their daily EE patterns over the course of months or years. Another promising application environment is within a vehicle, where the Smart pad could measure the EE of a person every single day during a 15 minute work commute. These use scenarios have great implications for clinical application, since the Smart pad could continuously transmit EE measurements to a clinician for optimal dietary planning based on real-time EE measurements. Alternatively, for research application, daily tracking of an individual's EE patterns would provide unparalleled insight into the physiological significance of EE fluctuations and factors that might influence them. In this work, many different measurement environments were validated for contactless REE accuracy of ±10% including a moving vehicle (3.1m^3), medical office (8.2 m^3), private office (14.0 m^3), and a curtained enclosure (18.8 m^3) within a larger room.

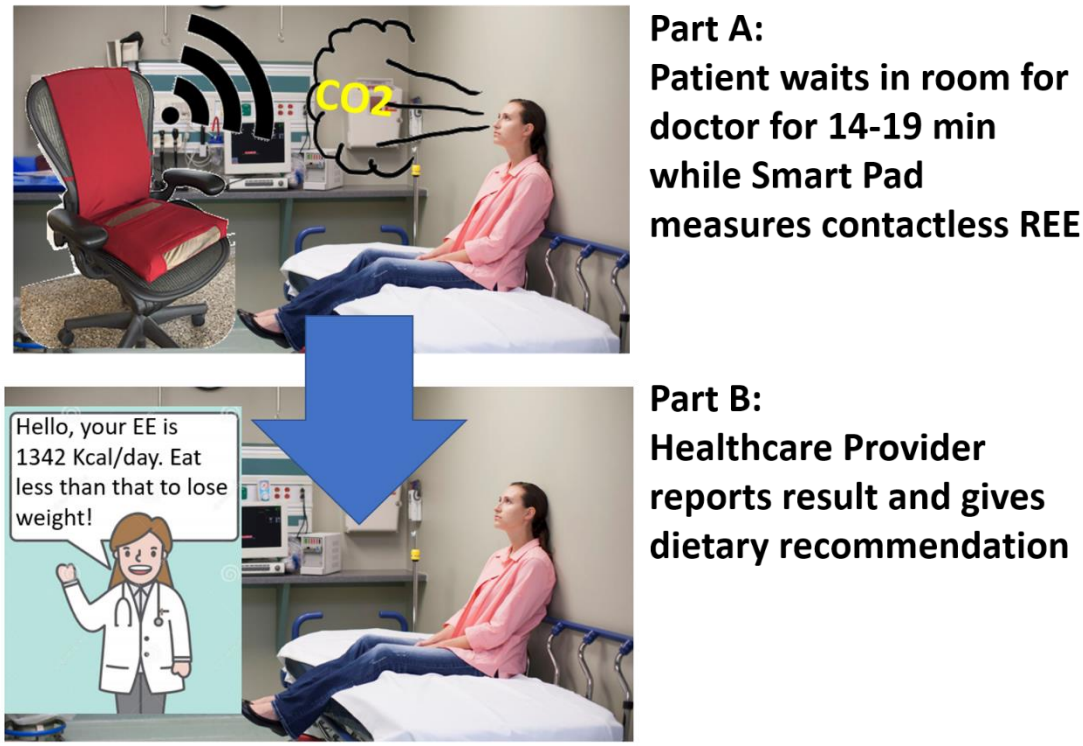

Figure 2: Smart Pad Target Application Environment. Patients often wait in an attending room for approximately 10-15 minutes to be seen by a healthcare provider. Given the Smart Pad's contactless measurements and short assessment length, it is realistic to expect that the Smart Pad can be integrated into this type of environment to provide patients with valuable metabolic data at almost no time or consumable cost.

2.3 Smart Pad Sensing Module

The Smart Pad sensing module is the main, namesake (module integrated into seat pad) feature of the system and serves the primary purpose of recording gas concentration measurements and transmitting them to a cell phone for analysis via the equations developed as a part of this work. The PCB at the heart of the Smart pad system has surface mounted sensors for measurement of 8 different parameters including temperature, pressure, relative humidity, CO_2 concentration, battery life, and also a

connector that allows the device to take measurements of 2 postural sensors. These sensors can potentially enable “occupancy determination” of whether or not a subject is seated on the Smart pad, but, more complex conclusions on a person’s posture may be made in the future from postural sensor data (i.e. slouching, seated upright, etc.). The sensing PCB has a built in Bluetooth module that allows for wireless communication of sensor data from the module to a user’s cell phone. The assembly process for the Smart Pad’s sensing module is shown below:

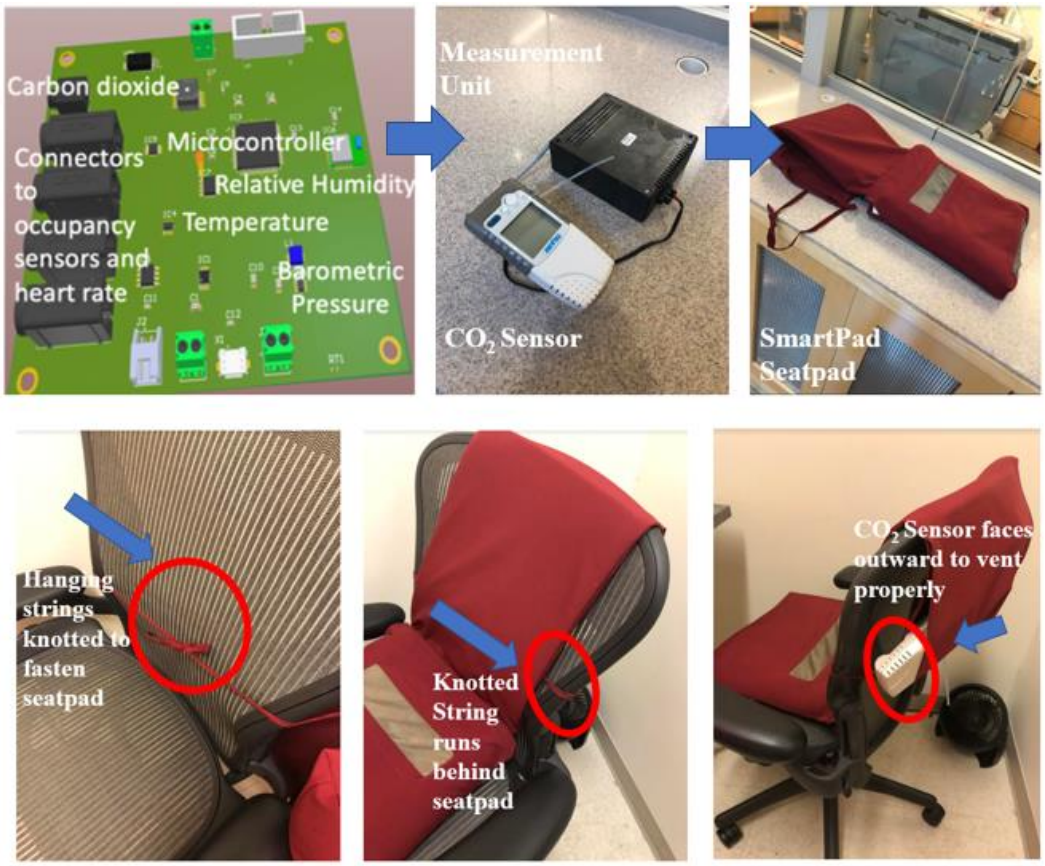

Figure 3: Smart Pad Hardware Components and Assembly Process. Measurement unit (houses sensor PCB shown in top left) and CO_2 sensor are fitted for Smart Pad seat cushion opening. The Smart Pad is tied around an office chair, where it is used to take EE measurements for the seated person.

2.4 Smart Pad Actuation Module and Testing Environment

Many different types of measurement environments were evaluated as a part of this dissertation research including a medical office, private building office, vehicle, and curtained area of a larger lab. All environments showed promising accuracy, ±10%, and comparable measures to FDA 510(k) cleared devices (see Table 19), but, in each case the ventilation system was modified in some way (with the exception of the vehicle, where recirculation mode was instead turned on). Over time, the CO_2 accumulation model was refined, and the device was refined to be functional for REE measurement from only 14-19 minutes of occupancy in a room with only the inlet and outlet HVAC vents blocked to disallow any significant airflow during CO_2 accumulation periods. In all human occupied environments, it is essential that CO_2 concentration within the metabolic chamber is kept below 2,000 ppm while occupied as a safety consideration, as concentrations exceeding this level have been observed to result in cognitive impairment (Allen et al., 2016; Satish et al., 2012; Zhang et al., 2015) after exposure for prolonged periods of time. To achieve this, an actuator system was developed which controls a set of inlet/outlet fans to allow for precise control of CO_2 concentration within the operating environment. The actuation system is an IoT (internet of things) connected device via Bluetooth and receives an on/off signal from the user's cell phone that turns the fans on to bring the CO_2 level within the room to baseline and start new data collection. This on/off signal is sent automatically from the user's cell phone or tablet depending on the lower/upper concentration threshold limits set within the mobile application for the experimental run. These lower/upper limits effectively define the length of the experiment and are of great operational importance, especially with regards to accuracy and measurement duration, as

covered later in this dissertation (Chapter 4). A commercially available Velcro door (Retrotec^{TM}) was also repurposed to fully seal the operating environment described in Chapters 3 and 4. Eventually, the team will strive like to implement the system without the installation of the door or ventilation system and future work strives to accomplish this goal. That being said, this dissertation research lays the foundational groundwork for those goals, by validating successfully for the first time a contactless and portable technique for REE measurement.

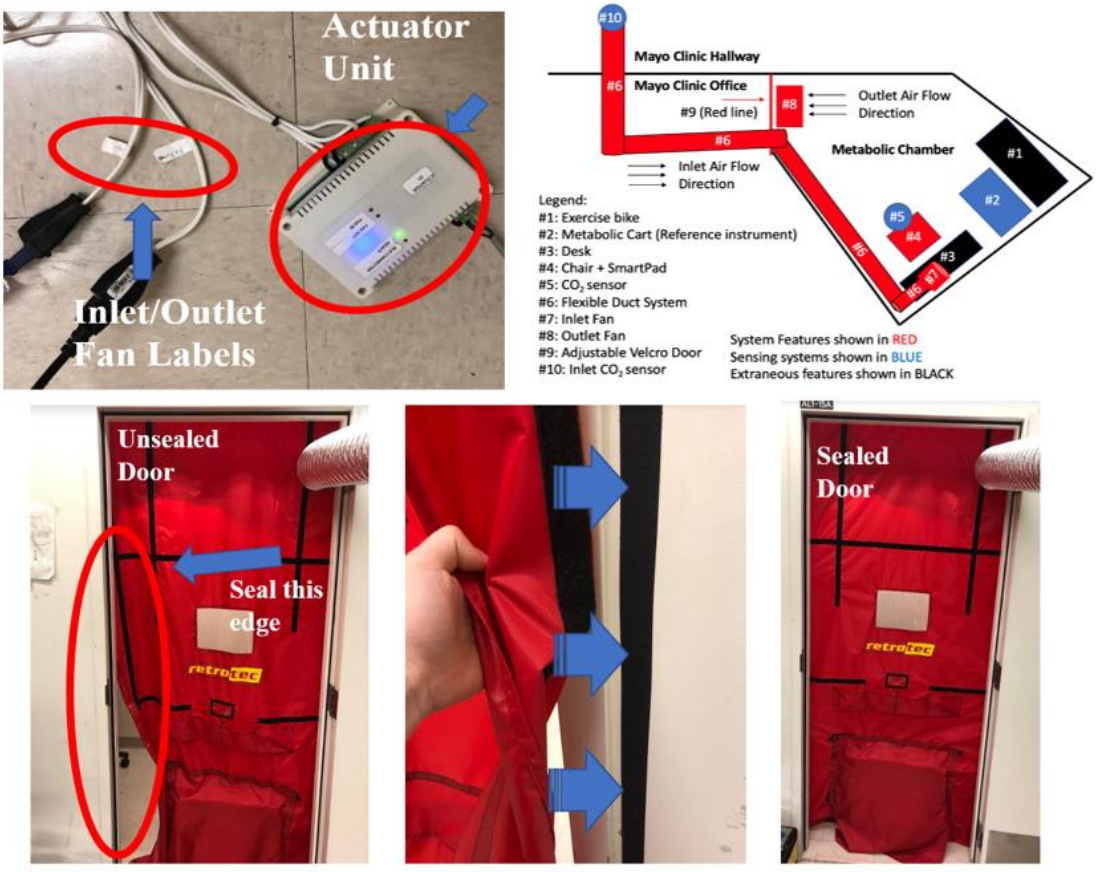

Figure 4: Smart Pad Measurement Environment and Actuator System. Top left: Shows actuation system (Bluetooth controlled) and connections to inlet/outlet fans. Top right: Bird's eye view of testing environment for Chapter 3 and ventilation system with major components labeled. Bottom panel: Sealing of Velcro door to create airtight environment.

2.5 Smart Pad Data Analysis

CO_2 concentration, temperature, relative humidity, and pressure data are all collected for a subject in a medium sized room. Established equations for describing transient CO_2 are applied to collected data, with only CO_2 accumulation data being analyzed (see Figure 5). The CO_2 accumulation model relates air exchange, mathematically represented by λ_{Acc} [$hours^{-1}$], also referred to as air exchange rate (AER) or number of air volume changes (ACH) (Claude-Alain & Foradini, 2002) in the room per hour, to CO_2 accumulation patterns. The term fundamentally represents the number of times the rooms volume is exchanged to the surrounding environment per hour. Prior to this work and the publication of the findings of Chapter 4, there was no distinguishment between λ (air exchange) assessed from CO_2 accumulation resulting from human occupancy (λ_{Acc}) or from CO_2 decay resulting after a human's departure (λ_0) in scientific literature. Since the findings of this work suggest there may be a significant difference between the two terms, this distinguishment is made here for consistency between λ_{Acc} and λ_0. A sample of analyzed CO_2 accumulation data is shown below in Figure 5.

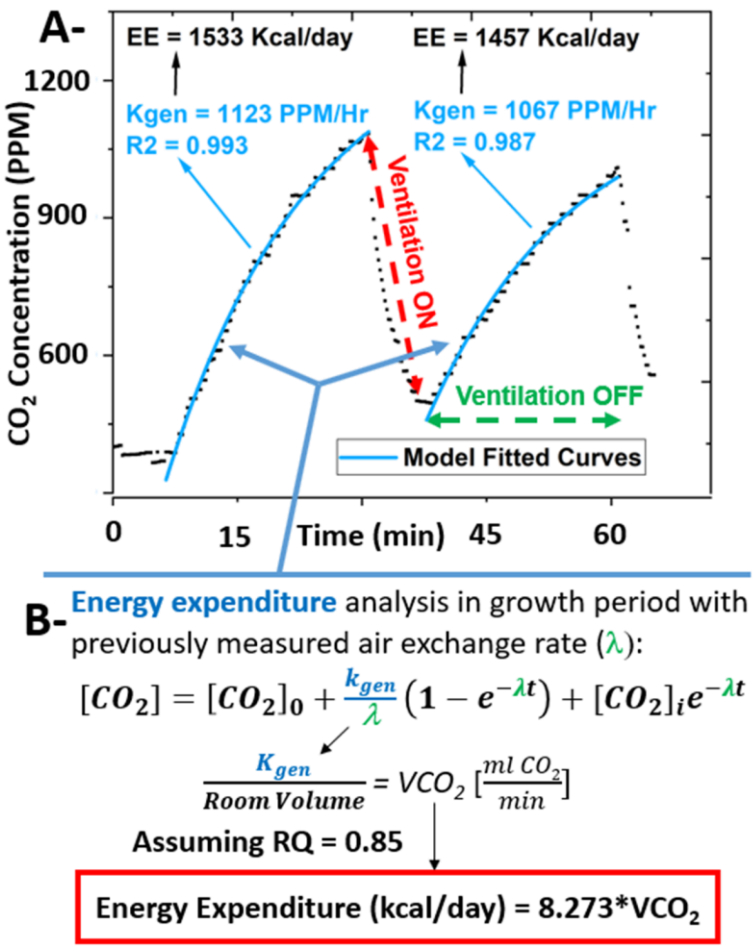

Figure 5: Smart Pad Data Analysis Algorithm. (A): Raw Smart Pad data for 2 EE measurement cycles. (B) model used in data analysis to determine EE from k_{gen}.

In the data analysis for the first growth curve, a VCO_2 value for the occupant is measured directly via a medical device considered a high accuracy reference instrument. This allows for the direct measurement of λ_{Acc} using the mathematical model shown above (see example λ_{Acc} measurement in Figure 14, Figure 21, or Figure 24). Once λ_{Acc} is measured, every proceeding growth curve utilizes that λ_{Acc} to measure the occupant's EE via analysis of the CO_2 accumulation curve. This λ_{Acc} value assessed for regression of CO_2 accumulation with known VCO_2/k_{gen}, based on generally accepted error propagation heuristics, should have a standard error closely correlated to standard error of VCO_2

measurement from the reference method. Since this is the first ever report of using a high accuracy medical device to assess VCO_2/k_{gen}, and tracer gas techniques cannot be successfully applied in occupied indoor environments (for safety concerns regarding breathable air, i.e. most popular tracer gas is SF_6 (Cui et al., 2015)), it is not unreasonable to state this work details the most accurate assessment of air exchange rate (λ_{Acc}) in an occupied environment.

The following equations are the foundation of the contactless REE measurement, all derived from mass balance on CO_2 within a defined volume where air exchange occurs to the surroundings. The equation does assume a first order relationship between CO_2 concentration and λ_{Acc}, supported by previous empirical measurements (Ruiz et al., 2018) and findings of other works (Batterman, 2017; Claude-Alain & Foradini, 2002; Haverinen-Shaughnessy et al., 2011):

$$[\boldsymbol{CO_2}] = [\boldsymbol{CO_2}]_{\boldsymbol{0}} + \frac{\boldsymbol{k_{gen}}}{\boldsymbol{\lambda_{Acc}}}\left(\boldsymbol{1} - \boldsymbol{e^{-\lambda_{Acc}t}}\right) + [\boldsymbol{CO_2}]_{\boldsymbol{i}}\boldsymbol{e^{-\lambda_{Acc}t}} \qquad (1)$$

Where $[CO_2]$ is the CO_2 concentration [ppm] measured within the room, $[CO_2]_0$ is the baseline CO_2 concentration [ppm] measured in the inlet duct during the experiment, k_{gen} is the CO_2 generation rate [ppm $hour^{-1}$], and λ_{Acc} is the air exchange rate [$hours^{-1}$].

It was experimentally determined that VCO_2 assessed did not fit perfectly with the assumptions made by the aforementioned model, one of which is that CO_2 is perfectly mixed within the environment. An empirical correction factor, CF_{Env}, is used to adjust for differences between "ideal" k_{gen} and "actual" k_{gen}, henceforth defined as k_{gen}'. This correction factor was validated for ±10% accuracy for contactless REE in 3 environments ranging in volume of 8.2-18.8m^3. By design, CF_{Env} should be a property of the

environment that corrects for non-ideality in that setting, although, findings of this work suggest it may not vary significantly in room of similar size and ventilation regime:

$$\boldsymbol{k_{gen}{}' = k_{gen} CF_{ideal}} \quad (2)$$

As described above, λ_{Acc} is assessed in the first measurement cycle, and then k_{gen} is assessed for each subject from the second measurement cycle using equation 1. k_{gen}' is then used in the following equation to determine the value of VCO_2 [ml/min]:

$$\boldsymbol{VCO_2 = k_{gen}{}' * V_{Room} * CF_{STPD}/60} \quad (3)$$

Where VCO_2 is the subject's volumetric production of CO_2 [ml/min], V_{Room} is the volume of the room [ml] (experimentally measured and accounting for the volume of objects within the environment), and CF_{STPD} [dimensionless] is a correction factor to correct the VCO_2 for standard temperature, pressure, and dry conditions, as the weir formula (shown below) utilizes VCO_2 at standard conditions. The correction factor is calculated as follows:

$$\boldsymbol{CF_{STPD} = \frac{P_{bar} - P_{H20}}{760} * \frac{273}{T + 273}} \quad (4)$$

Where P_{bar} [mmHg] is the barometric pressure inside the room, P_{H20} is the partial pressure of H_2O [mmHg] within the environment (with P_{Sat} calculated from the Antoine equation and then also considering measured relative humidity % to find P_{H20}), and T is the temperature within the environment [Celsius]. Finally, the EE [Kcal/day] of the subject was calculated using a simplified version of the Weir formula that assumes a constant respiratory quotient, or RQ, of 0.85 (although this changes due to study conditions e.g. fasting requirements). The respiratory quotient of a person is dependent on their ratio of fat to carbohydrate to protein consumption ratio specifically referring to

their body's metabolic state. Since total fat consumption corresponds to an RQ of ~0.7, protein as ~0.82-0.88, and carbohydrate as ~1.0, an RQ selection of 0.85 for the model is a conservative estimate that minimizes overall error from high carbohydrate and high fat consumption test subjects (FDA, 2003; Marra et al., 2004; Matarese, 1997). The RQ value depends heavily on subject fasting status with RQ typically steady decreasing in hours follow a meal (Reed & Hill, 1996)). As such, the value of RQ is heavily dependent on study execution and measurement protocol:

$$\boldsymbol{EE}\left(\frac{\boldsymbol{kcal}}{\boldsymbol{day}}\right) = \boldsymbol{3.941} * \frac{\boldsymbol{VCO_2}}{\boldsymbol{RQ}} + \boldsymbol{1.106} * \boldsymbol{VCO_2} \tag{5}$$

$$\boldsymbol{RQ} = \frac{\boldsymbol{VCO_2}}{\boldsymbol{VO_2}} \tag{6}$$

In this manuscript, λ_0 [hour^{-1}] refers to air exchange (λ) assessed through CO_2 decay data. Equation (7) is as follows:

$$[\boldsymbol{CO_2}] = [\boldsymbol{CO_2}]_{\boldsymbol{0}} + \ ([\boldsymbol{CO_2}]_{\boldsymbol{i}} - [\boldsymbol{CO_2}]_{\boldsymbol{0}})\boldsymbol{e^{-\lambda_0 t}} \tag{7}$$

Sample fittings of equation (7) can be found in Figure 19, Figure 29, Figure 30, and Figure 31.

The findings of Chapter 4 lead to the development of a new, simplified mathematical model for REE measurement from CO_2 accumulation data based equation (1). This model was developed by strong ($p<0.0001$) multicollinearity between λ_{Acc} and k_{gen} that is a result of hypothesized physical effects resulting from a human's presence (i.e. some combination of breath and/or heat appears to increase air exchange significantly) within the room.

To account for this multicollinearity, one may solve the system of equations of Eq (1) and the regression, Eq (8), shown in Figure 29, and reproduced below, leading to initial derivation of Eq (9) (see Chapter 4 for full derivation and sample regressions for each subject):

$$\boldsymbol{\lambda_{Acc} = \alpha\, x\, VCO_2} \quad (8)$$

This is a simple regression resulting from the findings of Chapter 4, where α [hours^{-1} min ml] is the change in λ_{Acc} resulting from a 1 unit increase in VCO_2. The value of this term was determined to be 0.0107 [hours^{-1} min^{-1} ml] in the private office evaluated in Chapter 4.

$$[\boldsymbol{CO_2}] = [\boldsymbol{CO_2}]_{\boldsymbol{0}} + \frac{\boldsymbol{1}}{\boldsymbol{\beta}}\left(\boldsymbol{1 - e^{-\beta * k_{gen} * t}}\right) + \left([\boldsymbol{CO_2}]_{\boldsymbol{i}} - [\boldsymbol{CO_2}]_{\boldsymbol{0}}\right)\boldsymbol{e^{-\beta * k_{gen} * t}} \quad (9)$$

Where variable meanings and dimensions are the same as for Eq (1), except for a new term, β [ppm^{-1}], which could be understood as a combined unit conversion (ml min^{-1} to ppm hour^{-1}) and factor from Eq (8) that represents the change in λ_{Acc} resulting from a 1 unit increase in k_{gen}. The value of β is calculated from measurements of the application environment (i.e. room volume, temperature, pressure, humidity), all of which are already present in Eq (1). β can be calculated from a combination of mass conservation and the regression shown in Figure 29. β is calculated follows, where α is multiplied by 1/60 hours min^{-1} to change units the Figure 29 regression finding from those of VCO_2 to k_{gen} (i.e. from change in λ_{Acc} resulting from a 1 unit increase in VCO_2 instead to k_{gen}):

$$\boldsymbol{\beta = \frac{\alpha}{60} * CF_{Env} * V_{Room} * CF_{STPD}} \quad (10)$$

Where variable and unit meaning are identical to those described in equation's (2), (3), and (4). Equation (8), key to the innovation leading to equation (9), was derived from N=26 measurements taken from section 4.6. The model was evaluated on an independent dataset, N=56 measurements from N=5 subjects and the results were accurate with precision that can be mitigated with repeated measures (Altman & Bland, 2005), up to levels of respectable FDA cleared devices (MGC Ultima CPX^{TM}, Korr ReeVue^{TM} (Cooper et al., 2009; FDA, 2003, 2006)) after only a few repeated measures. Without repeated measures using equation (9), equivalent accuracy to 4 FDA 510(k) cleared medical devices (including several metabolic carts) was observed in the N=56 subject dataset (see Table 19). This dataset contained no overlap in individual measurements with regards to model development dataset and included data from several months prior to the collection of training set data with no single outlier being removed the evaluation of the test set. The new model is accurate for REE measure in comparison to a reference instrument although imprecision is notable (Y=1.02X, R=0.761). High R^2 values can be observed in fittings of CO_2 data as well across multiple subjects in Figure 29, Figure 32, Figure 33, Figure 34, Figure 35, and Figure 36. Additionally, the model uses the exact same CF_{Env} as was determined during the medical office study conducted in Chapter 3. This is considered a step forward if the result is reproducible in other environments, given the revised equation 1 model developed as a part of this work in equations 8-10 simplifies the contactless REE assessment significantly with only 1 set of CO_2 accumulation data needed and no prior λ assessment from reference instrument (λ_{Acc}) or CO_2 decay (λ_0) measurements.

At all points within this dissertation, error relative to a reference instrument is defined as follows:

$$Error\ \% = \frac{Smart\ Pad\ measure\ - reference\ measure}{reference\ measure}\ x\ 100\% \qquad (11)$$

In the equation above, it is most important to consider that the Smart Pad measure is the first term in the numerator difference calculation. As such, negative errors suggest Smart Pad underestimates. Throughout this manuscript, the most common reference measure was the MGC Ultima CPX™, considered perhaps the best indirect calorimeter in the medical device industry. One may be wise to pay special attention to the parameter of interest with regards to error calculation, as in some occasions REE is evaluated and others VO_2 (typically for biking this parameter is reported).

2.6 Characterization of Smart Pad Sensors in Controlled Environments

2.6.1 Summary

An environmental chamber was used to assess the accuracy of temperature and relative humidity measurement for the Smart Pad system's environmental sensors, since these measurements (i.e. temperature and relative humidity) are fundamentally needed for correction to standard conditions via equation 4. The accuracy of temperature measurement was ±0.86 degrees Celsius across a range of 6-51 degrees Celsius, showing correlation of y=1.017x, R=1.000 with a reference measure. The accuracy for relative humidity measurement was ±10.0% across a relative humidity range of 3 to 98% showing a correlation of y=1.036x, R= 0.987 with a reference measure. Measurements for both parameters met or substantially exceeded measurement characteristics for a FDA cleared device for metabolic assessment, the Korr ReeVue™ (FDA, 2003). Additionally, there

was no significant effect of Temperature, correction factor, or relative humidity on VCO_2 measurement within the chamber using a CO_2 reference gas injection method and analyzing using equation (1), suggesting the model is robust across a wide range of environmental conditions.

2.6.2 Methodology

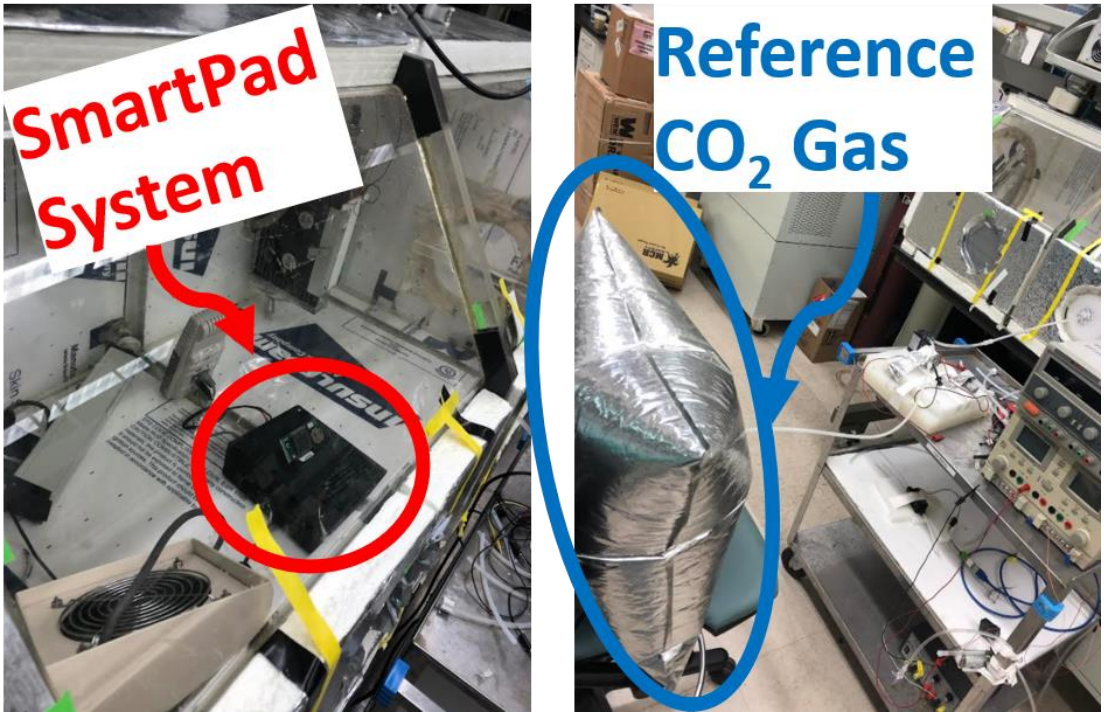

Figure 6. Environmental Chamber Set Up

Figure 6 above shows how the environmental chamber was set up. First, the chamber was conditioned to a certain temperature and relative humidity and allowed to come to equilibrium (i.e. no transient changes in RH or Temperature). A full factorial design was conducted with 3 levels of Temperature and relative humidity with 3 replicate measures for each level. The design of experiments is shown below in Table 2.

Table 2. Design of Experiments for Environmental Chamber Measurements

Factors	Levels		
	-1 (“low”)	**0 (“medium”)**	**+1 (“high”)**
RH (%)	Min achievable (~10%)	45%	Max achievable (~85%)
Temperature (Celsius)	Min achievable (5C)	25 C	50 C (Max rating for CO_2 sensor)

A minimum of 1 hour of data was collected at the equilibrium condition which included approximately 10 minutes of CO_2 injection and a minimum of 50 minutes of CO_2 decay (with longer decays collected for some runs but while maintaining the same environmental conditions). Over 10,000 parallel temperature and relative humidity measurements were collected from both the Smart Pad unit and reference device, referred to as the Hobo™ Unit.

2.6.3 Results

Sample data and CO_2 accumulation/decay analyses for the environmental chamber study is shown below in Figure 7:

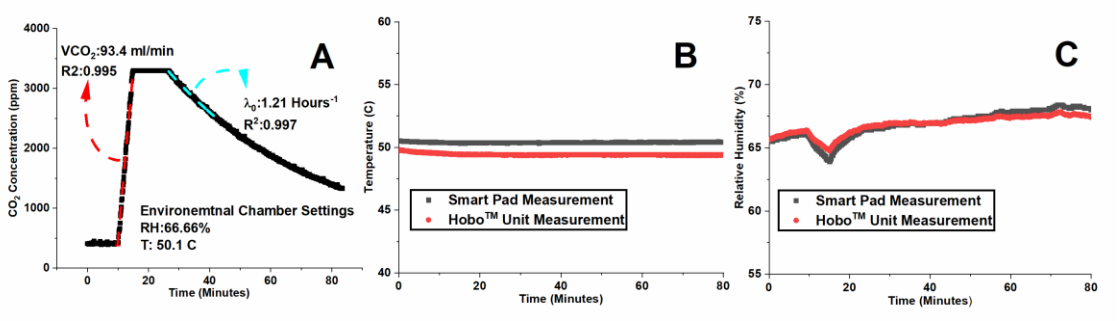

Figure 7. Environmental Chamber Study Sample Raw Data and Analysis

Temperature measurements correlated highly between both reference devices (R=1.000). Temperature accuracy was determined to be ±0.86 Celsius, comparable to specifications FDA 510(k) cleared devices used for metabolic assessment (FDA, 2003). The correlation between both devices is shown below in Figure 8.

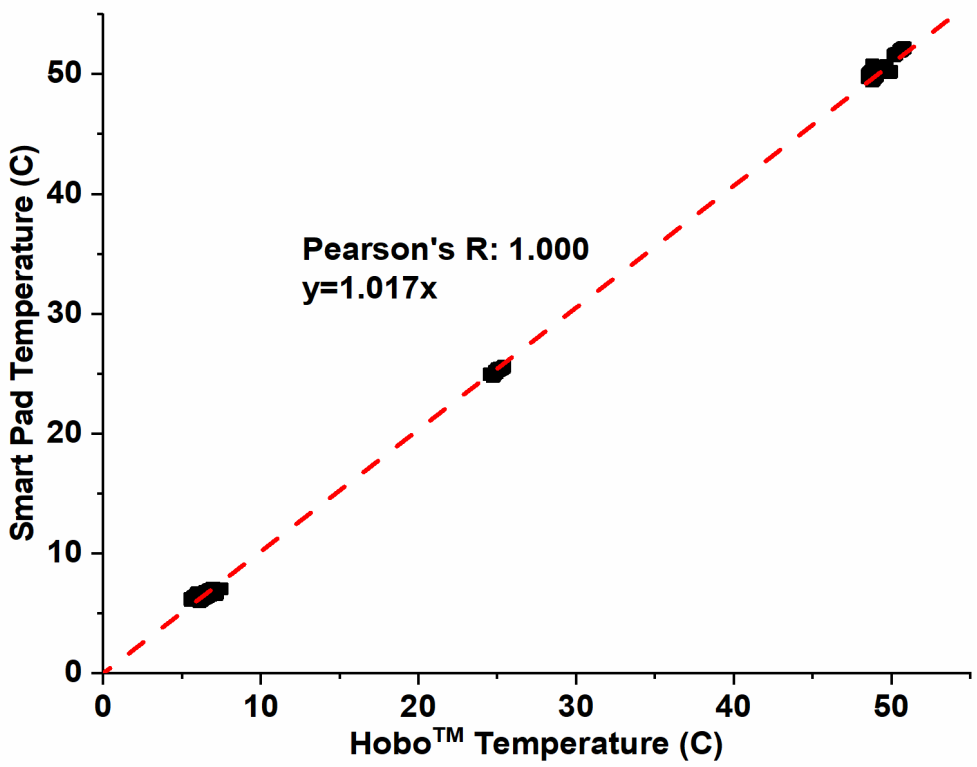

Figure 8. Comparison of Temperature Measured on Smart Pad and Reference Device

Relative Humidity measurements correlated highly between both reference devices (R=0.987). Accuracy was determined to be ±10.0%, comparable to specifications FDA cleared devices for REE measurement, of which errors of ±10% are reported (FDA, 2003). The correlation between both devices is shown below in Figure 9. Although this error may be considered large by some standards, the U.S. FDA finds this level of accuracy acceptable for REE measurement since humidity plays a minor, although

observable, effect in the calculation of the standard environmental condition factor, CF, as shown in equation 4. Clearly, the Smart Pad device is less accurate with regards to measurement of very humid (>90%) and very dry (<10%) conditions.

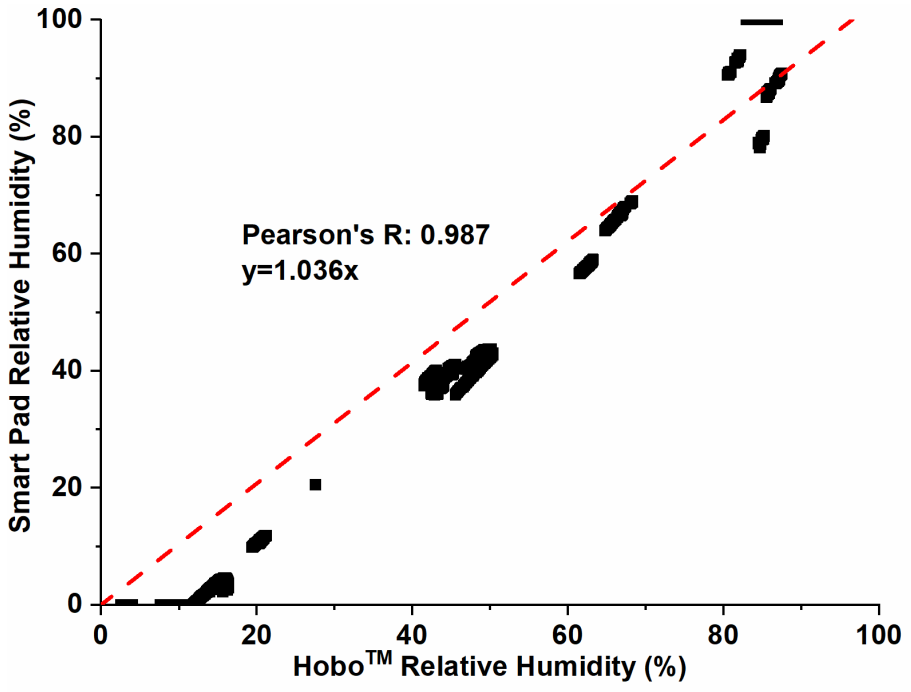

Figure 9. Comparison of Humidity Measured on Smart Pad and Reference Device.

The effects of various environmental conditions on the Smart Pad CO_2 accumulation model, equation 1, and CO_2 decay model, equation 7, were asessed via regression analysis. Regression between λ_0 and VCO_2 error %, between ideal VCO_2, calculated from mass balance with known injection gas concentration and flow rate, in specific were the outcome variables of interest. The effect of humidity on model outcomes are shown below in Figure 10.

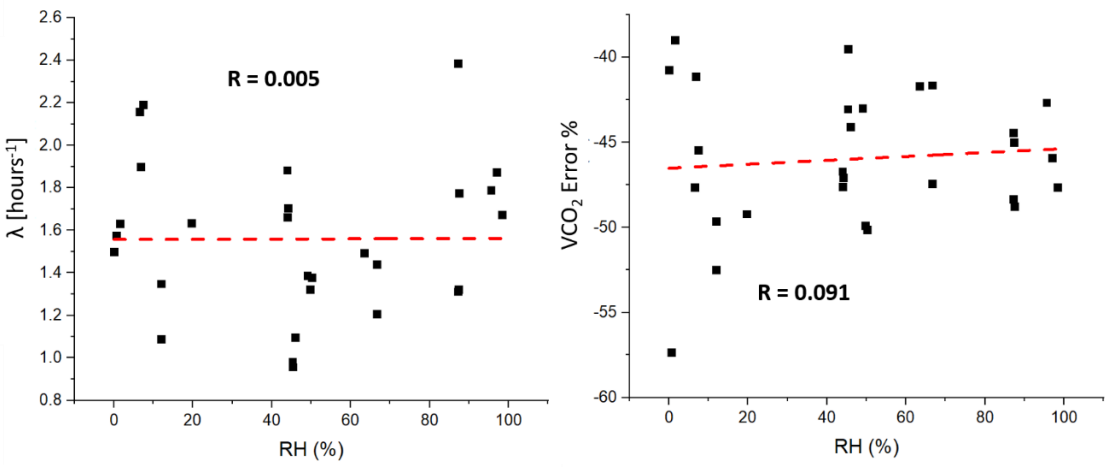

Figure 10. Effect of Humidity on Air Exchange (λ_0) and VCO_2 Error %

Clearly there is a low correlation between humidity and model parameters. The VCO_2 error is high (i.e. large negative), and this is an important finding considering the assumption that λ was equal for CO_2 decay and accumulation. This finding suggests that there may be some significant effect of CO_2 injection (whether it is from a person's breath, as observed in Chapter 4, or from a peristatic pump). The effect of temperature on air exchange and VCO_2 error is shown below in Figure 11.

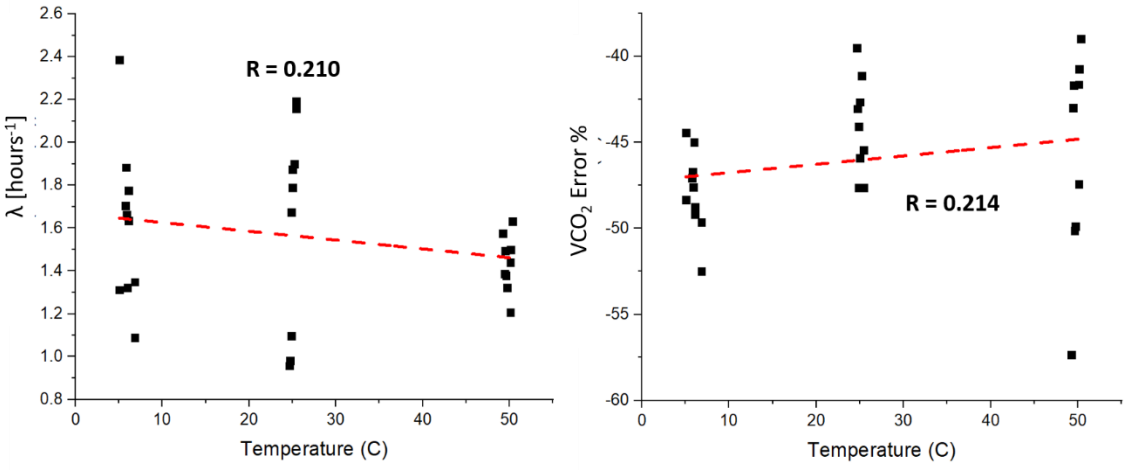

Figure 11. Effect of Temperature on Air Exchange (λ_0) and VCO_2 Error %.

Some correlation between temperature and air exchange can be observed in Figure 11, although this correlation is weak and considered insignificant by statistical heuristics (P=0.286). Similar regression analyses were performed for the CF as calculated via equation 4 and also between λ_0 and VCO_2 error. The findings are shown in Table 3 below.

Table 3. Effect of Temperature, CF, and RH on Smart Pad Measurement

Predictor Variable	Response Variable	Pearson's R	P-value (<0.05 = significant)	Conclusion
CF	λ	0.236	0.227	Not Significant
CF	VCO_2 Error	-0.226	0.250	Not Significant
RH	λ	0.005	0.980	Not Significant
RH	VCO_2 Error	0.091	0.646	Not Significant
Temperature	λ	-0.210	0.286	Not Significant
Temperature	VCO_2 Error	0.214	0.274	Not Significant
λ	VCO_2 Error	0.236	0.227	Not Significant

Table 3 shown above suggest that neither CF, RH, or temperature have any significant effect on λ_0 or VCO_2 error % as measured from the Smart Pad. Also, the finding above suggests that λ_0 has little to no effect on VCO_2 error, although, one should consider the injection gas supply rate in terms of VCO_2 was held constant across all 27 experiments.

2.6.4 Smart Pad Measurement Specifications

The Smart Pad device's physical measurement specifications are shown below in Table 4:

Table 4. Smart Pad System Measurement Specifications

Parameter (Measurement)	Accuracy and/or Precision	Operating Range
Temperature Measurement (°C)	±0.86 °C	6-51 °C
Relative Humidity Measurement (%)	±10.0%	3-98%
Barometric Pressure Measurement (hPa)	±0.1hPa	800-1100 hPa
CO_2 Measurement Accuracy	±50ppm (GE, 2021)	0-3300 ppm
CO_2 Measurement Repeatability	±20ppm (GE, 2021)	0-3300 ppm
Parameter (Device Operation)	**Classification/Value**	**Notes**
Sensing Device Communication Mode	BLE 4.2	iOS supported
Actuator Device Communication Mode	BLE 4.2	iOS supported
Mobile Application Operating System	iOS 14.5	iPhone/iPad OS
Operating Power Sensing Device (DC)	5 V/1A for Charging	microUSB B 2.0
Operating Power Actuator Device (AC)	120 V/60 Hz	U.S. Domestic Standard
Sensing Device Weight	<2.5 lbs (1.1kg)	
Sensing Device Dimensions	25c x 25cm x 10cm	
Battery life (Lithium Ion Rechargeable)	72 Continuous Hours	

2.6.5 Conclusions

The Smart Pad system as described in Chapter 2 has achieved comparable accuracy to a FDA cleared predicate device (Korr ReeVue™) for measurement of Temperature and Relative Humidity, two key parameters in the calculation of a clinically relevant VCO_2, corrected to standard temperature and dry conditions. Neither CF, RH, or temperature have any significant effect on λ_0 or VCO_2 error % as measured from the Smart Pad. From that information, one may reasonably conclude that the Smart Pad's measurement technique is effective across a wide variety of environmental conditions.

High errors in VCO_2 as measured using λ_0 from CO_2 decay were observed, suggesting that there may be some significant difference between λ as measured from CO_2 decay and accumulation, in line with findings from Chapter 4.

CHAPTER 3

3 CLINICAL EVALUATION OF SMART PAD MEASUREMENTS

3.1 Abstract

Twenty healthy subjects were tested in a cross-sectional study to evaluate the performance of the aforementioned technique in measuring both resting energy expenditure (REE) and exercise energy expenditure using the proposed system (the "Smart pad") and an U.S. Food and Drug Administration (FDA) 510(k) cleared reference instrument, MGC Ultima CPX^{TM}, for EE measurement. For VCO_2 and EE measurements, the method showed a correlation slope of 1.00 and 1.03 with regression coefficients of 0.99 and 0.99, respectively, and Bland-Altman plots with a mean bias of -0.2% with respect to the reference instrument. Furthermore, two subjects were also tested as part of a proof-of-concept longitudinal study where EE patterns were simultaneously tracked with body weight, sleep, stress, and step counts using a smartwatch over the course of a month, to determine correlation between the aforementioned parameters and EE. Analysis revealed moderately high correlation coefficients (Pearson's r) for stress ($r_{average}$=0.609) and body weight ($r_{average}$=0.597) for the 2 subjects and VCO_2 measurement accuracy of -1.2%±7.8 (SD) across 13 total longitudinal measures of both subjects. A correction factor, CF_{Env}, was developed, identified, and validated in 2 additional operating environments across N=57 total human measurements to ±10% accuracy for VCO_2 measurement. This corretion factor was later implemented successfully witin the equation (9) model, resulting in substantially equivalent performance to 4 FDA 510(k) cleared devices for VCO_2 measurement using no reference instrument calibrtion.

3.2 Experimental Set Up

The experimental set up is shown below in Figure 12. The subject stayed inside the room configured in the way shown in Figure 13. The room had the Smart pad system and the Smart pad with the sensing module in the back part of the seat. The subject was instructed first to stay seated on the Smart pad pad (red pad in Figure 12) while performing the study tasks described below. The subject simultaneously wore a nose clip and a mouthpiece attached to the reference instrument (MGC Diagnostics, Ultima CPX™ instrument (MGC)) during all CO_2 accunulation measurements. This allowed to evaluate the EE values and carbon dioxide production rate (VCO_2) of the subject using both systems: #1 the Smart pad – based method, and #2 – Reference MGC system. The subject's tasks included: Task 1: sitting in a chair, and Task 2: biking at a moderate, consistent pace in a Fitdesk V3.0 exercise bike or laying on a cot.

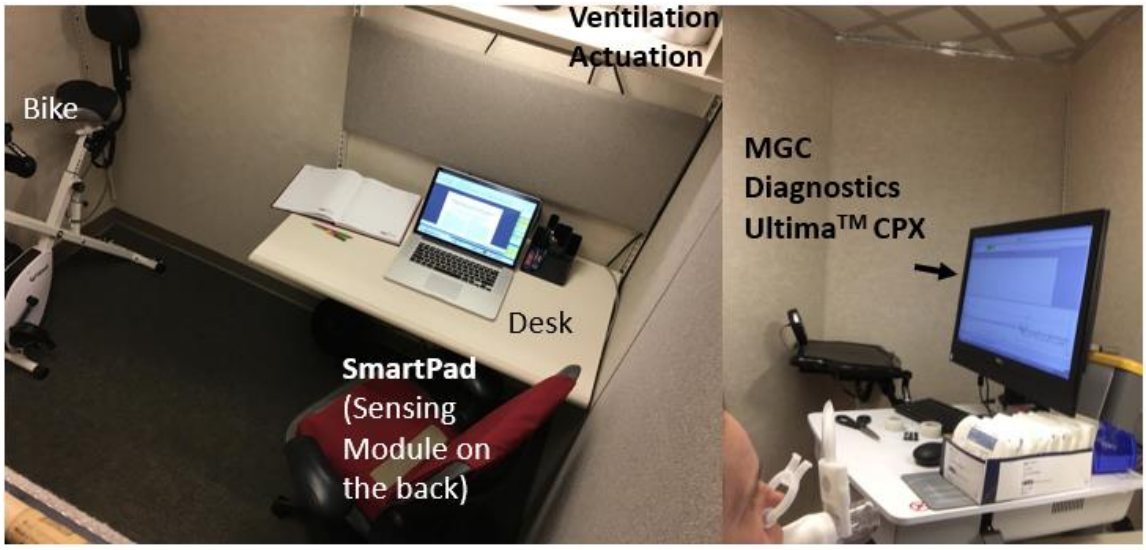

Figure 12. Experimental Set Up for Medical Office Validation Study. Photographs includes Smart Pad, reference instrument, and bike. Activity 1 (sitting) was performed at the desk and then activity 2 (biking) was performed on the bike.

Each experiment consisted of 2 measurement cycles, for a total of 4 measurement cycles between the 2 tasks. The first and second measurement cycle were performed with the subject sitting at the desk, and the third and fouth cycles were performed with the subject biking or lying on the cot. The first and third cycle were used to account for air exchange patterns between the room and the outside environment by experimental determination of the value of the air exchange rate [$hours^{-1}$] (i.e. λ_{Acc}) for the given experimental conditions. The air exchage rate value must be assessed prior to metabolic assessment according to our group's previously derived model (Ruiz et al., 2018). This first and third measurement cycles are termed "growth period #1 and #3" or "G1 and G3" for short. The growth period of the second and fourth measurement cycle (G2 and G4) to fit the new set of experimental data and then determine the exhaled CO_2 volume, VCO_2 [ml/min] for the subject at resting (G2) and biking or liying condition (G4), respectively. The determined VCO_2 value were used for estimation of EE, using a simplified version of the Weir equation (Weir, 1949) (see equation (6)) that assumes a constant value for the respiratory quotient, or RQ. In this way, the first and third measurement cycles provided air exchange data for that particular day since airflow patterns within the building could potentially differ from day to day. Since both the Smart Pad and the MGC Ultima CPX™ were used in parallel, a correlation study of measured VCO_2 and estimated EE values by both methods for each subject at resting and biking or laying conditions was performed.

During the metabolic assessment, a fan system within the room was turned on or off after fixed intervals of time. The fan system consisted of an inlet and outlet fan that cycled fresh air into the room when the system was turned on, to reduce the concentration of CO_2 and other bio effluents, allowing CO_2 specifically to return to baseline levels. The

fan system was turned off immediately prior to each metabolic assessment, to allow CO_2 levels within the room to increase. Other than the fan system, the room was specially sealed to insulate it from the building HVAC system. This special sealing includes both a Retrotec™ blower door with Velcro tape sorrounding the room door frame to prevent air leakage and the taping of interstitial space between ceiling tiles to fully minimize air leakage into/out of the plenum. Each measurement cycle lasted 25 minutes for task 1 (Fans on for 5 minutes then fans off for 20 minutes) and 15 minutes for task 2 (Fans on for 5 minutes then fans off for 10 minutes).

Inlet CO_2 concentrations were also measured for each run as a quality control procedure and to determine whether or not they varied significantly from run to run. To do so, a Telaire 7001 CO_2 sensor was placed in the initial opening inlet duct of the system on the hallway side. The geometry of the medical office and ventilation system can be seen below in Figure 13.

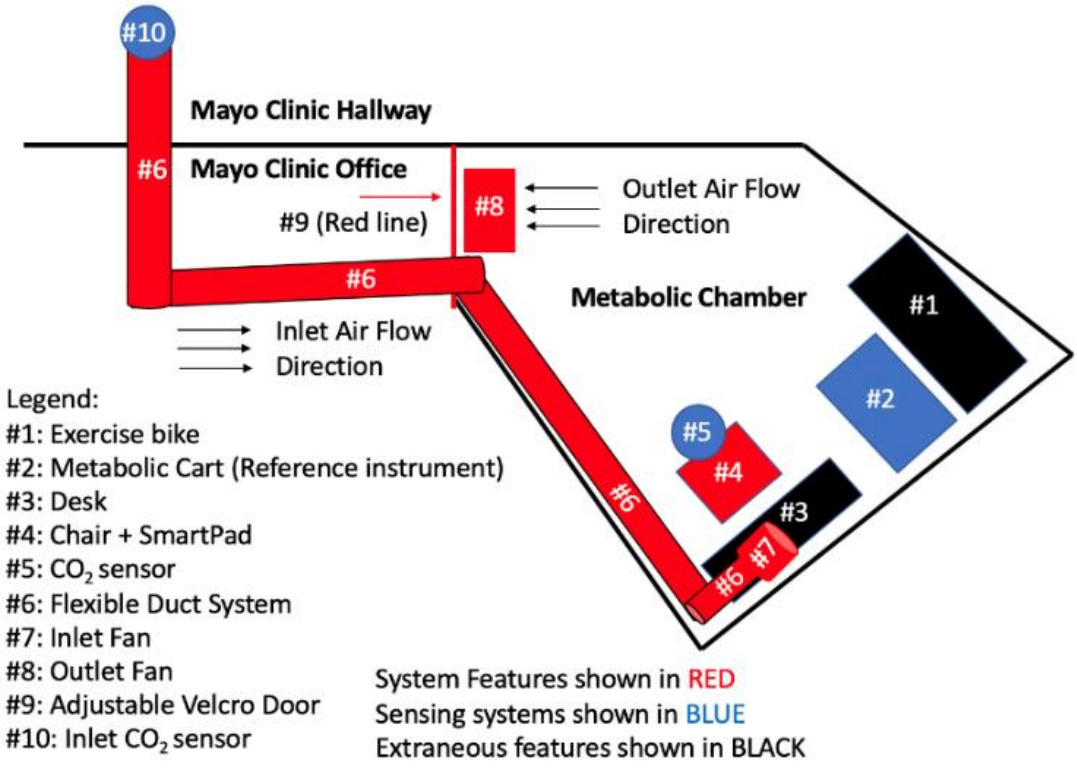

Figure 13. Diagram Showing Room Geometry for Medical Office Study.

3.3 Cross Sectional Study

3.3.1 Cross Sectional Study Methodology

Study participants were recruited primarily from ASU's Biodesign Insittute and Mayo Clinic Scottsdale and were carried out at Mayo Clinic, Scottsdale, Arizona. Subjects had their EE measured while performing a sequence of predetermined tasks under: *1. Resting condition* (sitting in a chair), *2. Activity* (fixed biking). During this study each subject's EE was assessed using both the Smart pad and a reference instrument for EE measurement: MGC Diagnostics Ultima CPX™. For the cross sectional study, 20 subjects were recruited within the age range of 18-65 years . The subjects had an average weight of 69.4 ± 16.2 (SD) kilograms and height of 171.0 ± 11.3 (SD) centimeters. The

study consisted of 10 males and 10 females. One subject elected not to bike for her assessment (due to pregnancy) and instead lied down on a cot for her metabolic analysis. Subjects were instructed to be fasted for at least 4 hours prior to the experiment, to ensure a negligible thermic effect of food, following the use protocol of a FDA cleared device for measurement of EE (Korr ReeVue™) and also within the REE measurement protocol for the reference instrument, MGC Diagnostics Ultima CPX™, which recommends 2 hours fasting prior to REE (resting EE) assessment. However, post hoc literature review has revealed that at least 5-6 hours fasting is likely better sceintific practice, as only 78% of total TEF occurs within the first four hours following a meal (meaning 22% of total TEF from a meal occurs after hour 4) from a wide varitey of meals across 131 TEF tests (Reed & Hill, 1996). The subjects were allowed to bring a laptop or cell phone to use during task 1.

3.3.2 Cross Sectional Study Results (n=20)

For each assessment, experimental data was analyzed manually using OriginPro 2017 (OriginLab™) and data was carefully selected by hand so that it would be best representative of the beginning/end of each assessment. Temperature and relative humidity data are also used to make corrections to standard temperature dry conditions. Sample data analysis records for subjects with low and high metabolic rates are shown below in Figure 14:

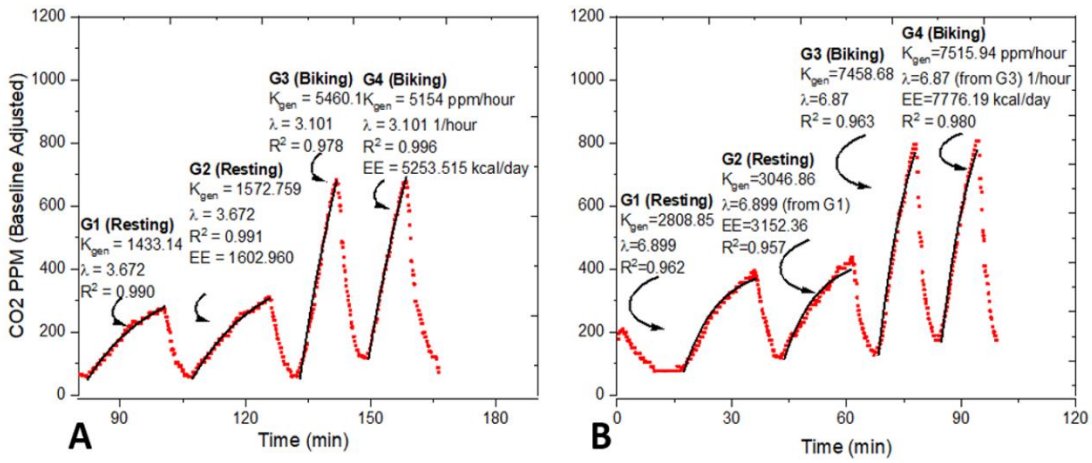

Figure 14: Example of Data Analysis During the 2019 Clinical Study. G1 & G3 are used to calibrate for environment specific factors (e.g. air flow). G2 & G4 are actual assessments from the Smart Pad system. A) low metabolic rate subject; B) high metabolic rate subject.

Each EE & VCO_2 result from G2 & G4 for each run were used to create a set of data with 40 data points total for all subjects tests and was compared to reference instrument readings for the same growth periods (G2 & G4). The resulting correlation plots were analyzed. Figure 15A shows the correlation plot for VCO_2 from the Smart Pad in comparison with the reference instrument. As it can be observed a slope of 1.00 and regression coefficient of 0.99 was obtained, indicating a good correlation for VCO_2 assessment between the methods. Figure 15B shows the corresponding Bland-Altman plot, which indicates a mean bias close to zero (-2.4%), and percentage errors between 10% to -15% for 95% confidence interval. A similar analysis was performed for EE values. Figure 15C shows the correlation plot for EE from the Smart Pad and MGC system with a slope of 1.03 and regression coefficient of 0.99, indicating a good correlation for EE between the methods. Fig. 4D shows the corresponding Bland-Altman

plot for EE assessment, indicating a mean bias close to zero (-2.4%), and percentage errors 15% to -20% for 95% confidence interval. In addition, Figure 15D shows the average variability in a person's energy expenditure (Black & Cole, 2000), which is in average of ± 11.8%. As it can be observed the averge daily EE variability measured from Black and Cole is comprised in ~93% of the total assessed points. As such, a strong case can be made that using the Smart Pad system and taking multiple measurements with the device may potentially be more accurate in estimation of average longitudinal EE than a single time point EE measurement system, even with the Smart pad's current 95% confidence interval for system accuracy. In terms of precision, these measurements indicate comparable perfomance characteristics with other respected indirect calorimeters (Cooper et al., 2009).

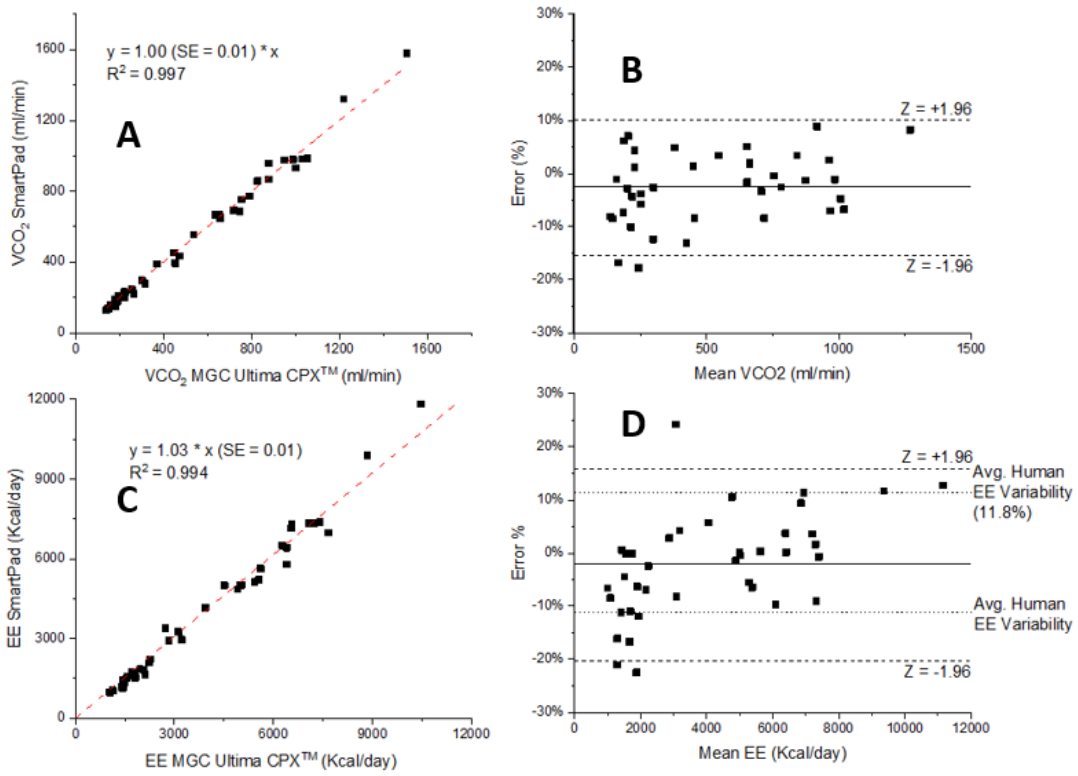

Figure 15: Smart Pad Accuracy During the 2019 Clinical Study for N=20 Subjects. A: Scatter plot of VCO_2 for Smart Pad system and MGC Ultima CPX™. Fig 7B: Bland–Altman plot of VCO_2 Error % for Smart Pad system and reference method for the cross sectional study. Solid black line represents the mean error % between the two systems; the dashed lines indicate +/- 11.8% (average variability in a person's metabolic rate (Black & Cole, 2000). Fig 7C: Scatter plot of EE for the Smart Pad system and reference method. Fig 7D: Bland–Altman plot of EE Error % for Smart Pad system and reference method for cross sectional study. Solid black line represents the mean Error % between the two systems; the dashed lines indicate +/- 1.96 SD (95% confidence interval).

3.3 Longitudinal Study

3.3.1 Longitudinal Study: Accuracy Across All Longitudinal Measurements

Figure 16 presents VCO_2 measurements for both subjects across the longitudinal study. The slope of this plot (1.00) suggests that the EE correction (shown in Figure 15) was effective and that the system is valid for measurement of EE for the longitudinal study. The resulting Bland-Altman plot Figure 16B confirms that the Smart Pad system is effective at assessing EE in terms of mean bias which is -1.23% and with promising precision (SD = 7.81%). The plotted results showing EE from the Smart Pad system are shown for both subjects (Figure 16C-D). These plots also show stress patterns (hassles survey score) and hours of sleep per night (steps and bodyweight data collected but not shown in Figure 16C-D for simplicity). Statistical analysis for determining any correlation between the aforementioned quantities & energy expenditure (EE) is described below in section 3.3.2 & shown below in Figure 17 and Figure 18. Given the low number of subjects (N=2) and the low number of EE measurements throughout the tests (4-9 depending on subject), results should be interpreted conservatively. The study consists of the presentation of two study cases as a proof of concept of assessment of EE and other complementary physiological data under daily conditions.

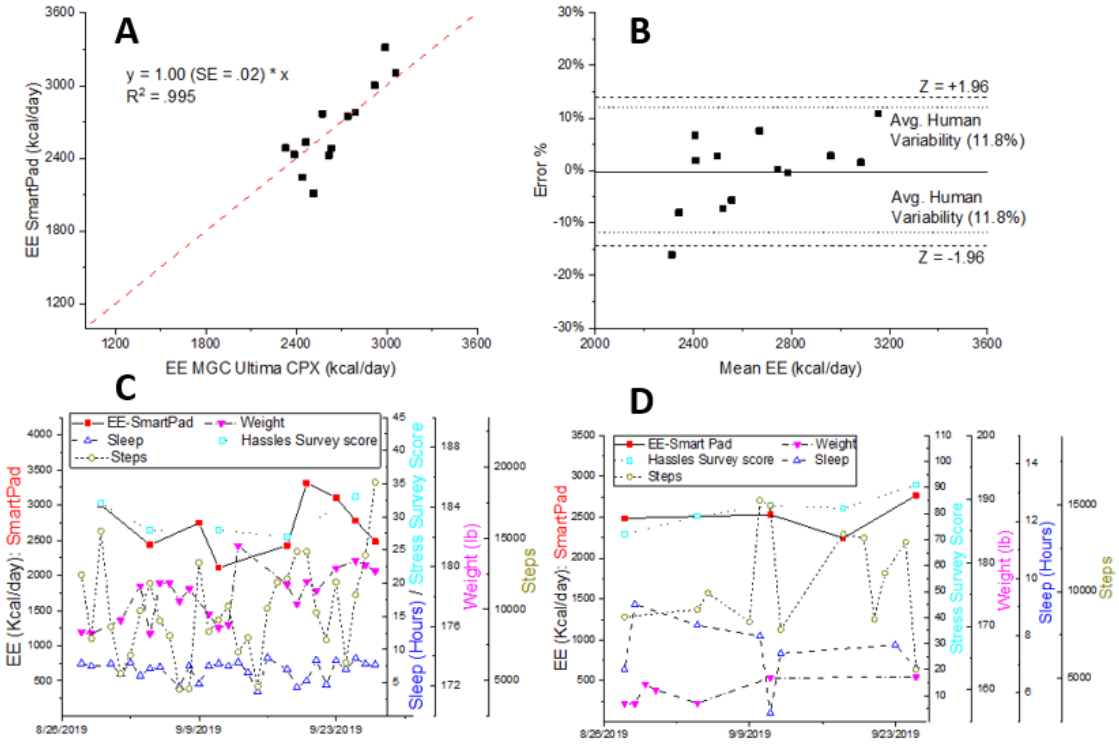

Figure 16: Results from Longitudinal Study of Metabolism and Lifestyle Patterns. A: Scatter plot of VCO_2 for the Smart Pad system and reference method (MGC Ultima CPX™). B: Bland–Altman plot of VCO_2 Error % for Smart Pad system and reference method. Solid black line represents mean Error % (-1.23%) between both systems; dashed lines indicate +/- 11.8%, the average variability in a person's metabolic rate (Black & Cole, 2000). C-D: Results of longitudinal study for 2 different subjects, one aged 22 (correlation analysis shown in Figure 17), the other aged 24 (correlation analysis shown in Figure 18).

3.3.2 Longitudinal Study: Correlation Analysis

Figure 16A-B shows the correlation plot and corresponding Bland-Altman plot for EE assessment during the longitudinal study by Smart Pad and the reference system.

The simulaneously collected EE data from both the Smart Pad and the MGC Ultima CPX^{TM} showed evidence to support (mean bias ~0% for EE measurement for longitudinal study) the accuracy level of Smart Pad necessary to perform further correlation analysis between EE and lifestyle parameters of sleep, activity (steps), stress and body weight. As mentioned in the experimental section, stress was taken using hassles survey, and body weight from the Wi-Fi scale records for the corresponding dat of the EE assessment. The metric used to assess correlation was "Pearson's r", which ranges from -1 (high negative correlation) to +1 (high positive correlation) with a value close to 0 suggesting little to no correlation. The results of this correlation analysis are shown in Figure 17A-D for the 22 year old male (subject A) and in Figure 18A-D for the 24 year old male (subject B).

The correlation coefficients resulting from correlation analysis between stress survey score and EE were r = 0.823 (n=5) for subject A, and r = 0.514 (n=4) for subject B. The correlation coefficients resulting from correlation analysis between body weight and EE were r = 0.602 (n=7) for subject A and r = 0.644 (n=3) for subject B. Stress and body weight showed the highest correlations with EE. The positive correlation between body weight and EE confirms a well known correlation (Roza & Shizgal, 1984). The correlation between hours of sleep the night before to the metabolic assessment and EE rendered r = -0.309 (n=8) for subject A, and r = 0.386 (n=3) for subject B did not show strong correlation. Evidences in literature suggest poor sleep generally results in lowered REE (Sharma & Kavuru, 2010) . The correlation between the number of steps the day of the assessment day (measured using a smartwatch) and EE measured the same day did

not show correlation with energy expenditure: r=0.263 (n=9) for subject A and r = -0.674 (n=4) for subject B.

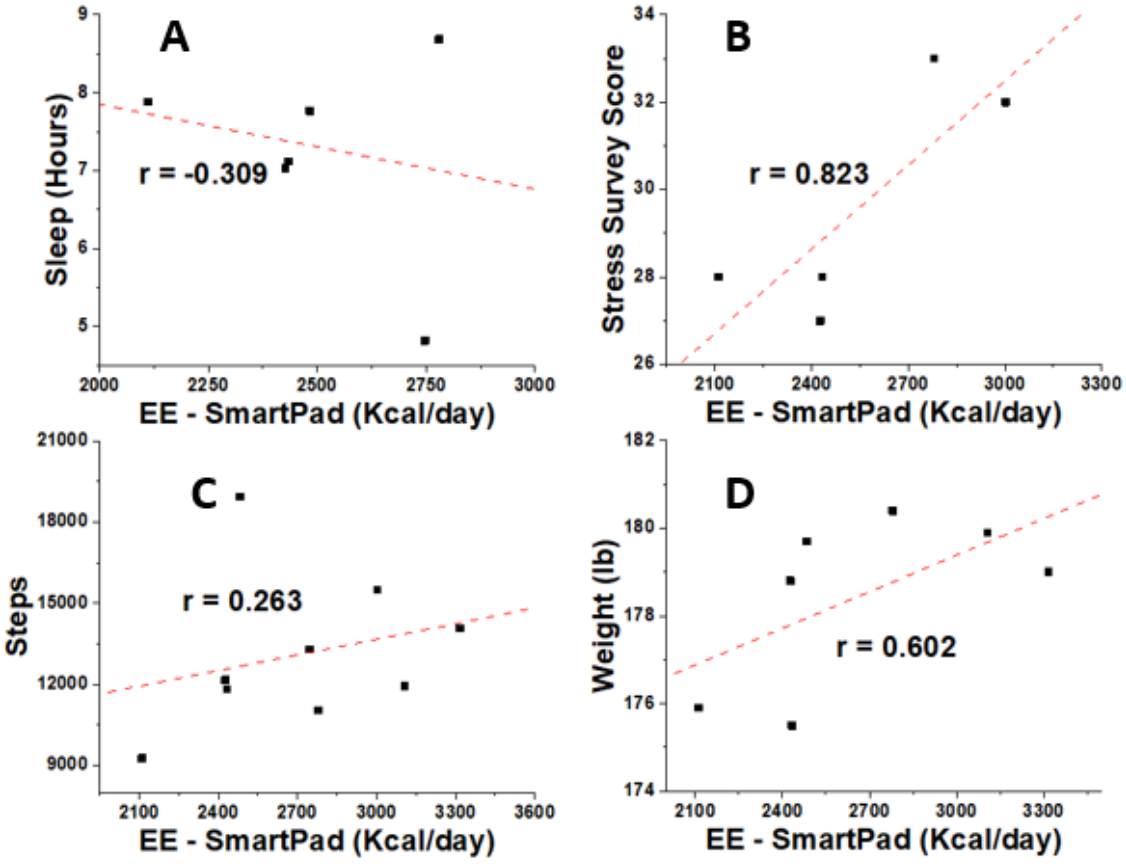

Figure 17: Longitudinal Study Correlation Results for the 22 Year Old Male. Pearson's r values for EE [kcal/day] and the various parameters measured: (A) sleep [hours] night before test, (B) stress questionnaire score, (C) steps measured on Withings^{TM} smartwatch, and (D) weight

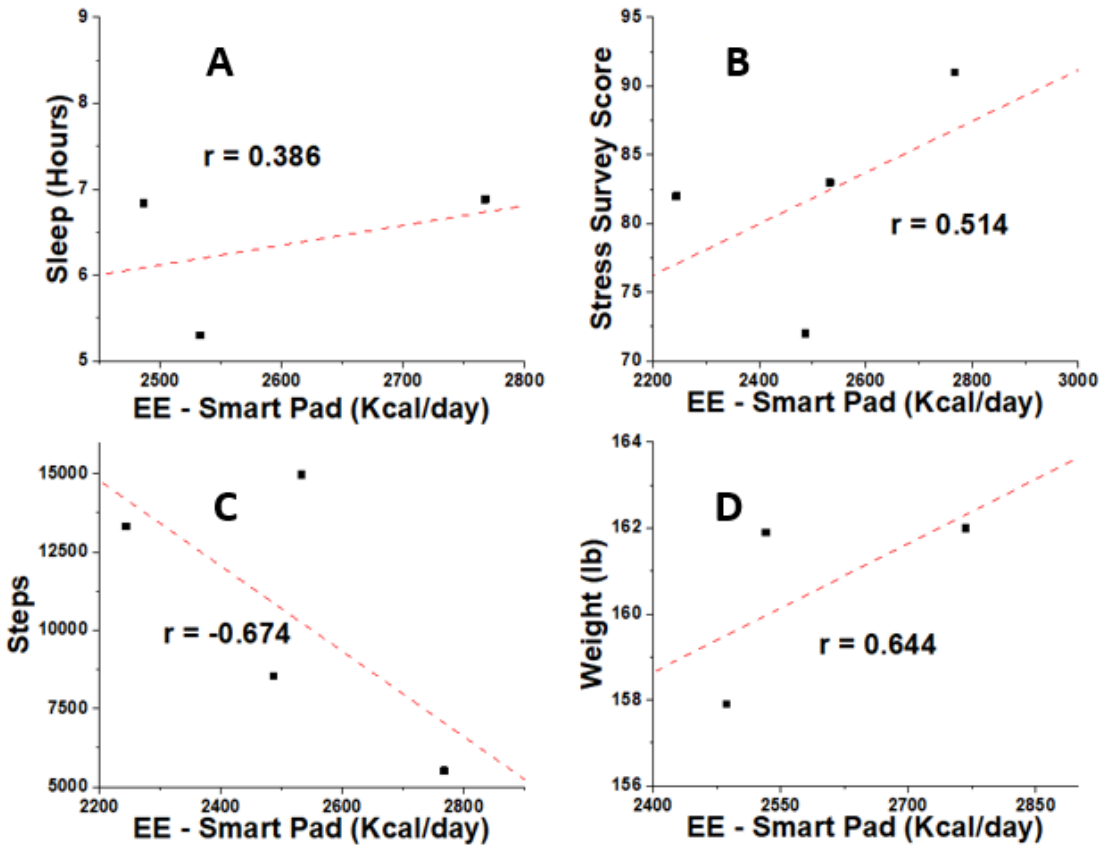

Figure 18. Longitudinal Study Correlation Results for the 24-Year-Old Male. Pearson's r values for EE [kcal/day] and the various parameters measured: (A) sleep [hours] night before test, (B) stress questionnaire score, (C) steps measured on smartwatch, and (D) weight

3.4 Conclusion

The technique presented in this work has been shown to be an effective method of VCO_2 measurement under free-living conditions in comparison with a reference method, and therefore, has value in determination of energy expenditure (EE). The measurement technique is truly novel, being the first ever EE measurement technique that is both portable and capable of physical contact free measurements, therefore potentially

providing great utility for clinical treatement of obesity. The system presented has relatively good accuracy as evidenced by low mean biases when compared to the reference method for both the cross sectional and longitudinal studies. The system is unparalleled in its ability to be used daily and the fact that it does not require any wearable technology on part of the user (e.g. breathing tubes and noseclips).

CHAPTER 4

4 ENGINEERING A FASTER, FULLY AUTOMATED SMART PAD

4.1 Abstract

Energy Expenditure (EE) [kcal/day], a key diagnostic for obesity treatment, is measured from CO_2 production, VCO_2 [ml/min], and/or O_2 consumption, VO_2 [ml/min]. Current technologies are limited due to prevailing designs requiring wearable facial accessories presenting accuracy, precision, and usability concerns with regards to free-living measurement. A novel system is evaluated, the Smart Pad, which measures EE via VCO_2 from transient changes in a room's ambient CO_2 concentration. Resting EE (REE) (N=113) and exercise VCO_2 (N=46) measurements were recorded using Smart Pad and a reference instrument, MGC Ultima CPX^{TM}, to study measurement duration's influence on accuracy. The Smart Pad displayed 90% accuracy (68% Confidence Interval (CI)) for 14-19 minutes of REE measurement and for 4.8-7.0 minutes of exercise VCO_2 measurement after air exchange rate (λ [hour^{-1}]) calibration using a reference instrument. Additionally, the Smart Pad measured the REE of N=5 subjects with a wide range of body mass indexes (BMI) for a minimum of 5 measurements each, successfully validating system accuracy across a range of subject BMI's (18.8 to 31.4 kg/m^2) and REE's (~1200 to ~3000 kcal/day). High correlation between subjects' VCO_2 (N=26) and λ [hour^{-1}] for CO_2 accumulation was observed (P<.00001, R=0.785) in a 14.0 m^3 sized room used for this study. This finding lead to development of a new model for REE measurement from ambient CO_2 without λ calibration using a reference instrument. The model correlated in high agreeance with reference instrument measures (y = 1.06x, R=0.937) using an independent averaged dataset (N=56).

4.2 Smart Pad: Physical Characteristics, Design, and Testing Environment

The Smart Pad system is comprised of three components: a measurement system (seat pad comprised of sensors and an IoT enables electrical system shown in Figure 1A), actuator system (optional IoT controlled electrical system allowing for precise control of CO_2 concentration within a room shown in Figure 1C), and iOS app (for logic control of the actuator system, and, eventually data analysis) with a portion of the user interface shown in Figure 1B and Figure 19A. The measurement system is a pad that fits over a chair with the red seatpad serving to house a commercial CO_2 sensor (Telaire™ 7001D CO_2 monitor) with CO_2 measurements based on non-dispersive infrared (NDIR) absorption, and bluetooth™ enabled data logger that also records temperature, barometric pressure, and relative humidity using widely available electronics (but with electrical system and packing designed by our lab). A brand new CO_2 measurement device was used for the entire study and factory calibration was validated using a CO_2 reference gas and outdoor air, which is well known to contain approximately 415 ppm CO_2 in most areas of the world (Tans & Keeling, 2020), to the rated accuracy of the CO2 measurement device (±50ppm). An inlet tube with a diameter of approximately 0.3 cm was connected to the sample inlet port of the CO_2 sensor, sealed with parafilm, and then allowed to rest approximately 5 cm out of the red seatpad. Data resolution was 1 measurement/5 seconds for CO_2, relative humidity, barometric pressure, and temperature.

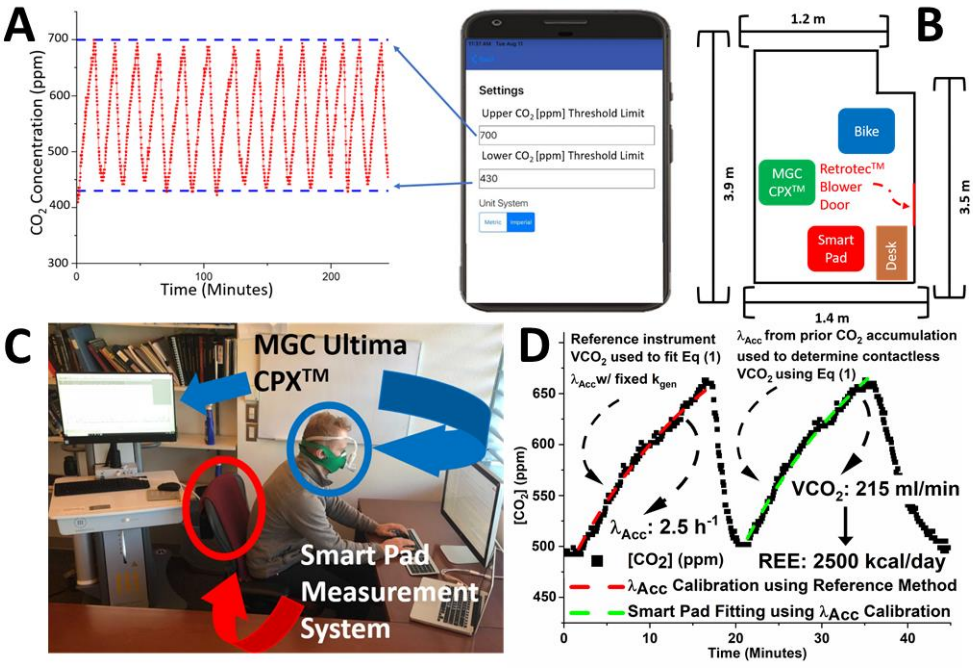

Figure 19: Study Design for Optimization of Smart Pad Operating Parameters. (A) Graphic showing Smart Pad mobile application and settings allowing for precise control of CO_2 concentration. (B) Graphic showing top view of room layout and locations of various objects. (C) Subject during test procedure for parallel REE measurement with Smart Pad and Reference Instrument. (D) Graphical demonstration of Smart Pad's k_{gen} assessment with two CO_2 accumulation data, using known λ_{Acc} from first CO_2 accumulation data. In the first CO_2 accumulation cycle, the CO_2 accumulation fitting is done using equation (1) and known k_{gen} from the reference instrument. In the second CO_2 accumulation cycle, λ_{Acc} from the first accumulation cycle is used to determine k_{gen} using equation (1). k_{gen} is then used to calculate EE via combination of equations (3-6).

The Smart Pad was installed on a chair in a rectangular room with a measured volume of 14 m^3, which accounts for the size of objects, and approximate dimensions of 2.7m x 1.4m x 3.7m (shown below in Figure 20). The room was well sealed using tape to cover interstitial space between ceiling tiles and cardboard panels to block the room's

built-in HVAC (heating, ventilation, and air conditioning) system. A special Retrotec™ (https://retrotec.com/) blower door was installed on the doorway fixed with an outlet fan and also a transparent plastic window allowing for observation of test subjects. Despite this, there was still a significant amount of leakage present, with almost all observed λ values greater than 1 $hour^{-1}$, which is in agreeance with similar findings for unoccupied administrative offices (Cheong & Chong, 2001), suggesting that significant air exchange will still occur even with the room mostly sealed from the surrounding environment (Retrotec™ door's opening for an outlet fan was likely the primary air exchange medium). Additionally, two 40 cm diameter mixing fans were pointed towards each other at opposite corners of the measurement environment to support mixing of CO_2 in the room. The fans were left on continuously during both CO_2 accumulation and decay periods.

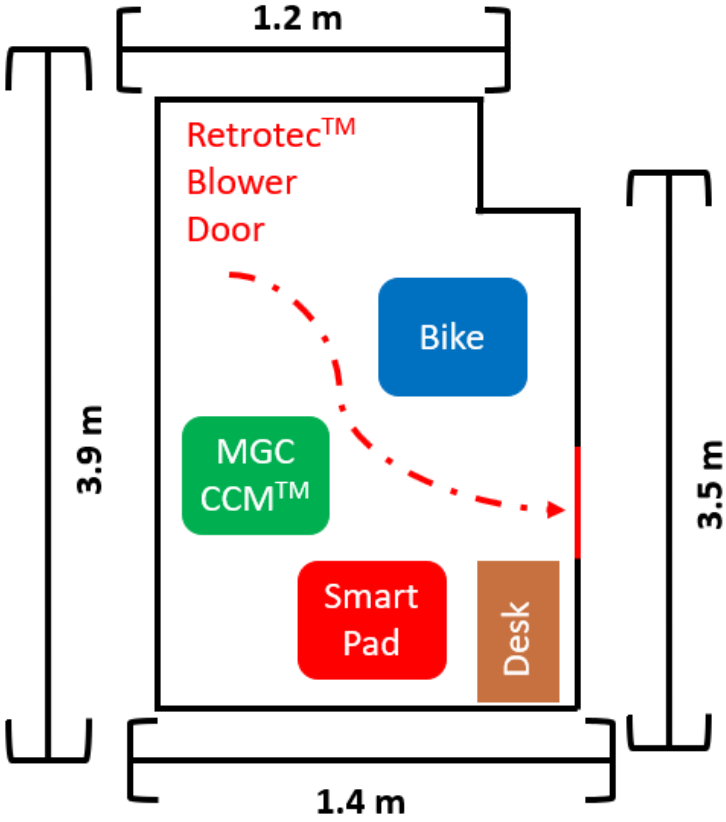

Figure 20. Schematic of Testing Environment Layout for Chapter 4. The room was a rectangular prism with one irregular corner. The MGC CPX™ Ultima would need to be moved slightly for biking assessments, but, the Smart Pad and bikes were kept in a constant location.

4.3 Methodology: CO_2 Measurement Range Optimization for REE assessment

A single subject performed 113 REE measurements with both the Smart Pad and an MGC Ultima CPX™ Indirect Calorimeter (MGC Ultima CPX™), a FDA cleared device, considered a reference method for both VCO_2 and REE measurement. The device is considered a highly accurate reference instrument since it measures both VCO_2 and VO_2, which it does by direct physical measurement of flow rate (via pitot tube), O_2 concentration (via galvanic cell potential), and CO_2 (via NDIR absorption). The 113 REE

measurements were split between 5 CO_2 threshold ranges [ppm]: 500-600, 500-625, 500-650, 500-675, 500-700. Multiple CO_2 accumulation cycles are measured sequentially. λ_{Acc} was calibrated for using the first CO_2 accumulation curve from that day and a reference k_{gen} value generated from gold standard VCO_2. The subject was fasted for 8 hours prior to each REE assessment to minimize the well-studied effect of the thermic effect of food which is known to increase EE by a significant margin (Calcagno et al., 2019).

This section of the study was performed to build upon previous work published in the journal of breath research (Sprowls, Victor, Serhan, et al., 2021) showing relatively good system accuracy in measurement of VCO_2 from 20 minute CO_2 accumulation periods in a similarly sized room. This study strove to reduce the measurement time to lower than 20 minutes without sacrificing measurement efficacy. All 113 REE measurements were performed with both the Smart Pad and a FDA cleared (FDA, 2006), gold standard method for both VCO_2 and REE measurement, the MGC Ultima CPX™ (https://mgcdiagnostics.com/products/ultima-ccm-indirect-calorimeter). A minimum of 16 measurements were performed for each measurement cycle and up to 32 measurements for the most promising threshold ranges in terms of accuracy. The λ_{Acc} value used for analysis was assessed from reference instrument VCO_2, as follows. First, Multiple CO_2 accumulation cycles are measured sequentially. For the first CO_2 accumulation cycle in the sequence, equations 2-3 are used to generate a reference k_{gen} from the gold standard method's VCO_2 measurement. Then the reference k_{gen} is applied to equation (1), fitting the CO_2 accumulation data from the first measurement cycle. A λ_{Acc} value can be ascertained from this first CO_2 accumulation curve and can be applied

to every CO_2 accumulation curve occurring after the first one to generate Smart Pad k_{gen} values that lead to corresponding VCO_2 and EE measurements from equations 2-6. This procedure can be seen in Figure 21, Figure 23, and Figure 24 below. Often times 8-12 sequential CO_2 accumulation curves were collected on the same day, all analyzed using the λ_{Acc} value (measured using the gold standard's VCO_2 reading) taken from the first CO_2 accumulation curve from that day. For each new day of collected data, a λ_{Acc} value was always extracted from the first CO_2 accumulation curve and applied to the CO_2 accumulation curves that followed that one (i.e. λ_{Acc} value applied to CO_2 accumulation data was always assessed from that day's collected data and no CO_2 accumulation curve was analyzed using the λ_{Acc} value collected from a different day). All N=113 measurements were performed on subject #1 (physical characteristics shown in Table 5). Since many CO_2 accumulation curves were used for λ_{Acc} assessment, there are a total of N=135 growth curve measurements, which allowed for an assessment of the effect of CO_2 threshold range on measurement duration.

The Smart Pad showed evidence of substantial equivalence to multiple FDA cleared predicate devices based on the results of the study (see Table 19) and when λ_{Acc} was calibrated for using a well-respected reference method for VCO_2 measurement. In this Chapter, the results of 4.7 are compared to (Cooper et al., 2009). Although differing units are reported, we believe both (Cooper et al., 2009) and the authors of this work have calculated CV and error SD in fundamentally the same manner and therefore both results could be reported together. That being said, one should take interpret differences in precision referred to above conservatively given (Cooper et al., 2009) does not provide a

formal definition (see Table 1 of the referenced work), although we suspect it does match our own.

4.4 Methodology: CO_2 Measurement Range Optimization for Exercise assessment

Subject 1 (physical characteristics shown in Table 5 below) performed N=46 simultaneous Smart Pad and MGC Ultima CPX^{TM} VCO_2 and exercise EE assessments while using a stationary bike. The subject often biked at a high intensity; however, no formal measure of exertion was recorded. The stationary bike was facing the Smart Pad unit (kept in the same geometric location between 4.3 and 4.4) and was approximately 1 meter away from the seat pad (see Figure 19 for illustration of biking subject and nearby Smart Pad). Regression analysis was performed based on app settings and end/beginning points of CO_2 accumulation data (not necessarily absolute CO_2 [ppm]).

There was a stationary bike also located in the measurement environment (shown in Figure 20) which was used to perform exercise EE measurements using the Smart Pad and gold standard. Analysis was performed in an identical manner to the method of 4.3, except that the λ_{Acc} assessment from gold standard instrument VCO_2 always assessed λ_{Acc} from a CO_2 accumulation curve occurring as a result of subject biking. The same set of threshold ranges were analyzed as in section 4.3 (i.e. 500-600, 500-625, 500-650, 500-675, 500-700) for a total of N=40 measurements or N=8 measurements for each threshold range. Additionally, N=6 measurements were taken for an extended CO_2 threshold range of 500-900 ppm. VCO_2 measurement accuracy for the Smart Pad is the focus of this sub-study, however, exercise EE is studied and reported as well within this section.

4.5 Methodology: Effect of REE on Accuracy for Optimized Measurement Range

Test subjects were recruited with Arizona State University's institutional review board's approval (STUDY00006547) after giving consent to participate in the study and were asked to perform 6 sequential MGC Ultima CPX^{TM} and Smart Pad measurements at the CO_2 threshold range of 500-650 ppm (1 for λ_{Acc} assessment from reference method VCO_2 and 5 comparative measurements). This was done to determine if subject BMI, VCO_2, or EE have any significant effect on Smart Pad accuracy or λ_{Acc}.

The physical characteristics of each subject are shown below in Table 5.

Table 5: Subject Physical Characteristics for Optimized Smart Pad Study

Subject #	Height (cm)	Weight (kg)	BMI (kg/m^2)	Clinical Body Type Classification *(CDC, 2021)*	Age (Years)	Sex (male, female, or non-binary)
1	178	79.4	25.1	Overweight	24	Male
2	153	44	18.8	Normal Weight	27	Female
3	185	107.3	31.4	Obese	26	Male
4	155	63.5	26.4	Overweight	35	Female
5	185	78.5	22.8	Normal Weight	25	Male

4.6 Methodology: CO_2 Decay: Study of Unoccupied Room Air Exchange (λ)

In scientific literature (Batterman, 2017; Gall et al., 2021; Ramalho et al., 2013; Turanjanin et al., 2014), there is a general assumption that λ_0 from CO_2 decay following subject departure should be in agreeance with λ_{Acc}. In this study, reference measurement for VCO_2 measurement was used to assess λ_{Acc} with high accuracy and compare it with

λ_0 from CO_2 decay following subject departure. N=26 CO_2 accumulation periods and subsequent CO_2 decay periods were collected with the actuator system turned off continuously to assess CO_2 decay as a predictor of λ_{Acc} during CO_2 accumulation periods. N=5 minimum assessments were performed for each of the following CO_2 concentration ranges (ppm): 500-600, 500-625, 500-650, 500-675, and 500-700. For the 500-650 ppm data set, CO_2 accumulation and subsequent CO_2 decay was collected using N=1 measurement from each subject # 2-5 and N=2 measurements from subject #1.

4.7 Results: Measurement Range Optimization for REE assessment

To control for the effect of REE, subject characteristics, and experimental methodology execution, a single subject was used as the population within this study section. That subject performed N=113 parallel REE assessments with the Smart Pad and reference instrument. Results shown below in Figure 21:

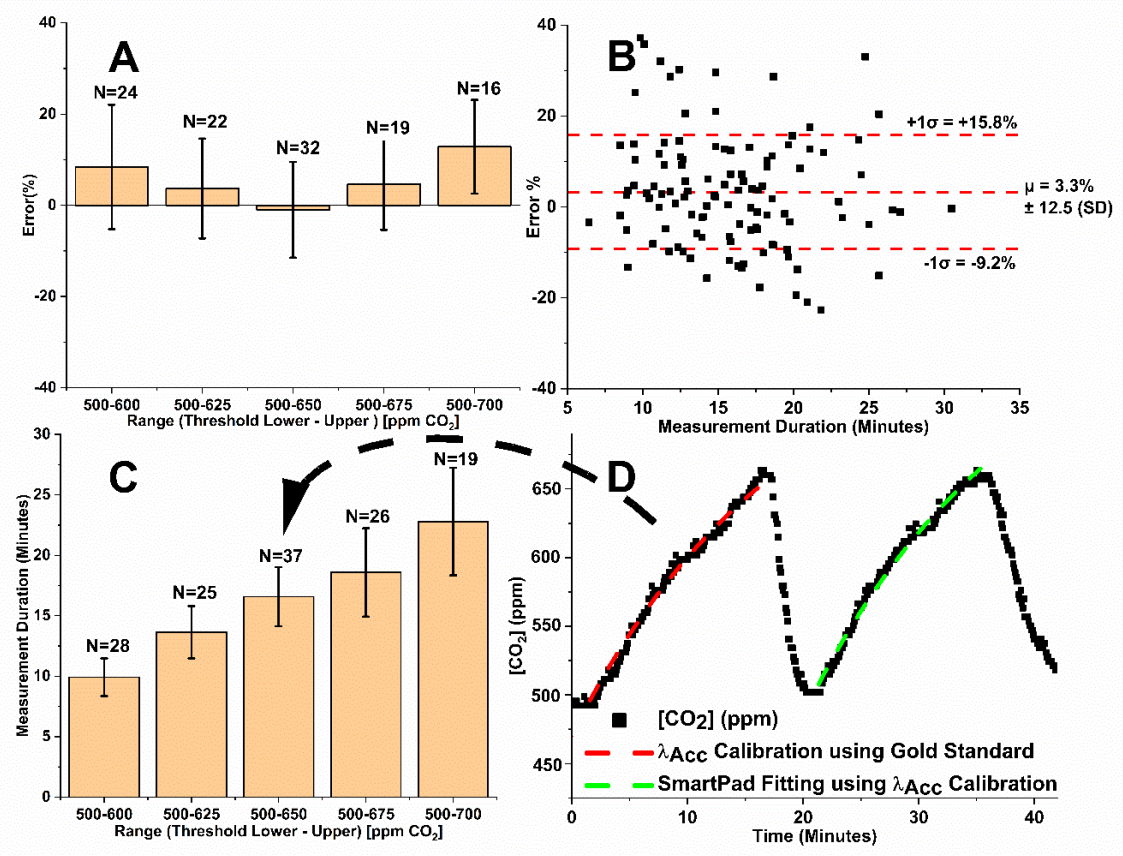

Figure 21. Effect of Measurement Duration on REE Measurement Accuracy (A) Effect of upper and lower threshold range settings on Smart Pad accuracy for REE measurement; (B) Effect of time per measurement on REE accuracy across all N=113 measurements; (C) Effect of threshold range settings on the time per measurement. (D) Sample data analysis for 500-650 ppm threshold range.

Figure 21 details the effect of Smart Pad threshold range on system precision and accuracy. The 500-650 ppm CO_2 concentration range was concluded to be the most accurate and precise operating range with performance characteristics of -1.0% ± 10.5% (SD) for the subject across N=32 total REE measurements ranging from 1420 to 2990 kcal/day. Figure 21B shows the effect of measurement duration directly on system accuracy and provides evidence of the overall robustness of Eq (1) with a low mean bias

(3.3%) across all 5 threshold ranges. Figure 21C shows the effect of CO_2 threshold range on time per measurement, with time per measurement increasing consistently with increasing CO_2 threshold range, an expected result as, in general, larger sets of data should take longer to collect. From Figure 21C, it is possible to provide a confidence interval for the expected time per measurement for the tested subject at the tested CO_2 threshold ranges. From this information, one may reasonably conclude that the 500-650 ppm CO_2 threshold range provides the optimal precision and accuracy, with REE measurement characteristics of 88.5% (68% CI) accuracy for 14-19 minutes per measurement (68% CI). For a singular measurement in the given experimental conditions on the singular subject with N=32 measurements for 500-650 ppm, the Smart Pad showed comparable accuracy to the most accurate REE estimating equation (at least as reported in (Frankenfield, 2013) for their N=337 subject population): 81.5% accuracy for the Smart Pad compared to 82% accuracy for the Mifflin St. Joer equation (both for a 90% CI). Repeated measures can improve the Smart Pad accuracy significantly (see section 4.11) to levels above the Mifflin St. Joer, an inference based on implications of standard error (Altman & Bland, 2005). It is also interesting to note that the system when used the 500-650 ppm range shows evidence of similar precision by an alternative definition, the "within subject coefficient of variation (CV)" (relative to gold standard) as does current FDA cleared/approved medical devices for REE measurement (Cooper et al., 2009): the Korr ReeVue™ (FDA, 2003) and MedGraphics CPX Ultima™ (FDA, 2006): Smart Pad error SD (68% CI): 10.5%, Korr ReeVue™ CV (68% CI): 11.1%, MedGraphics CPX Ultima™ CV:12.2% (68% CI).

A linear regression on the results of Figure 21B produced a R value of -0.193, suggesting “little to no correlation between Smart Pad Error percentage and measurement duration”. However, one should be skeptical of this conclusion, given a hypothesis test on the slope of the aforementioned regression resulted in a p-value of 0.041 (possibly deflated due to high sample size, N=113, which is known to inversely correlate with p-value (Thiese et al., 2016)), only marginally significant by common statistical heuristics, and still suggesting the conclusion that per measurement has a significant effect on Smart Pad analytical accuracy. A similar, less refined Smart Pad system already did show relatively good accuracy for EE measurement in a N=20 subject study in collaboration with Mayo Clinic (Sprowls, Victor, Serhan, et al., 2021). This study section significantly builds on those results by effectively reducing the measurement time of the system by several minutes, an important consideration for medical practices with a limited number attending rooms and also for the purpose of repeated measurements as described in section 4.11.

The authors suspect fitting in the reference instrument mask and potential leaks in the facial accessory to partly have influenced reproducibility (and therefore precision and final rated accuracy in this manuscript). Since fundamentally the observed variance in the results is an additive product of the total errors in both Smart Pad and MGC Ultima CPX^{TM} systems, one might expect the rated precision of the presented device to decrease if errors in gold standard EE measurement were eliminated by using a more robust breath gas collection accessory (e.g. a mouthpiece accessory provided by supplier) or using a quality control product for respirator fitting such as Bitrex^{TM} as enumerated in the U.S. Occupational Safety and Health Administration regulatory statutes (OSHA, 2020).

Sample data fittings for Subject #1:

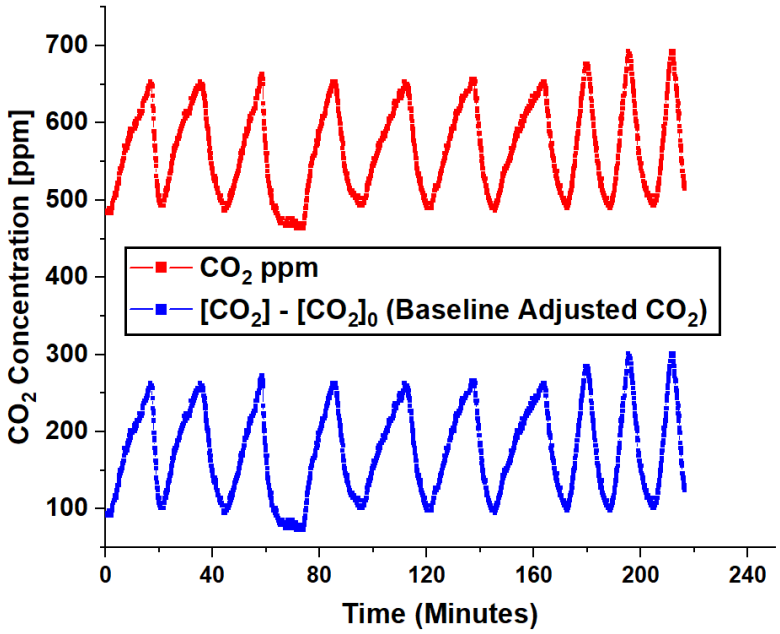

Figure 22: Sample Raw Data for a CO_2 Threshold Range of 500-650. Red curve shows CO_2 concentration measured from the Smart Pad. Blue curve shows the baseline adjusted CO_2 concentration, which is used to fit an identical model to equation (1) but with simplification that the $[CO_2]_0$ term is subtracted from both sides of the equation.

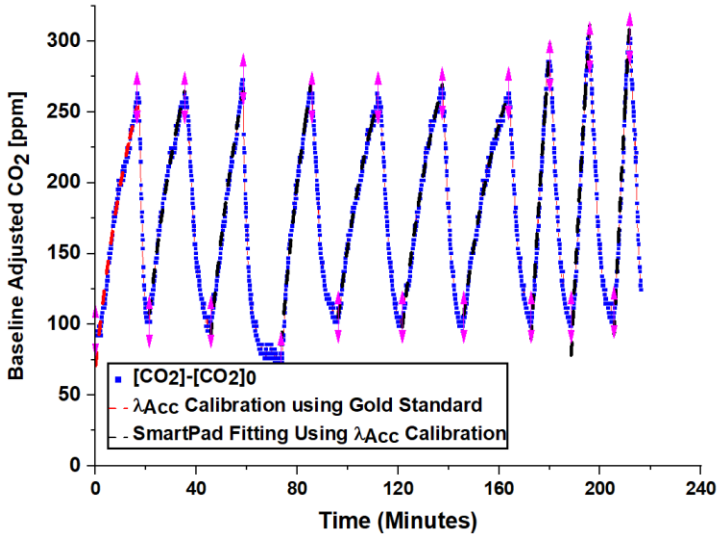

Figure 23: Baseline Adjusted Fitting for REE using Reference Method Calibration. First CO_2 accumulation curve is fit with reference k_{gen} to determine $\lambda_{Acc.}$ Each sequential curve is analyzed with that same λ_{Acc} value. Last three CO_2 accumulation curves are for biking assessment (i.e. for 4.4), with first being to calibrate for λ_{Acc} and second and third for Smart Pad VCO_2/EE measurement.

Table 6: Results from Contactless REE Measurement (for Figure 23)

Fitting # (Shown in Figure 23)	REE Smart Pad [kcal/day]	REE Reference Method [kcal/day]	Error %
#1	2552	2609	-2.2
#2	2767	2618	5.7
#3	3012	2987	0.8
#4	2345	2187	7.3
#5	2504	2225	12.5
#6	2279	2199	3.7

4.8 Results: Measurement Range Optimization for Exercise assessment

Figure 24 (A-D) below shows Smart Pad VCO_2 measurement performance for exercise (biking on a fixed bike).

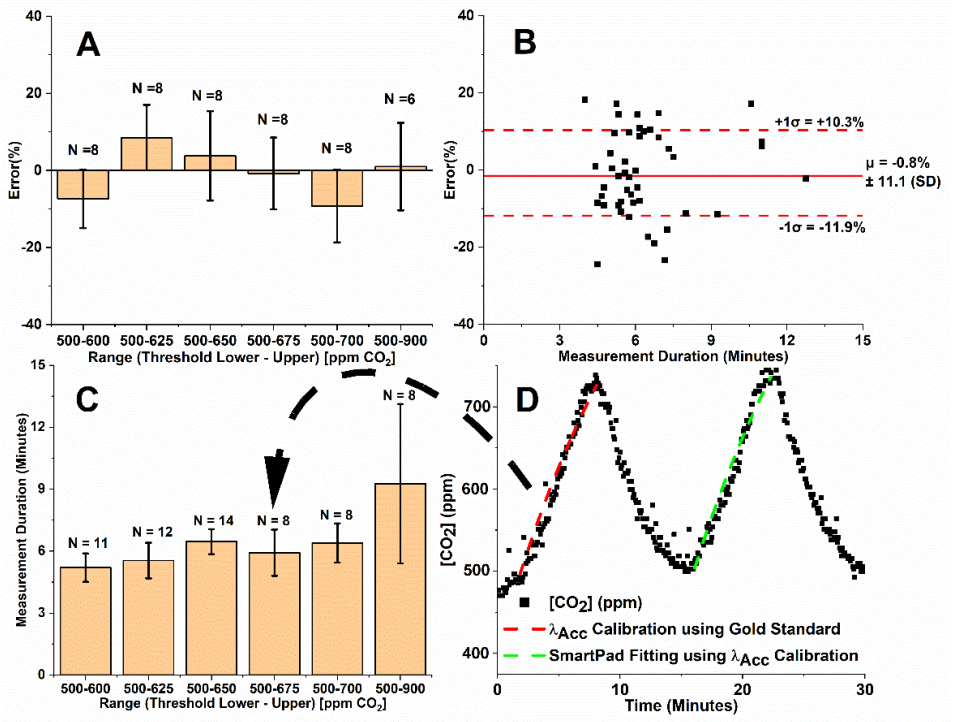

Figure 24: Effect of CO_2 Operating Range on VCO_2 Measurement for Exercise. (A) Effect of threshold range settings on Smart Pad accuracy for VCO_2 measurement for exercise VCO_2 assessment; (B) Effect of measurement duration on Smart Pad VCO_2 accuracy across all N=46 parallel measurements; (C) Effect of threshold range settings on the measurement duration for a biking subject. (D) Sample data analysis for 500-675 ppm threshold range.

Figure 24A shows how the Smart Pad app's CO_2 threshold range affects system accuracy for VCO_2 measurement, with the 500-675 threshold range showing optimal measurement characteristics (-0.8% mean bias). Figure 24B shows the effect of time per measurement on VCO_2 assessment accuracy. Across all N=46 measurements spanning the six concentration ranges from 500-600 ppm to 500-900 ppm, a mean bias of -0.8% can be observed, suggesting that equation (1) is robust across a variety of CO_2

concentration ranges. Figure 24C shows the effect of CO_2 threshold range on measurement duration. A consistent increase in measurement duration with increasing size of CO_2 threshold range was not observed, a logical result given the study design, given effort level on the bike was not a control variable of the study (a notable oversight). One promising note from Figure 24C is conveniently low time per measurement. For VCO_2 measurements in the 500-675 ppm threshold range, errors of -0.8% ± 9.3% were observed from only 4.8-7 minutes of CO_2 accumulation (68% CI).

It is important to note that results reported thus far in section 4.8 are concerned fully on VCO_2 measurement, the key parameter in measurement of EE. The other key parameter of consideration in the calculation of EE via the Weir formula (see equation (6)), RQ, is more difficult to confidently assume based on this study design for measurement of exercise EE. From this information, one may reasonably conclude that the Smart Pad is 83% (68% CI) accurate for a 4.8-7.0 minute exercise measurement when an RQ value of 0.85 is assumed. Users of this technique for exercise EE assessment should take great consideration of RQ assumption given the physiological parameter's tendency to vary significantly during the course of exercise (Gorostiaga et al., 1989; Issekutz & Rodahl, 1961).

According to current scientific knowledge of exercise physiology, RQ depends more highly on both exercise intensity (Issekutz & Rodahl, 1961) and the length of time for which the subject has been exercising (Gorostiaga et al., 1989) than it does fasting state. As such, results for exercise VCO_2 are shown within 4.8 instead of EE since RQ can vary significantly during the course of the first five minutes of moderate intensity exercise (typically within the range of 0.7 to 1.0) a well-studied phenomenon which

occurs in both men and women within a wide range of exercise intensities (Issekutz & Rodahl, 1961). Since RQ is known to vary significantly during this time, and, since the majority of exercise EE assessments in the present study lasted approximately 5 minutes in length, an RQ 0.85 was assumed (median value from references described above). The 500-900 range data was excluded for exercise EE assessment only (it is presented for VCO_2 in the above text and Figure 24) since it lasted longer than 5 minutes, under which condition RQ should be expected to increase above 0.9 for continuous exercise (Gorostiaga et al., 1989). Under this RQ assumption, across all 5 lower concentration ranges spanning from 500-600 to 500-700, and specifically for EE measurement of a biking subject, the analytical accuracy and precision of the Smart Pad were (-) 6.2±10.7% (SD).

Sample fitting of exercise EE data:

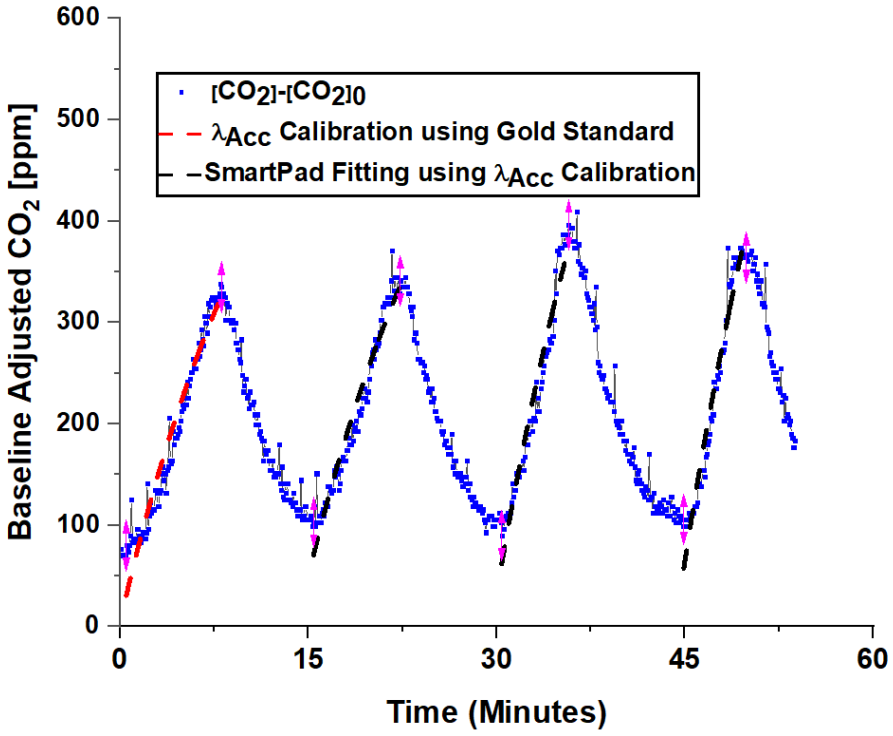

Figure 25. CO_2 Fitting for Exercise EE using Reference Method Calibration.

Table 7: Results for Exercise VCO_2 Assessment (from Figure 25)

Fitting #	**VCO_2 Smart Pad [ml/min]**	**VCO_2 Reference Method [ml/min]**	**Error 100%**
#1	787.4	728.1	8.5
#2	1090	952.8	14.4
#3	1208.8	1158.5	4.4

4.9 Results: Effect of REE on Accuracy for Optimized CO_2 Measurement Range

Specifically for the target application of this medical device, to aid in weight management for individual's whose BMI is outside of a healthy range via accurate metabolic diagnostics, it is critical to have the capability of accurate measurement across a wide range of BMIs and EE values. To study this effect, 5 subjects with a relatively

wide range of BMIs were assessed using the Smart Pad for a minimum of 5 parallel measurements each. Subject #1 performed a total of N=32 measurements as part of the sub-study detailed in 4.7. As such, the full dataset of assessments for 4.5 contained N=52 data points relating BMI with Smart Pad analytical accuracy. All assessments were performed at the CO_2 threshold range of 500-650 ppm to control for the effect of CO_2 threshold range. Figure 26A-C below illustrates results of 4.5:

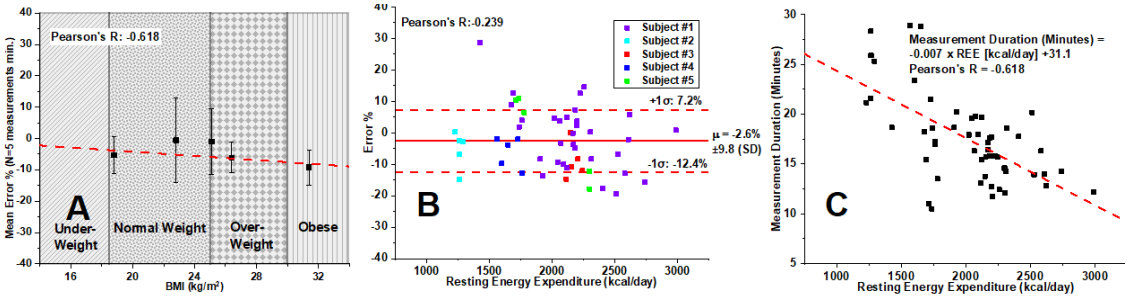

Figure 26. Effect of BMI on Smart Pad REE Measurement Accuracy and Duration. (A) Mean accuracy of the Smart Pad for measurement of REE categorically grouped based on BMI and ranging from just above the underweight cutoff (18.8 kg/m^2) to obese (31.4 kg/m^2); (B) Accuracy of the Smart Pad for measurement of REE; (C) Effect of REE on measurement duration.

Figure 26 shows a consistent effect of BMI on Smart Pad system measurement accuracy, however, despite this, all mean biases across all 5 subjects were within ±10% of the analytically accepted REE value for measurement. Even with the Pearson's R = -0.618, the slope was determined to be statistically insignificant (P=0.267) suggesting that the Smart Pad is accurate over a wide range of BMI values. Figure 26 confirms the low mean bias between the MGC Ultima CPX™ and the Smart Pad in accuracy for EE measurement across all N=52 measurements performed on the N=5 subjects (μ= -2.6%).

The figure also suggests that there is little correlation between REE and Smart Pad accuracy (Pearson's R:-0.239) and a significance test on the slope suggests "here is no statistically significant effect of subject REE on Smart Pad accuracy (P=0.088). Figure 26C shows the relationship between EE and the Smart Pad's time per measurement while the CO_2 threshold range is held constant at 500-650 ppm. There is a somewhat consistent (Pearson's R = -0.618) trend between decreasing time per measurement with increased EE. This is an intuitive result based on the design of the system, as, while holding upper CO_2 level constant, elevated CO_2 generation rates will reach the upper CO_2 level more quickly than would a reduced CO_2 generation rate. In general, from regressions shown in Figure 26A and B, we conclude that neither subject BMI (P=0.267) nor subject REE (P=0.088) have statistically significant effects on Smart Pad accuracy when using a reference method to calibrate for λ_{Acc}.

Measurement technique precision was not equal among subjects (±13.5% for subject 5 versus ±4.9% for subject 4), which, may potentially suggest a particular methodological error in the study with regards to the reference method instrument usage. Subject 4, who saw the highest level of precision for their 5 measurements (SD=±4.9%), had been previously trained to administer tests using the reference instrument, and, by their own estimate, had administered 50+ EE assessments previously using the MGC Ultima CPX^{TM}. On the other hand, Subject 5, whose assessments were characterized by a much greater variance in Smart Pad accuracy (SD=±13.5%) had never used the reference instrument previously and was somewhat unfamiliar with its operation. As such, the authors reason inconsistency in observed Smart Pad accuracy may be a result of small leaks in the reference instrument's wearable facial accessory, resulting in less apparent

precision within the REE measurement result. Three measurements from subject #2 were replaced with averages from 3 other measurements on the same subject due to an obvious error with the gold standard method (but with the Smart Pad still operating as intended). The author reason this is a logical approach, given the sample size of other recorded measurements (N=3) and low variance in other measurements (<3% Coefficient of variability). Within this study section, no datapoints were removed, with the exception of several runs that were not analyzed due to clear MGC Ultima CPX^{TM} errors (i.e. errors on device display interrupting data collection).

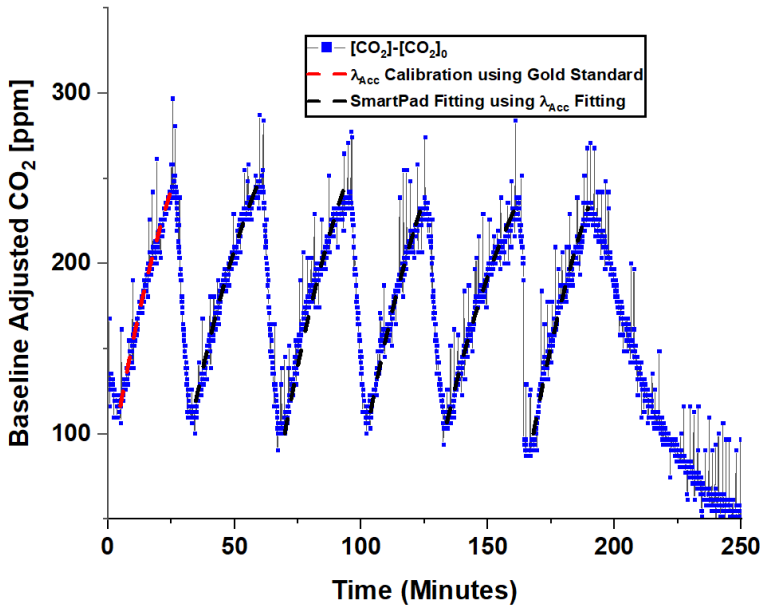

Figure 27: CO_2 Accumulation for Subject #2 using Reference Method Calibration

Table 8: Results for Subject #2 REE Assessment (from Figure 27)

Fitting # (Shown in Figure 27)	REE Smart Pad [kcal/day]	REE Reference Method [kcal/day]	Error (%	R^2 of Fitting
#1	1178	1264	-6.8%	0.969
#2	1255	1291	-2.8%	0.924
#3	1232	1229	26.8%	0.931
#4	1075	1261 (estimated)	-14.8%	0.941
#5	1230	1261 (estimated)	-2.5%	0.934

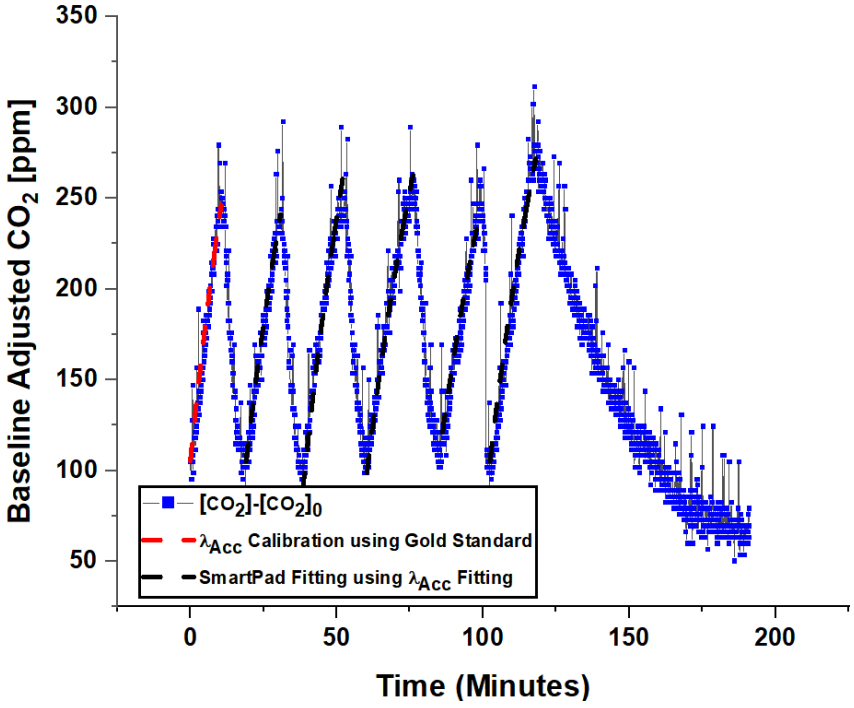

Figure 28: CO_2 Accumulation for Subject #3 using Reference Method Calibration

Table 9. Results for Subject #3 REE Assessment (from Figure 28).

Fitting # (Shown in Figure 28)	REE Smart Pad [kcal/day]	REE Reference Method [kcal/day]	Error 100%	R^2 of fitting
#1	2021	2206	-8.4%	0.947
#2	2146	2146	0.5%	0.944
#3	1921	2154	-10.8%	0.952
#4	1802	2113	-14.7%	0.940
#5	1974	2244	-12.0%	0.946

4.10 CO_2 Concentration Decay: Evaluative Study of Room Air Exchange Rate (λ)

A room's air exchange rate (λ) can be determined safely within indoor environments with estimation of subject VCO_2 during CO_2 accumulation periods (λ_{Acc}) (Batterman, 2017; Haverinen-Shaughnessy et al., 2011), or recording CO_2 decay following exit of human occupants from an environment (λ_0) (Batterman, 2017; Gall et al., 2021; Ramalho et al., 2013; Turanjanin et al., 2014). In our previous study, λ_{Acc} was determined using a medical device to provide a measurement for VCO_2 to use in equation (1) (Sprowls, Victor, Serhan, et al., 2021), and previous reports of λ_{Acc} assessed from CO_2 accumulation data (Batterman, 2017; Haverinen-Shaughnessy et al., 2011) were based on REE estimating equations (e.g.(ASTM D 6245, 2007; Mifflin et al., 1990)), widely reported to be limited in accuracy and therefore leading to propagation of standard error of regression for determination of λ_{Acc}. Here, we build upon the previous work by performing a correlative study between λ_{Acc}, using the most well respected indirect calorimeter device to provide a high accuracy value of k_{gen}, and λ_0 for CO_2 decay in the exact same environment following the subject's departure. In general, there is an

assumption that these results (i.e. λ_{Acc} and λ_0) are in agreeance. However, in this experimental set up, we observed a significant disagreeance between those parameters. Subject #1 performed N=26 measurements of sequential CO_2 accumulation and decay at the 5 threshold ranges (500-600, 500-625, 500-650, 500-675, 500-700 ppm) for a minimum of N=5 sequential measurements for each CO_2 threshold range. Figure 29A shows the results of this correlative study of λ between sequential CO_2 accumulation (λ_{Acc}) and decay (λ_0) data:

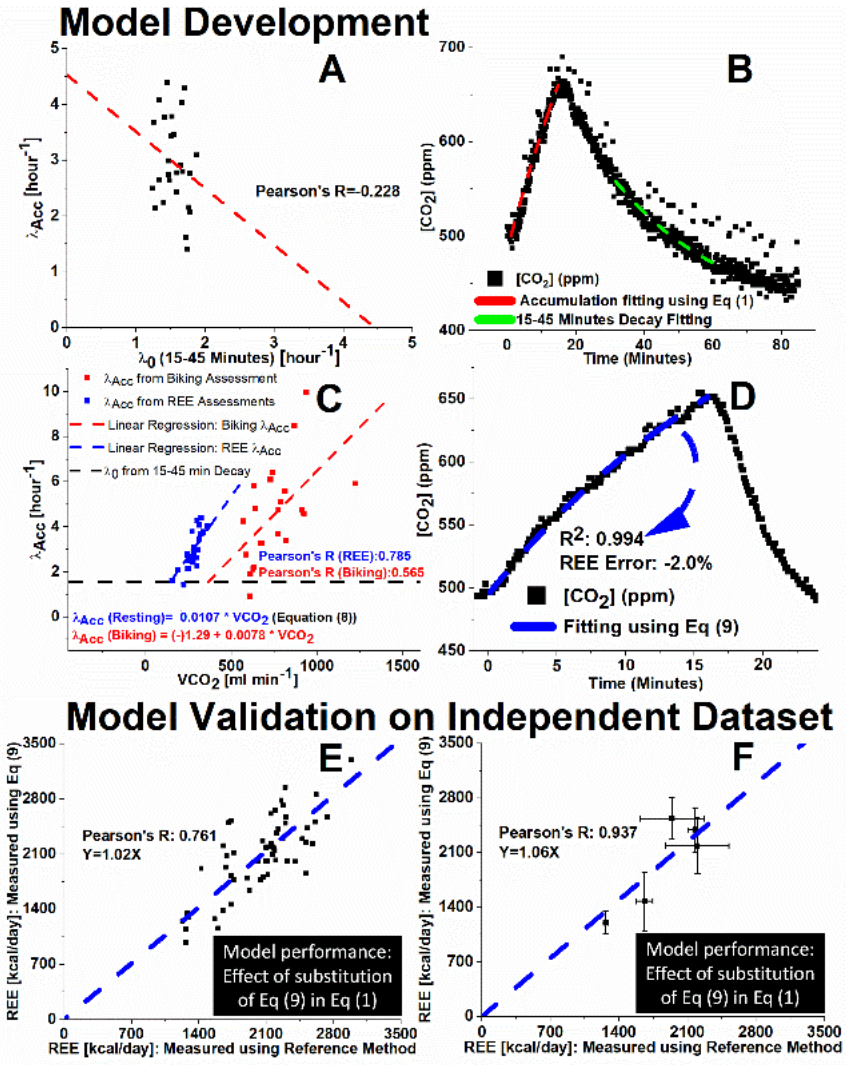

Figure 29. Results of λ_{Acc} Correlative Study and Simplified CO_2 Accumulation Model. (A) λ_{Acc} and λ_0 scatter plot showing little to no correlation (R=-0.228); (B) Correlation between VCO_2 measured from the MGC Ultima CPX™ and λ_{Acc}; (C) Sample data analysis for sequential CO_2 decay/accumulation experiments. (D) Sample data analysis using Eq (9) (E) Correlation between REE measured using Eq (9) and REE measured using MGC Ultima CPX™ for N=56 total measurements on N=5 subjects, (F) Correlation for the same dataset as (E) but presenting mean REE ± SD for each subject.

Surprisingly, Figure 29A shows little correlation (R=-0.228) between λ_{Acc} and λ_0 in the exact same measurement environment with the decay performed immediately following the accumulation period. Correlations between λ_{Acc} values were also regressed linearly with λ_0 values from 15, 30, and 45 minutes of CO_2 decay with similarly low correlation values: R=0.020, -0.138, and -0.234, respectively. In general there was relatively low variance in λ_0 assessed from CO_2 decay, with sample means of 1.9±0.2 $hour^{-1}$ (CV=11%), 1.9 ±0.2 $hour^{-1}$ (CV=11%), and 1.8 ± 0.2 $hour^{-1}$ (CV=11%) for 15, 30, and 45 minutes of CO_2 decay respectively, whereas λ_{Acc} was characterized by a much greater level of variance, with a sample mean of 3.0±0.8 $hour^{-1}$ (CV=27%) across the N=26 assessments performed in this sub study. Assuming there is no effect of the person's occupancy on λ_{Acc} (the prevailing assumption of the scientific community), this is an odd observation, however, there is fundamental science supporting the observed results (discussed below).

VCO_2 measured from the reference method correlated highly with λ_{Acc} (R=0.785, P<.00001), also a surprising observation. From the data shown (Figure 29B), in general larger VCO_2 values result in larger λ_{Acc} values. The authors suggest this is due to multicollinearity between VCO_2, k_{gen}, and λ_{Acc} where there was an unexpectedly high impact of the subject's body heat and/or breath volume and/or movement (all expected to correlate with VCO_2) on λ_{Acc}. A possible explanation is that the λ_{Acc} observed in this measurement environment is strongly influenced by aerodynamic effects of a subject's presence, leading to a rise in air exchange across openings connecting the room with adjacent spaces. Such changes may be due to increased convection associated with body movements (which results in elevated EE and therefore VCO_2), vertical stratification

(Auerswald et al., 2020; Novoselac & Srebric, 2003) due to human heat dissipation (which correlates with EE and therefore VCO_2 (Lyden et al., 2014)), and increased convection associated with respiration where VCO_2 is proportional to the produced breath volume, V_e (ml/min). These effects are maximized during biking tests where the subject's heat flux is elevated from exercise and there is additional air perturbation due to pedaling.

Since λ_0 does not adequately predict λ_{Acc} for CO_2 accumulation, it is vitally important to predict λ_{Acc} by some other method. To do so, one may solve the system of equations of Eq (1) and the regression, Eq (8), shown in Figure 29B leading to initial derivation of equation (9) (see 2.5 for equations):

Where variable meanings and dimensions are the same as for Eq (1), except for a new term, β [ppm^{-1}], which could be understood as a combined unit conversion (ml min^{-1} to ppm $hour^{-1}$) and factor from equation (8) that represents the change in λ_{Acc} resulting from a 1 unit increase in k_{gen}. The value of β is calculated from measurements of the application environment (i.e. room volume, temperature, pressure, humidity), all of which are already present in equation (1). β can be calculated from a combination of mass conservation and the regression shown in Figure 29B (equation (8)) and is shown in 2.5

Where variable and unit meaning are identical to those described in Equations (2), (3), and (4). Equation (8), key to the innovation leading to Eq (9), was derived from N=26 measurements taken as part of the 4.6 sub study. The model was evaluated on an independent dataset, N=56 measurements from N=5 subjects analyzed using equation (1) originally in section 4.5. This dataset contained no overlap in individual measurements with regards to model development dataset. The results of the application of equation (9)

to independent data are shown in Figure 29E-F. Figure 29E shows how the REE measurement from equation (9) correlates with the REE measurement from the MGC Ultima CPX^{TM}. The results show a low mean bias relative to reference instrument (Figure 29E slope=1.02 versus 1.00 for ideal measurement), however, variance (R=0.761) is notable. Taking the mean of multiple repeated REE measures (Figure 29F) increases correlation with reference method (Pearson's R=0.937), a logical consequence of standard error (Altman & Bland, 2005) and the general ability of measurement devices to mitigate imprecision using repeated measures, relevance and reasoning for the Smart Pad specifically are extensively discussed 4.11. This new model represents an important step forward from the progress made in (Sprowls, Victor, Serhan, et al., 2021) towards development of an contactless IoT device for REE measurement, given the promising application of equation (9) requires no calibration for λ_{Acc} using a VCO_2 measurement reference method.

Important note on all regressions shown in Figure 29: For Figure 29C, D, E, and F all y-intercepts were determined to be statistically insignificant (P>0.05) and Pearson's R is shown for datasets (not regression lines, which are fitted with y-intercept set as zero). Regression lines for Figure 29B, C, and D were all fitted with no y-intercept, since it was determined to be statistically insignificant and slope is shown for that regression with no y-intercept.

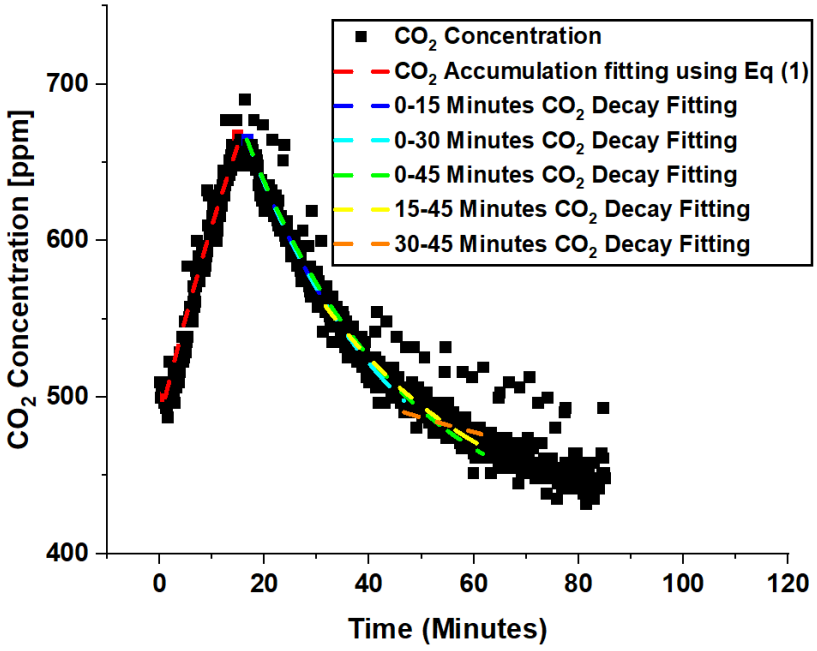

Figure 30: Sample CO_2 Accumulation/Decay Fittings for Subject #5. 5 discrete fittings performed for each of the N=26 decay experiments: 0-15, 0-30, 0-45 min and also 15-45, 30-45 min. Figure 29B shows the one with the highest Pearson's R). 30-45 min fittings showed relatively low R^2 values for many runs.

Table 10. Results for λ Evaluation from CO_2 Accumulation and Decay (for Figure 30)

Fitting (Shown in Figure 30)	λ [hour^{-1}]	R^2
CO_2 Accumulation fitting	1.41	0.953
0-15 Minutes CO_2 Decay Fitting	2.05	0.895
0-30 Minutes CO_2 Decay Fitting	2.04	0.963
0-45 Minutes CO_2 Decay Fitting	1.96	0.966
15-45 Minutes CO_2 Decay Fitting	1.74	0.870
30-45 Minutes CO_2 Decay Fitting	0.71	0.276

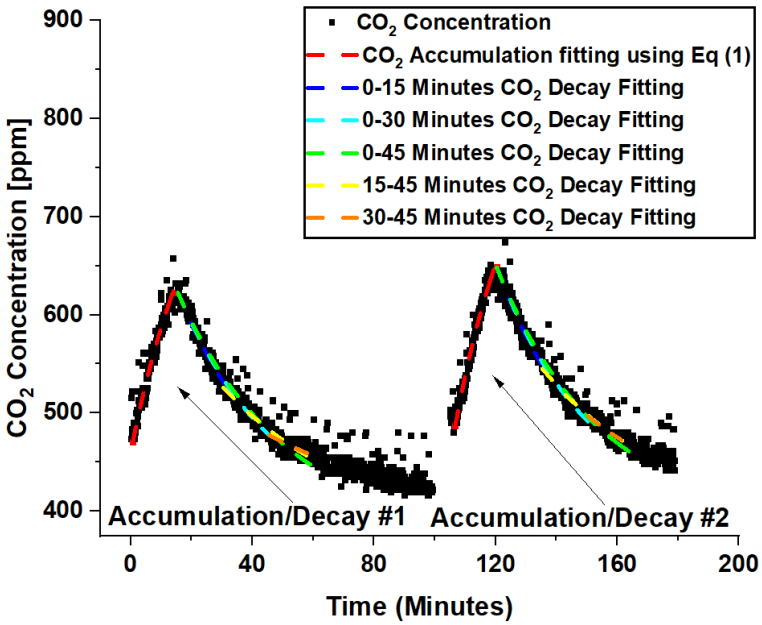

Figure 31. Sample CO_2 Accumulation/Decay Fittings for Subject #1.

Table 11. λ_{Acc} Evaluation from CO_2 Accumulation and Decay #1 (for Figure 31)

Fitting (Shown in Figure 31)	λ [hour^{-1}]	R^2
CO_2 Accumulation fitting	2.65	0.945
0-15 Minutes CO_2 Decay Fitting	1.84	0.931
0-30 Minutes CO_2 Decay Fitting	1.77	0.960
0-45 Minutes CO_2 Decay Fitting	1.69	0.960
15-45 Minutes CO_2 Decay Fitting	1.34	0.845
30-45 Minutes CO_2 Decay Fitting	0.94	0.282

Table 12. λ_{Acc} Evaluation from CO_2 Accumulation and Decay #2 (for Figure 31)

Fitting (Shown in Figure 31)	λ [hour^{-1}]	R^2
CO_2 Accumulation fitting	2.99	0.965
0-15 Minutes CO_2 Decay Fitting	1.98	0.876
0-30 Minutes CO_2 Decay Fitting	1.88	0.948
0-45 Minutes CO_2 Decay Fitting	1.80	0.960
15-45 Minutes CO_2 Decay Fitting	1.47	0.881
30-45 Minutes CO_2 Decay Fitting	1.42	0.602

Equation (9) Derivation:

Start with system of equations (1) and (8).

$$[\boldsymbol{CO_2}] = [\boldsymbol{CO_2}]_{\boldsymbol{0}} + \frac{\boldsymbol{k_{gen}}}{\boldsymbol{\lambda_{Acc}}}\left(\mathbf{1} - \boldsymbol{e}^{-\boldsymbol{\lambda_{Acc}} \boldsymbol{t}}\right) + \left([\boldsymbol{CO_2}]_{\boldsymbol{i}} - [\boldsymbol{CO_2}]_{\boldsymbol{0}}\right)\boldsymbol{e}^{-\boldsymbol{\lambda_{Acc}} \boldsymbol{t}} \quad (1)$$

$$\boldsymbol{\lambda_{CO_2\ Accumulation}} = \boldsymbol{\alpha\ x\ VCO_2} \quad (8)$$

Combine equations (2) and (3) from the to produce equation (12):

$$\boldsymbol{VCO_2} = \boldsymbol{k_{gen}} * \boldsymbol{CF_{env}} * \boldsymbol{V_{Room}} * \boldsymbol{CF_{STPD}}/\mathbf{60} \quad (12)$$

Solve equation (8) for VCO_2 and substitute into equation (12) to develop equation (13)

$$\boldsymbol{\lambda_{CO_2\ Accumulation}} = \left(\frac{\boldsymbol{\alpha}}{\mathbf{60}}\right) * \boldsymbol{CF_{Env}} * \boldsymbol{V_{Room}} * \boldsymbol{CF_{STPD}} * \boldsymbol{k_{gen}} \quad (13)$$

Then defining a new term, β, to simplify equation (13):

$$\boldsymbol{\beta} = \left(\frac{\boldsymbol{\alpha}}{\mathbf{60}}\right) * \boldsymbol{CF_{Env}} * \boldsymbol{V_{Room}} * \boldsymbol{CF_{STPD}} \quad (10)$$

This results in the simplified version of equation 13, which is equation 14:

$$\lambda_{Acc} = \beta * k_{gen} \quad (14)$$

This can simply be substituted into equation (1), resulting in equation (9):

$$[CO_2] = [CO_2]_0 + \frac{1}{\beta}\left(1 - e^{-\beta * k_{gen} * t}\right) + ([CO_2]_i - [CO_2]_0)e^{-\beta * k_{gen} * t} \quad (9)$$

Sample equation (9) fittings:

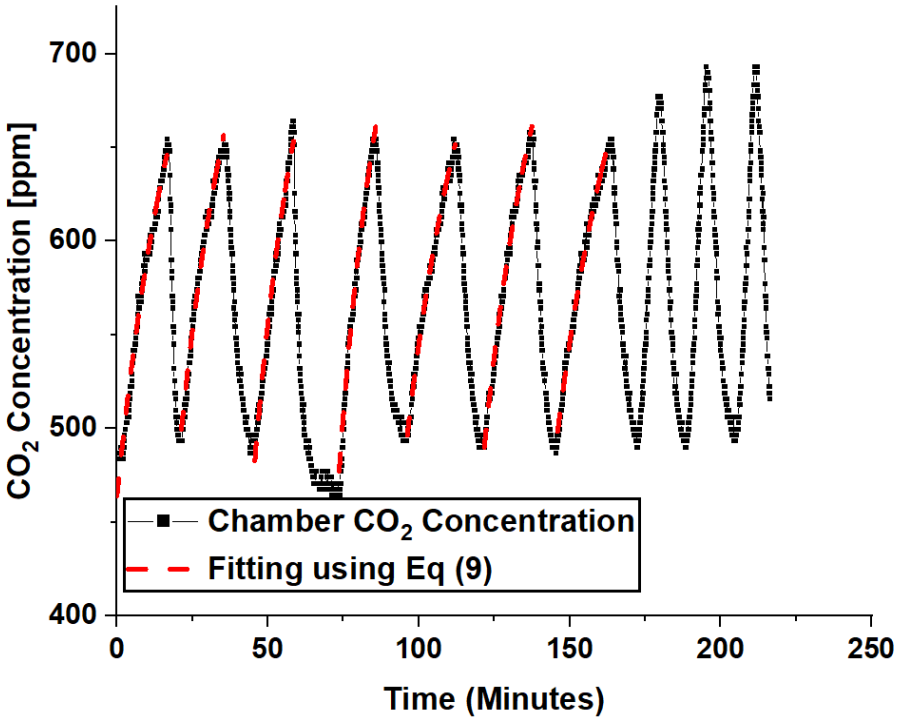

Figure 32. REE Measurements for Subject #1 using Simplified Accumulation Model. No training set data shown for either experimental run (performed on separate day). Last 2/3 CO_2 accumulation curves for each day were not analyzed using equation (9) given they are for biking assessments. Analyzed data taken from 2+ months prior to training set data collection.

Table 13. Smart Pad Accuracy for Subject #1 using Simplified Accumulation Model.

Fitting # (Shown in Figure 32)	REE Smart Pad using Eq (9) [kcal/day]	REE Reference Method[kcal/day]	Error %	R^2 of Eq (9) Model
#1	2242	2518	-11.0%	0.988
#2	2511	2609	-3.8%	0.990
#3	2856	2619	9.1%	0.986
#4	3295	2988	10.3%	0.990
#5	2144	2187	-2.0%	0.994
#6	2419	2225	8.7%	0.994
#7	2021	2199	-8.1%	0.994

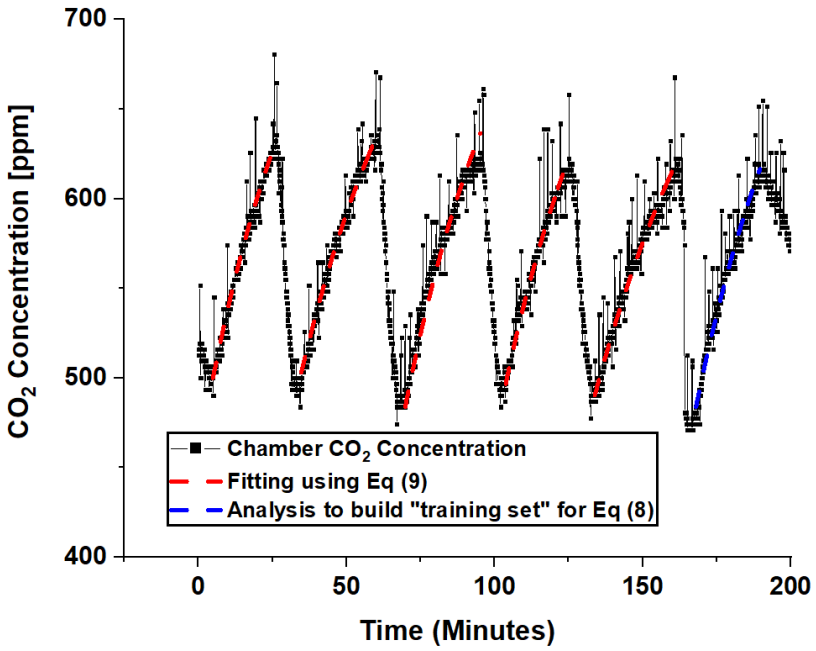

Figure 33: REE Measurements for Subject #2 using Simplified Accumulation Model. G6 not included in Figure 29E-F (model validation dataset) since it was used to build the training set from Figure 29C.

Table 14. Smart Pad Accuracy for Subject #2 using Simplified Accumulation Model.

Fitting # (Shown in Figure 33)	REE Smart Pad using Eq (9) [kcal/day]	REE Reference Method [kcal/day]	Error %	R^2 of Eq (9) Model
#1	1346	1261	5.1%	0.961
#2	1145	1264	-9.4%	0.968
#3	1292	1291	0.0%	0.926
#4	1245	1229	1.3%	0.931
#5	975	1261	-22.7%	0.938

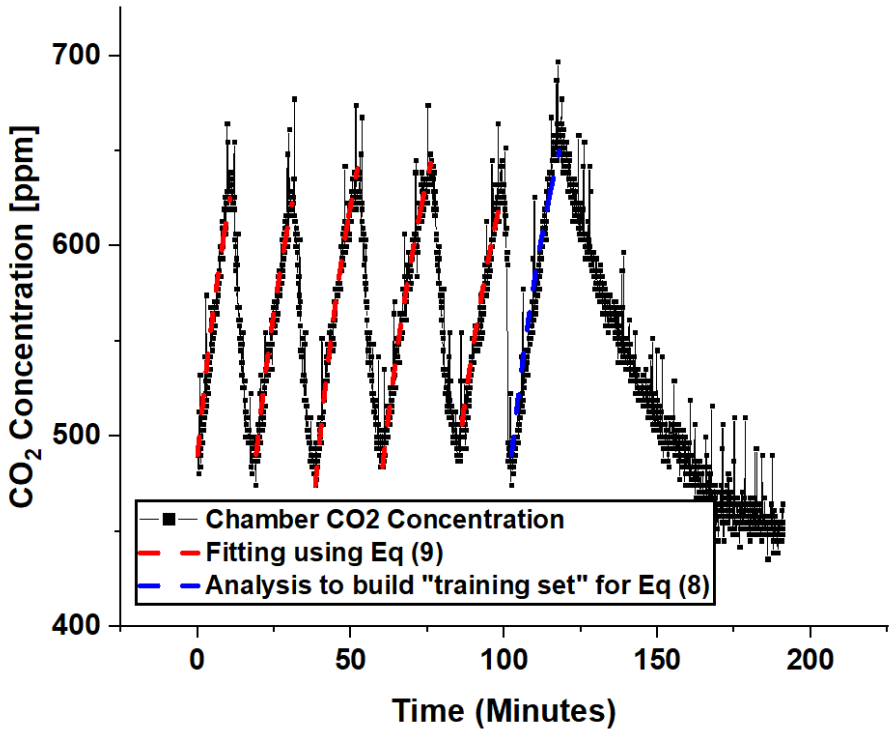

Figure 34: REE Measurements for Subject #3 using Simplified Accumulation Model. G6 not included in Figure 29E-F (model validation dataset) since it was used to build the training set from Figure 29C.

Table 15. Smart Pad Accuracy for Subject #3 using Simplified Accumulation Model.

Fitting # (Shown in Figure 34)	REE Smart Pad using Eq (9) [kcal/day]	REE Reference Method [kcal/day]	Error %	R^2 of Eq (9) Model
#1	2717	2277	19.3%	0.929
#2	2371	2206	7.5%	0.942
#3	2612	2146	21.7%	0.958
#4	2238	2154	3.9%	0.956
#5	2017	2113	-4.6%	0.933

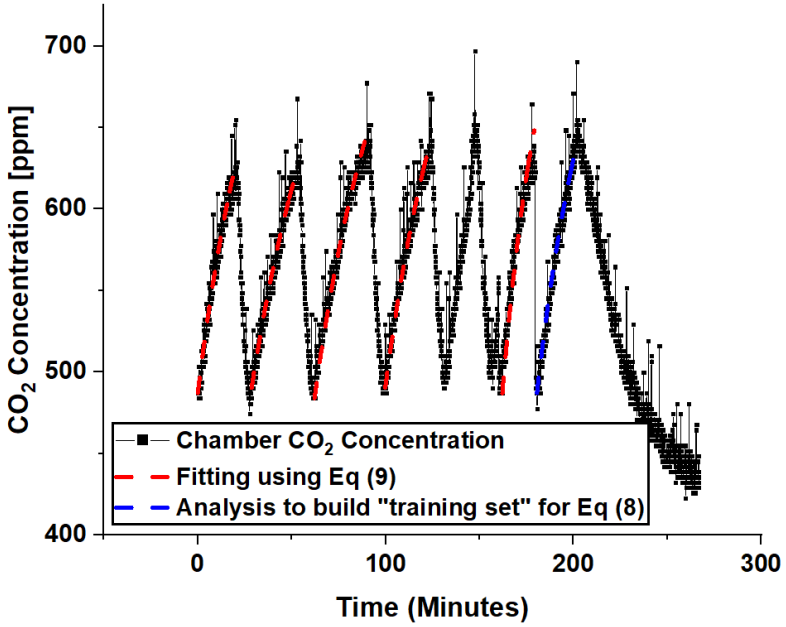

Figure 35: REE Measurements for Subject #4 using Simplified Accumulation Model. 5th CO_2 accumulation not analyzed due to gold standard method operating system error. G6 not included in Figure 29E-F (model validation dataset) since it was used to build the training set from Figure 29C.

Table 16. Smart Pad Accuracy for Subject #4 using Simplified Accumulation Model.

Fitting # (Shown in Figure 35)	REE Smart Pad using Eq (9) [kcal/day]	REE Reference Method [kcal/day]	Error %	R^2 of Eq (9) Model
#1	1462	1735	-15.6%	0.946
#2	1155	1600	-27.8%	0.949
#3	1275	1563	-18.4%	0.941
#4	1377	1650	-16.6%	0.932
#5	2117	1760	20.3%	0.904

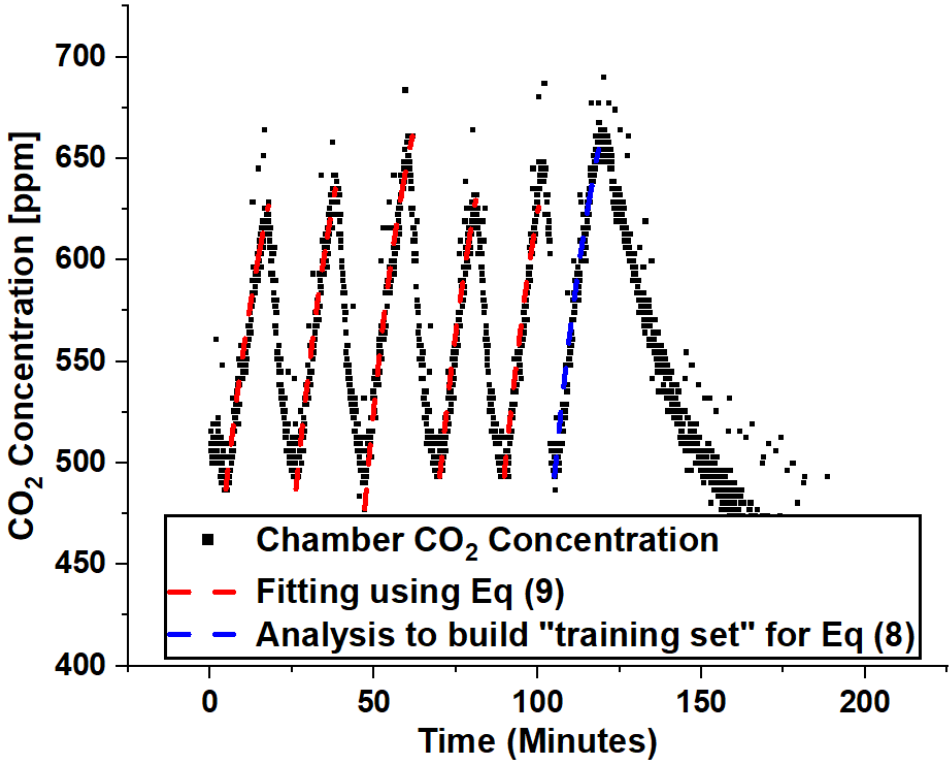

Figure 36: REE Measurements for Subject #5 using Simplified Accumulation Model. G6 not included in Figure 29E-F (model validation dataset) since it was used to build the training set from Figure 29C.

Table 17. Smart Pad Accuracy for Subject #5 using Simplified Accumulation Model.

Fitting # (Shown in Figure 36)	REE Smart Pad using Eq (9) [kcal/day]	REE Reference Method [kcal/day]	Error %	R^2 of Eq (9) Model
#1	2206	1659	33.0%	0.942
#2	2494	2301	8.4%	0.952
#3	2946	2298	28.3%	0.936
#4	2499	1713	45.9%	0.937
#5	2529	1735	45.7%	0.940

4.11 Discussion: Compensation for Imprecision using Repeated Measures

It is well known that repeated measurements can increase statistical confidence in a final result, even in the scenario where a measurement instrument is relatively imprecise. In fact, this is a major motivator and distinction between standard deviation and standard error (Altman & Bland, 2005). Standard error of a particular measurement is correlated with the inverse square root of the number of measurements. Assuming the same level of accuracy as was observed during this study (a large assumption, only posed to offer the reader the "vision" of the Smart Pad), a user of the device would potentially see a substantial increase in the confidence of their final average REE measure via repeated assessment (which could be relatively easy, given the Smart Pad performs contactless measurements). This could be in the form of multiple monthly visits to a weight loss clinic, or, could potentially be in the form of 10 separate occupancy sessions (e.g. times that the subject has occupied the given environment for a minimum of 14-19 minutes) of a home study, bedroom, bathroom, vehicle cabin (Deng et al., 2020), or office space (e.g. inside a business/institution). For the Smart Pad measurement technique

based on equation (9), the realized accuracy across the N=56 measurements were 2.2±16.7% (68% CI).

Here, accuracy is defined as the maximum error expected for a given confidence interval based on experimental findings for the Smart Pad, as follows:

$$Accuracy\ \% = \ 100\% - (|Mean\ Error\ \%| + standard\ Error) \qquad (15)$$

Table 18. Implications of Standard Error with Regards to Equation (9)

Number of Repeated Measurements	Smart Pad Accuracy for Equation (9) (68% CI)
1	81.1%
3	88.2%
5	90.3%
10	92.5%

This extrapolation based on generally accepted consequences of standard error was further analyzed to account for the effect of total measurement time across multiple measurements. Here, the extrapolated results are for the 500-650 ppm CO_2 threshold range (where the 2.2±16.7% (68% CI) error was observed for the equation (9) model) was used, for which contactless REE measures were recorded in 14-19 minutes. For that reason, a mean measurement duration of 16.5 minutes was modelled below in Figure 37:

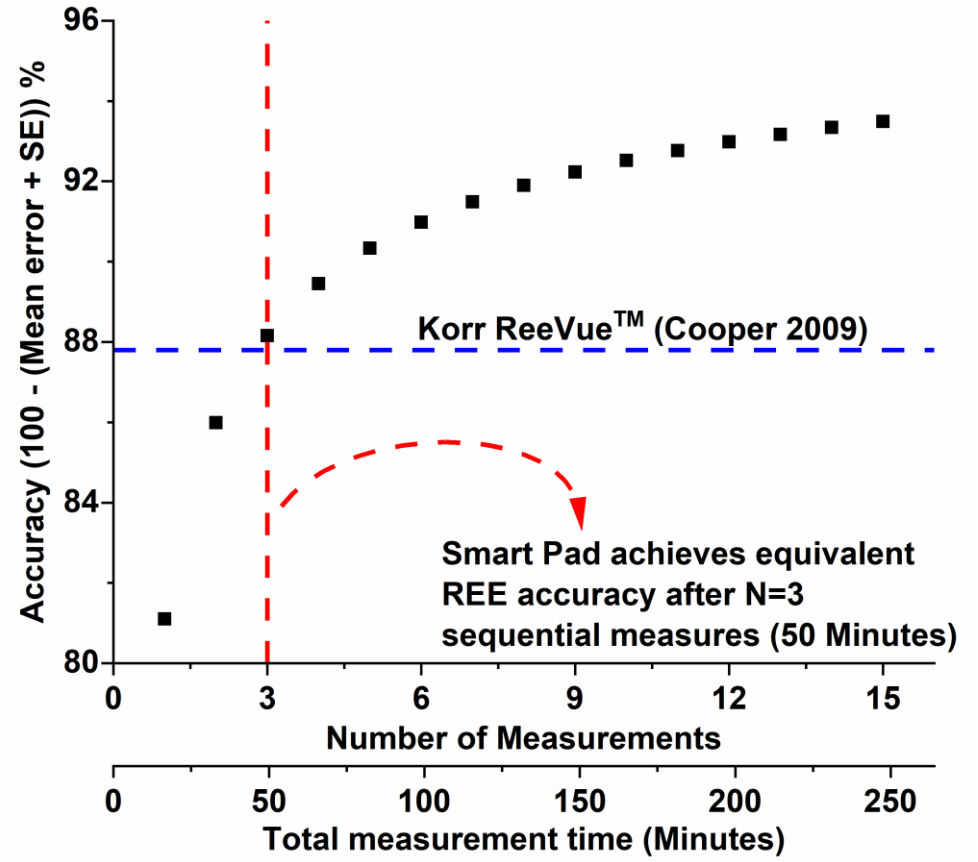

Figure 37. Smart Pad Accuracy using Eq (9) and Extrapolating from Standard Error.

4.12 Conclusions

A new contactless IoT device is evaluated, the Smart Pad, which displayed promising accuracy characteristics for contactless resting energy expenditure (REE) and exercise CO_2 production rate (VCO_2) measurements in a medium size room after calibrating for air exchange rate with a VCO_2 measurement gold standard method once. The Smart Pad is capable of performing accurate REE measurements in 14-19 minutes and exercise VCO_2 measurements in 5-7 minutes after calibrating with the gold standard once. In this configuration, measurement characteristics were comparable to multiple wearable (i.e. with facial accessories) FDA 510(k) cleared devices as reported by another

study and FDA sourced 510(k) submissions from several device manufacturers (see Table 19). Additionally, by performing the first ever study of sequential CO_2 accumulation and decay air exchange rates using a high accuracy VCO_2 measurement device, disagreement between air exchange for CO_2 accumulation and decay was observed in the same measurement environment. This led to development of a new model for REE assessment from ambient CO_2, which does not require air exchange rate calibration using a gold standard method or CO_2 decay rate. The model shows good agreeance for REE assessment (Y=1.02X, R=0.761) when evaluated on a dataset independent from the one used to develop the model. Limitations of the study include errors in reference method VCO_2 measurements due to potential differences in fitting of the wearable facial accessory, a lack of air exchange assessed from subjects with low VCO_2, and control of subject exercise intensity during biking EE assessments. Future work will focus on validation of equation (9) in a new environment and development of a contactless VO_2 max test.

CHAPTER 5

5 SMART PAD: VALIDATION IN AMBULATORY ENVIRONMENT AND DEVELOPMENT OF A CONTACTLESS EXERCISE TEST

5.1 Abstract

A new testing environment for the Smart Pad was developed and a subject was evaluated to study the effect of an ambulatory (enclosed by a curtain, as in many hospital rooms) measurement environment on accuracy. The testing environment is unique given it is not surrounded by rigid walls of a room, rather, the testing area is enclosed by a flexible curtain. Additionally, this is the largest environment tested as part of this thesis work, having a measured volume of approximately 18.8 m^3. The area was enclosed and only one simple modification was made to the area's inbuilt HVAC system with the inlet vent being sealed with a vinyl fabric. One outlet fan, connected to the Smart Pad's actuator system, was installed in line with the curtain. In preliminary testing of the environment, the Smart Pad's equation (1) resulted in errors of -3.1% for REE and 10.6% for exercise VCO_2. The environment's λ_0 value was determined to be ~5.5 hours ^{1}, approximately 3X larger than the private office evaluated as part of Chapter 4, suggesting that even in environments with significant leakage and significantly larger than the typical private office, the Smart Pad's measurement principle is still accurate. Additionally, a contactless exercise test based on thermodynamic efficiency (CTET) was evaluated before final modifications were made to further seal the testing environment, showing similar characteristics to reference data upon visual analysis. This set up resulted in high unoccupied air exchange (12.0 $Hours^{-1}$), yet, visually similar data to the reference

method, showing the technique captures a strong metabolic signal even in an ambulatory, semi-sealed environment.

5.2 Methodology

A room was developed for testing the Smart Pad at Arizona State University's Health Futures center building in Phoenix Arizona. The room was built using a long curtain and Velcro^{TM} with adhesive backing inside of a larger lab space of approximately 3-5X the volume of the curtained area (18.8m^3). Several experiments were performed at various stages of the curtained area's construction and preliminary results suggested that the entire curtained area should be sealed to ensure adequately low unoccupied air exchange, λ_0. A photo of the ambulatory area prior to sealing the top air gap is shown below in Figure 38 :

Figure 38. 4th Smart Pad Operating Environment During Construction. Exercise bike, cot, and reference instrument all visible. Inlet fan (can be seen attached to ceiling) was totally sealed for all ambient VCO_2 assessments. Photo taken from outside the ambulatory area through a window visible from the hallway.

As part of the testing environment development process, preliminary data was collected for a newly funded study to develop a contactless physical fitness test. The test evaluates the thermodynamic efficiency of a human by evaluating the ratio of work output to total energy expenditure over the course of the CTET evaluation. The protocol for the preliminary data is shown below in Figure 39:

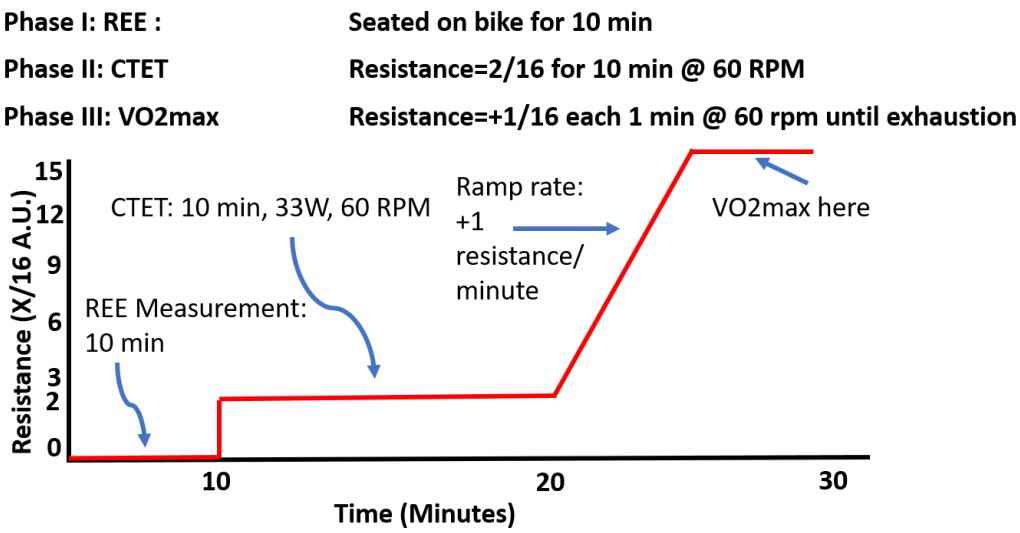

Figure 39. Test Protocol for Contactless Physical Fitness Assessment. "CTET" simply stands for contactless thermodynamic efficiency test. Resistance refers to the braking resistance of electromagnetically braked exercise bike (Nautilus NB2000^{TM}).

Phase I of the test protocol serves to acclimate the subject to the instrument and record a 5 minute measurement of resting energy expenditure (REE) which is common practice for indirect calorimeter measurement in a clinical setting (Horner et al., 2001). This practice eliminates unusually high respiratory quotient values in some subjects and generally provides the most consistent results. After 10 minutes, the subject bikes at a fixed low intensity for 10 minutes at a fixed work capacity (33W for this test), which can be achieved by monitoring pedalling speed (RPM) and keeping bike resistance constant across all subjects, providing a constant mechanical workload across all subjects. This practice can be used to provide a measure of thermodynamic efficiency (Jabbour & Majed, 2019), termed "CTET" (contactless thermodynamic efficiency test) for this project. Pedal velocity is also kept constant at 60 rpm to control for the effect of pedalling velocity/acceleration on air currents within the measurement environment. The CTET

score can be defined as follows, and is referred to net mechanical efficiency in some other works (Jabbour & Majed, 2019):

$$CTET\ (\%) = \frac{Power\ output\ \ (kcal)}{Energy\ expenditure\ (kcal) - REE(kcal)} \tag{16}$$

In equation (16) above, CTET refers to "contactless thermodynamic efficiency test", with the general physical meaning of thermodynamic efficiency of the human body, considering energy expenditures over resting (i.e. accounting for the fact that REE produces no measurable work external to the body). After 10 minutes of biking during the CTET, a standard biking $VO_{2,\ Max}$ test (Fleg & Lakatta, 1988; Storer et al., 1990) is performed. This simply consists of ramping resistance by a fixed interval (for example, 1/16 as shown in Figure 39) after fixed intervals of time (for example, 1 min as in Figure 39) until the test subject can no longer increase the electromagnetic braking force successfully while maintaining 60 RPM of biking cadence. Data is recorded simultaneously using the Smart Pad and MGC Ultima CPX™ and an in house developed python algorithm was used to calculate overlapping 30 second VO_2 averages from the MGC Ultima CPX™, the maximum of which is generally accepted to be the person's maximal oxygen consumption $VO_{2,\ max}$ (Fleg & Lakatta, 1988; Storer et al., 1990). The $VO_{2,\ max}$ assessment is generally accepted as the gold standard for cardiovascular physical fitness assessment and the future goal of this line of research is to find a correlation between the low intensity CTET test and the $VO_{2,\ max}$ test using the protocol described in Figure 39.

After preliminary biking data was collected, a decision was made to seal the top of the curtained area as well to increase sensitivity of the REE measurement by

decreasing λ_{Acc}. To do so, a metal collar was secured around a piece of plastic vinyl blocking the curtained area's inlet vent after the air supply duct was disconnected (i.e. isolating the environment from the building's HVAC system). Following this modification, the room's layout and appearance from outside the curtained area shown below in Figure 40:

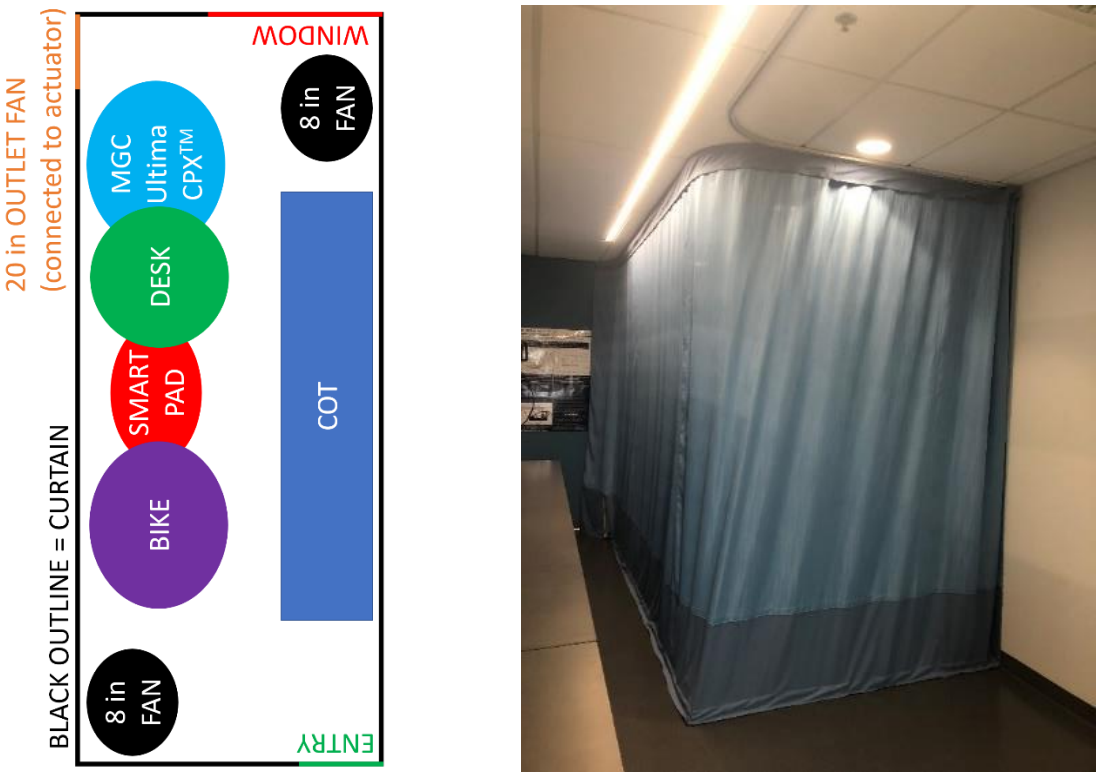

Figure 40. Layout of Measurement Environment at Health Futures Center. Left: diagram of curtained area. Right: Photograph taken from the curtain's exterior. The right side of the curtain was used as an entry and sealed with Velcro™ during experiments (including CO_2 decay data collection).

A photo from inside the curtained area is shown below in Figure 41:

Figure 41. View from within Health Futures Center Ambulatory Testing Environment.

For pilot data collected in this environment, 2 sequential CO_2 accumulation datasets were collected for both contactless REE and biking VCO_2 measurements, following the same reference instrument λ_{Acc} calibration procedure as described in Chapters 3 and 4.

5.3 Results

Pilot results of initial testing of the protocol shown in Figure 39 and the environment photographed in Figure 40 is shown below:

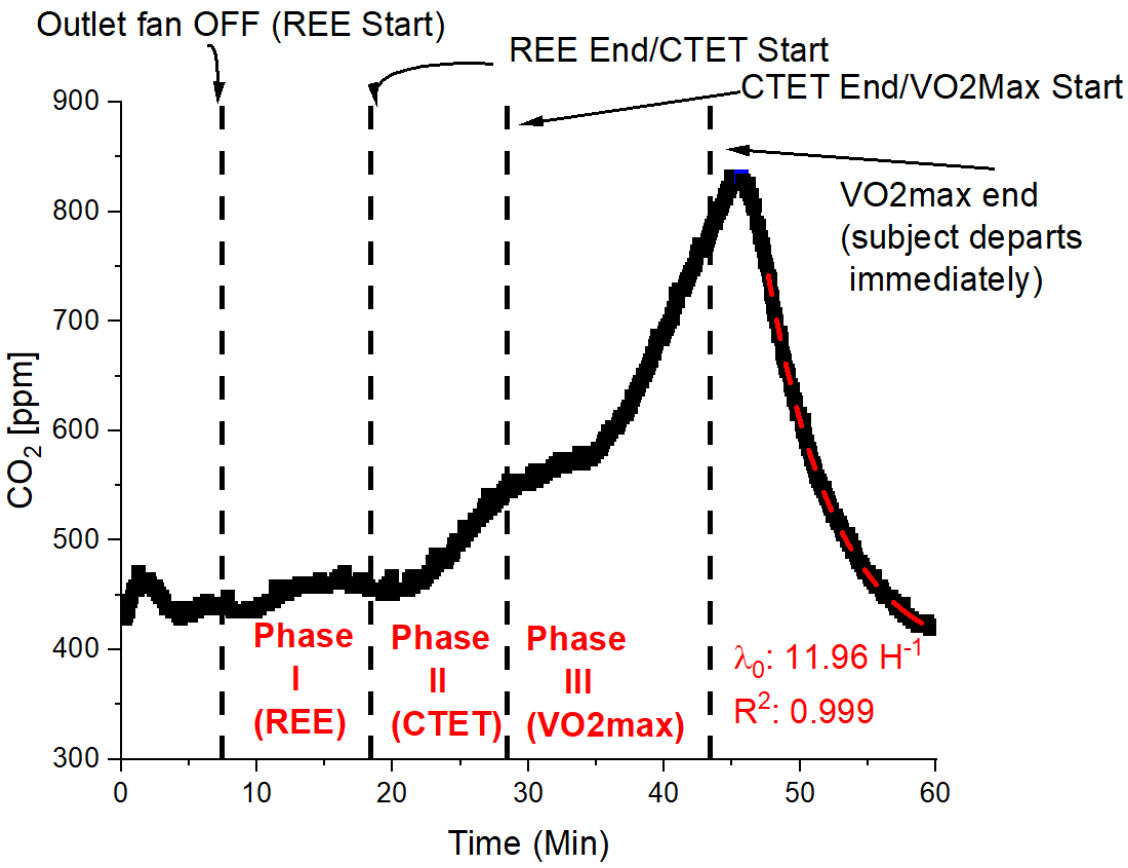

Figure 42. Pilot Data for Smart Pad CTET Test at Health Futures Center. Drop lines added to indicate start/end times for each phase and were determined by recording local time at the start/end of each event. A such, there is likely a slight time delay between event (i.e. start of CTET test) and CO_2 sensor signal due to mass transport effects.

Clearly differing shape in curves can be observed for each phase, showing clear metabolic difference in activity even with high air exchange (11.96 Hours^{-1} is approximately six times the decay λ_0 observed in Chapter 4). Phase I shows a slight increase in CO_2 concentration due to the subject's resting energy expenditure. The air exchange is too high in this set up to achieve a usable resting VCO_2 signal in this environment (one motivation for the modifications made to seal air gaps near the top of the curtained area). There is a clear signal for the CTET test as well as the $VO_{2,\,max}$ data

suggesting that even this high air exchange environment could be used to assess human CO_2 production from contactless CO_2 concentration modelling. There was very little noise in the CO_2 data and no data filtering was performed. The corresponding data from the reference instrument for parallel measurement and presenting VCO_2 (analysed in Python using in house developed code) is shown below in Figure 43. There are clear differences in both plots, however, one might imagine that the VO_2 signal shown below (expected to correlate highly with VCO_2 via the respiratory quotient, RQ, (Weir, 1949)) would follow closely the first derivative of k_{gen} (which changes due to increasing physical workload during the exercise test) in equation (1). To address this, Python code was developed to measure transient VCO_2 (which results in a changing k_{gen}), using 30 second averages from Smart Pad data (not reported in this work, code still under development).

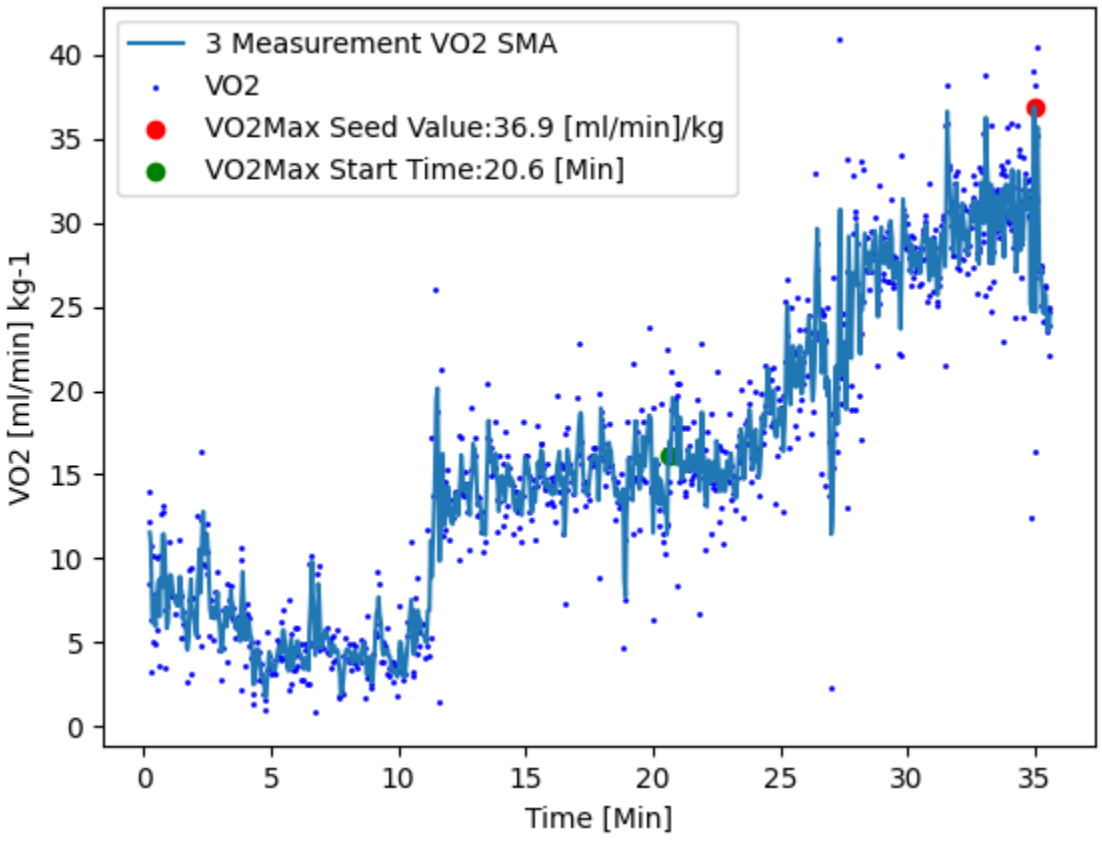

Figure 43. MGC CPX Ultima^{TM} $VO_{2,\,max}$ Test Data for CTET Pilot Testing. 3 measurement smoothed moving average (SMA) is the 3-point rolling moving average of raw VO_2 meatuses, a practice used to better visualize raw gas exchange data which is often noisy.

For the code developed for Figure 43, 30 second averages of VO_2 near the relative maximum seed value (shown as red datapoint above) are analysed and the maximum of which is taken as the true $VO_{2,max}$ of the subject. The result of 30 second averaging can be visualized below in Figure 44. For this test, the subject's $VO_{2,max}$ was 31.0 ml min^{-1} kg^{-1}. Results for a $VO_{2,\,max}$ test are typically reported in weight adjusted (kg^{-1}) units to control for the effect of subject body mass (Fleg & Lakatta, 1988; Storer et al., 1990).

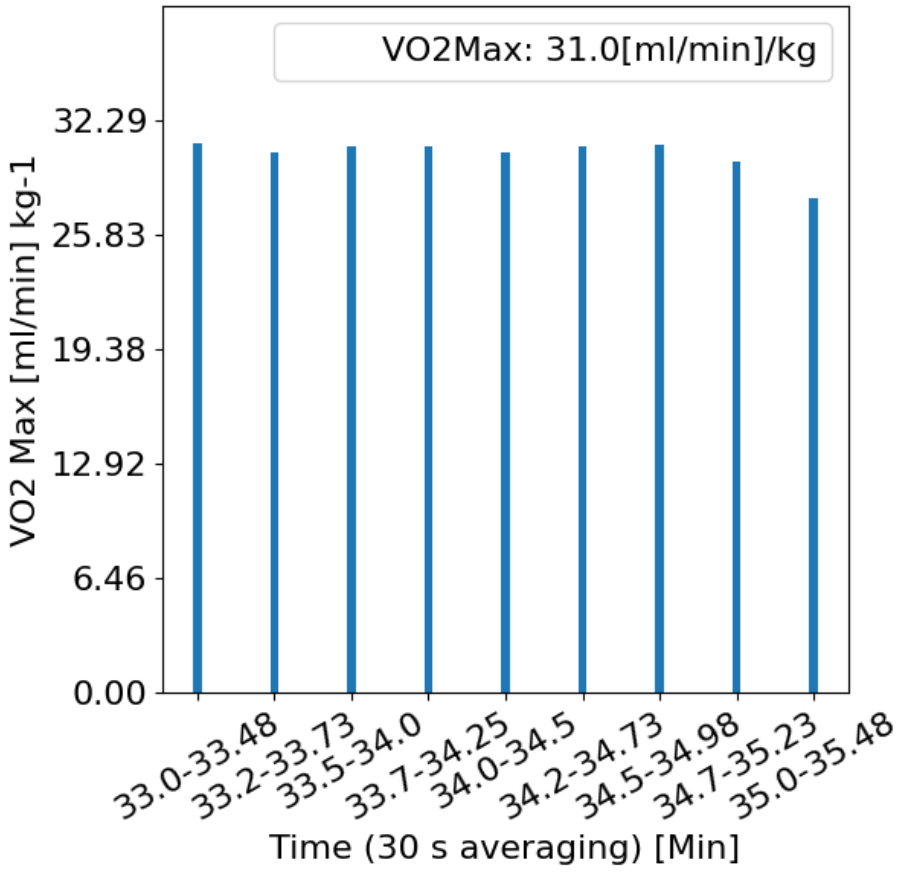

Figure 44. Automated $VO_{2,\,max}$ Analysis Results from Developed Python Code. The maximum $VO_{2,\,max}$ result from the 30 second overlapping averaging window is reported as the subject's true $VO_{2,\,max}$.

The python algorithm developed has clear advantages of current techniques used to analyse $VO_{2,\,max}$ data from a breath gas analyser like the MGC Ultima CPX™, which is to, by hand, find the largest 30 second average interval for VO_2 data. Considering that tedious and error prone process, the python code described above provides the most accurate 30 second averaging interval, since it can provide all possible 30 second averages that would take a human much effort to calculate by hand, and can be ran with little to no technician input unlike current techniques for analysing $VO_{2,\,max}$ data. The $VO_{2,\,max}$ python program also has preset functions for automated CTET analysis for this project using reference instrument data (developed in house). The results of one pilot CTET test and analysis using the automated python code are shown below:

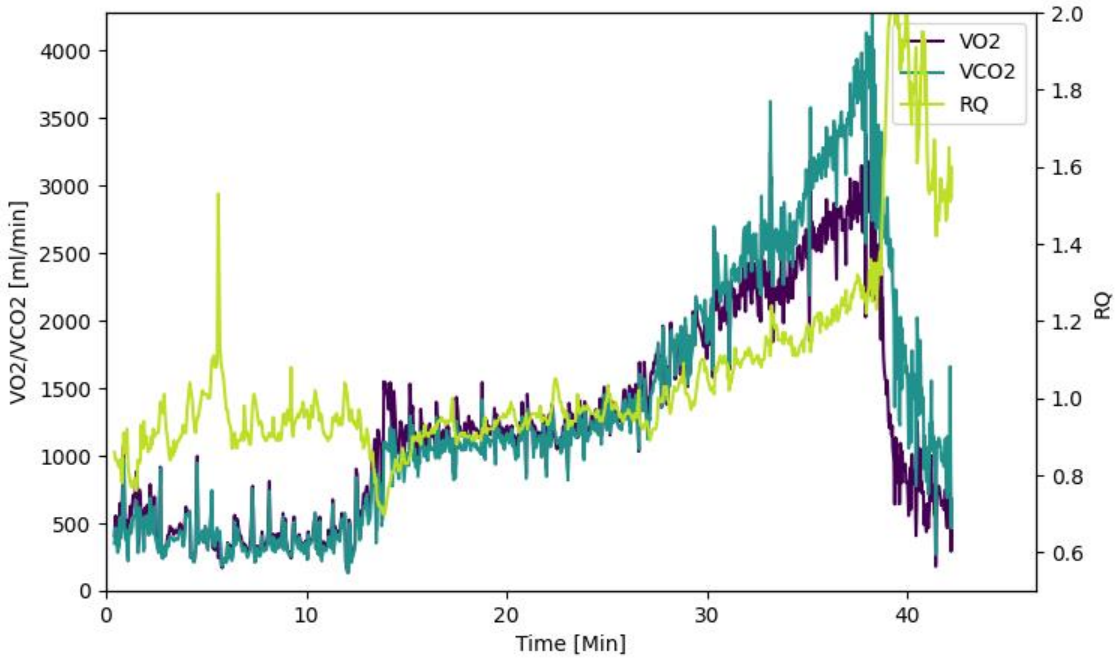

Figure 45. Raw Data from MGC Ultima CPX™ for CTET. Protocol for CTET test described in Figure 39.

In Figure 45 above, the 3 distinct phases of the CTET test can be observed. The average REE from Phase I is subtracted from the known workload of the subject on a fixed electromagnetically braked exercise bike. The bike's workload is simply calculated by the manufacturer, Nautilus, whose device calculated power output through the bike's crankshaft from the bike's RPM and known electromagnetic braking resistance forces. The RPM was kept constant at 60 rpm and was validated to 0.0% error using a video recording technique with triplicate measures, showing perfect agreeance to counting rotations per minute by visually (by pausing video each rotation). The results for the preliminary CTET test are shown below in Figure 46.

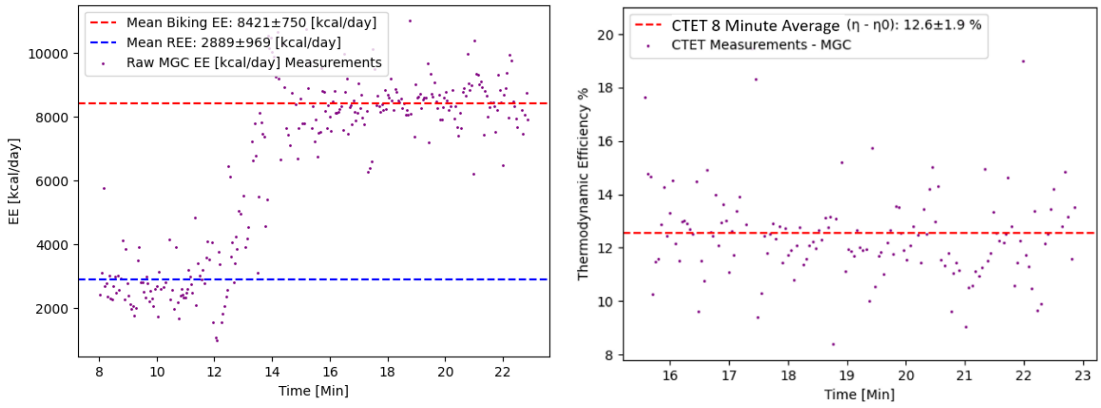

Figure 46. Results of Preliminary CTET Measurement. Left: Raw energy expenditure (EE) measurements from the MGC Ultima CPX™. Blue line shows average for REE. Red line shows average for biking EE. Right: CTET score derived from MGC Ultima CPX™. Red line shows average of derived CTET measures over 8 minutes.

In comparison with literature values for net mechanical efficiency for the subject's BMI group (Jabbour & Majed, 2019), CTET values from the MGC Ultima CPX^{TM} are in agreeance with expected results. For the test shown, the CTET score was 12.6%±1.9, meaning 12.6% of the energy consumed (above REE) during biking was actually transferred to mechanical work. The CTET test is also being developed for the Smart Pad, but, further research is needed within this project to understand the best way to predict RQ, shown in equations 5-6, a key term relating VO_2 (which the Smart Pad does not measure) to VCO_2 (which the Smart Pad does measure) and energy expenditure. RQ is relatively easy to predict for REE measurements where it typically can assumed as 0.85 for calorically balanced (in terms of energy intake in comparison with energy expenditure) subjects fasted for several hours (Marra et al., 2004; Matarese, 1997). The first 5 minutes of the REE assessment and first 2.5 minutes of the CTET assessment are ignored as the subject's body takes some time to achieve equilibrium with the reference instrument or once they start biking, which typically increases EE until steady state is achieved.

From preliminary testing in the ambulatory environment, it was clear modifications were necessary to the room, as described and shown in Figure 40 and Figure 41. The primary modification was sealing the top air gap of the curtain. Preliminary results following this change in environment are shown below for the Smart Pad system:

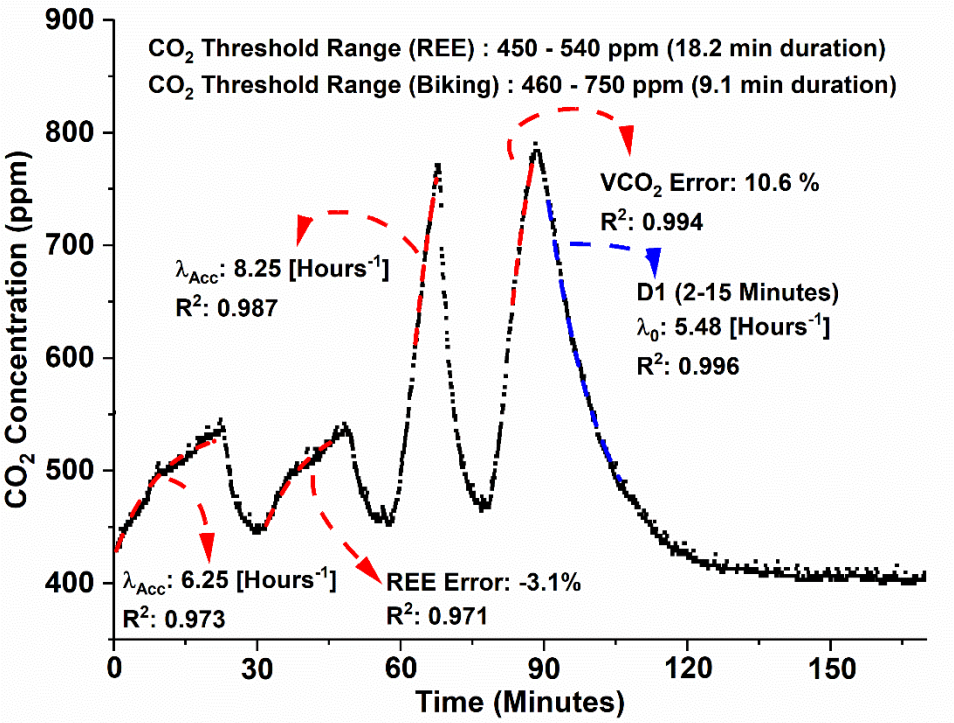

Figure 47. Preliminary Smart Pad Performance at Health Futures Center. Red dashed lines show fitting with equation (1) and blue lines show fitting with equation (7).

From Figure 47 it may be observed that the Smart Pad's measurements were accurate in high air exchange, given the observed λ_0 of ~5.5 Hours^{-1} which is approximately 3 times the air exchange observed in the environment from Chapter 4. Beyond that, good accuracy was maintained in the large environment, given the ambulatory area is 4/3 the size of the environment from Chapter 4 and 2 times the size of environment from Chapter 3. In these two ways, combined with the fact that the environment was filled with many different objects (Cot, metabolic cart, table, test subject, 2 mixing fans, and an exercise bike) and also that the curtain fabric itself is very flexible, the curtained area could certainly be considered non-ideal. Despite the many challenges posed by this environment, the ±10% accuracy of the device, comparative to

several FDA cleared devices (Cooper et al., 2009; FDA, 2003, 2006) considered respectable indirect calorimeters, was maintained during pilot testing. The results shown in Figure 47 are analyzed using the λ_{Acc} reference instrument calibration procedure utilized throughout Chapter 3 and 4. For contactless REE measurement, the Smart Pad was observed to have an accuracy of -3.1%. For contactless biking VCO_2 measurement, the accuracy was observed to be 10.6%. In Figure 47 above, contactless exercise VCO_2 data is only analyzed as the second half of the CO_2 accumulation curve. This is done to avoid errors due to a well-established human tendency to produce a large variance in respiratory quotient (RQ) during the first few minutes of exercise (Gorostiaga et al., 1989; Issekutz & Rodahl, 1961). For REE assessment the same measurement time was preserved as within Chapter 4 (14-19 minutes) and a slightly larger timeframe of biking VCO_2 data was collected the analyze the effect of performing ½ CO_2 accumulation curve fittings, as shown in Figure 47 where the second ½ of CO_2 accumulation data was fitted successfully with low error.

It is also interesting to note that covering the top (approximately 1/10- $1/15^{th}$ of the height of the full curtain) of the curtained area decreased the air exchange (λ_0) by a factor of 2, from ~12.0 $Hours^{-1}$ in Figure 42 to ~5.5 $Hours^{-1}$ in Figure 47. These λ_0 values are significantly higher than in the typical administrative office (Cheong & Chong, 2001), which typically are within the range of 1.5 to 4 $Hours^{-1}$. It is reasoned this substantially increased air exchange is due to the construction of the curtained area as a "semi-enclosed" environment given it truly is part of a larger room 3-5X the volume of the curtained area alone, making this curtained enclosure the perfect area for characterization of the Smart Pad's performance in an environment that is on the limits of non-ideality

that might be encountered in practice. Additionally, the findings of Figure 47 suggest the Smart Pad system is effective at contactless REE/VCO_2 assessment while maintaining good air quality using only 1 outlet fan (no inlet fan or vent). The authors suggest this works as the curtained area (as any room) is nearly impossible to fully seal and the air displacement of one fan is sufficient for the purpose of exchanging high CO_2 air to the surrounding, resulting in displacement of low CO_2 concentration air into the curtained enclosure from the surroundings. This finding also makes sense with regards to other measurements, as the air pressure has been observed not to increase by any significant margin during ventilation on periods of subject tests in Chapter 3 or during any CO_2 accumulation period by more than a few mbar (the Smart Pad measures barometric pressure and it's values are often observed to be unchanging throughout all phases of contactless REE measurement including when the actuator system is on).

These findings suggests the revised equations (especially with regards to CF_{Env}, which corrects for non-ideality in equation (1)) presented in Chapter 3 are conclusively accurate for contactless VCO_2 measurement, given they were validated in Chapter 3's longitudinal study (N=10+ parallel measures), Chapter 4 (N=52+ parallel measures), and now in the findings of Chapter 5 (N=2 pilot testing). To clarify, no training set data was collected with regards to equations 1-7 since the completion of the 20 subject Mayo Clinic study and therefore it is reasonable to conclude the technique is definitively accurate for REE measurement. See Table 19 for more details on comparison with current FDA 510(k) medical devices from past 25 years used as indirect calorimeters.

5.4 Conclusions

The Smart Pad's contactless VCO_2 measures was tested in an ambulatory enclosure to validate design controls as to the most challenging environment for device application. The testing area was a large, high air exchange, object-filled, environment connected to a larger room and enclosed with a flexible curtain. The system only used one outlet fan. Preliminary results only using previously established equations show validated ±10% accuracy, comparable to in respectable, FDA 510(k) cleared indirect calorimeters commonly used in clinical practice suggesting the Smart Pad system as part of this study is accurate even in the non-ideal environments, such as an ambulatory enclosure. A contactless exercise test was developed, and experimental results show similar curvature to reference instrument measure in a very high air exchange environment (12.0 $Hours^{-1}$), however, additional system development is needed to accurately capture subject's with non-constant energy expenditure, as is typical during a graded exercise test where intensity is increased over time.

CHAPTER 6

6 VEHICLES: A USEFUL ENVIRONMENT FOR METABOLIC ASSESSMENT

6.1-Abstract

This work investigated the effects of air recirculation mode and vehicle speed on transient CO_2 accumulation profiles within a mid-size sedan. CO_2 concentration profiles were measured during driving at five different speeds in the range 0 – 70 MPH. Air exchange rate (λ_{Acc} [$hours^{-1}$]) was assessed for several vehicle speeds, and was observed to have the following relationship: $\lambda_{Acc} = 0.060*(speed) – 0.88$ when driving faster than 17 MPH. The driver's energy expenditure was estimated as *EE* = 1620±140 kcal/day, by determining CO_2 generation rates from 16 CO_2 accumulation curves, which compares well with reference measurements for the same subject by conventional indirect calorimetry, *EE* =1550±150 kcal/day, from the average of 10 measurements. CO_2 concentration profiles were simulated to predict effects of vehicle speed, air exchange rate, presence of multiple occupants within the vehicle and driver's energy expenditure, providing broader insights on the factors affecting transient CO_2 accumulation within vehicle cabins.

6.2 Methodology

During the test, the sensing system was placed on top of the front passenger seat, approximately one meter from the driver. Real-time CO_2 concentration, temperature, and humidity were recorded with a resolution of 1 s^{-1}. All tests were conducted at times of low traffic for consistent driving speed and to avoid introducing CO_2 by air exchange with the outside environment, since CO_2 effluent from surrounding vehicle exhaust could

enter the vehicle cabin as car exhaust is a form of highly concentrated CO_2 (relative to regular atmospheric levels). Additionally, it is reasonable to postulate exhaust streams are at a higher pressure than the internal car cabin pressure (due to engine heat, among other factors) and are high in CO_2 concentration since they are fuel effluent which would serve as a source of error for observed CO_2 accumulation patterns if it were not controlled by driving at low traffic times.

A picture of the vehicle model used in the study is shown in Figure 48a. Figure 48b shows the AC dashboard, including 4 fan speed levels and an independent control to select between RC or air exchange mode.

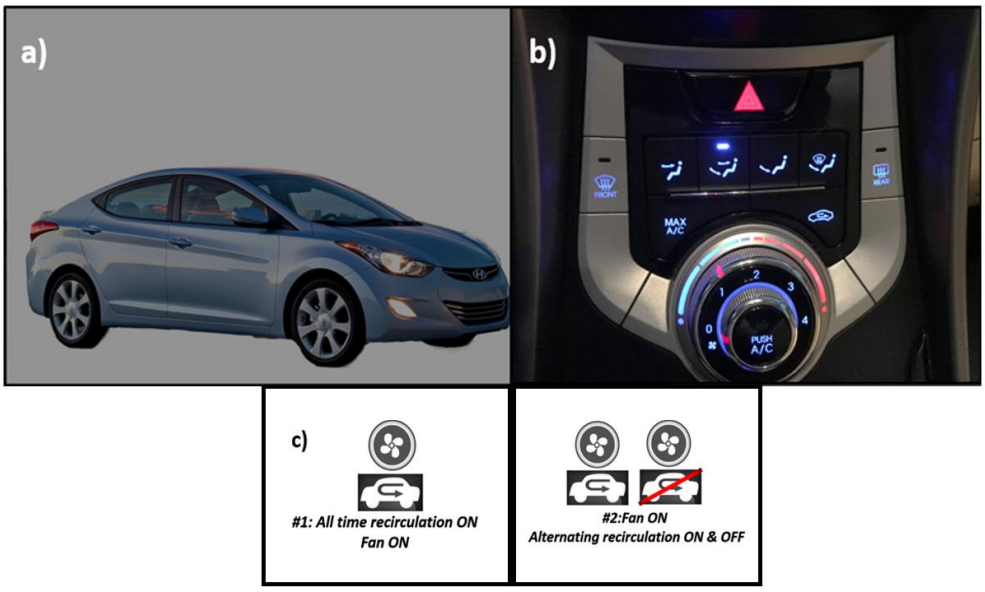

Figure 48. Vehicle Used and Study Design. a) Vehicle used in this study; b) AC control panel; c) Two different testing conditions, see text for detail.

Two different ventilation conditions were evaluated, as described in Figure 48c and enumerated in more detail below:

Ventilation Condition #1: All-time RC (recirculation) mode was on and the fan was kept at level 1 during the tests. Five different driving speeds were tested under this condition: 0 MPH (miles per hour), 15-17 MPH, 33-35 MPH, 48-50 MPH and 68-70 MPH. To achieve different level of speed, the tests were conducted on residential roads (Broadway and Rural road in Tempe, AZ) and highway (AZ Loop 101, Loop 202 and Interstate 10 in Arizona) accordingly. The speed log of each test was recorded with the RunKeeper® app (ASICS Digital, Boston, MA). The test was stopped once the cabin CO_2 concentration reached 2000 ppm or if the test had lasted 0.8 h. These tests were performed 3 times at each speed. One growth curve is provided at each speed as an example. This experimental condition was used to assess the air exchange rate, λ_{Acc} [$Hours^{-1}$], for the vehicle at various speeds. It was determined experimentally that there is a linear relationship between the velocity of the vehicle and the apparent air exchange rate as analyzed from CO_2 vs. time data.

Ventilation Condition #2: Fan level 1 with air conditioning mode alternating between RC mode on and off, depending on the CO_2 level within the cabin. The RC mode was initially on and was turned off for five minutes once the cabin CO_2 concentration reached around 1000-1100 ppm, to allow for air exchange with the external environment and reduction of CO_2 levels within the vehicle cabin. Under this condition, four different driving speeds were tested: 0 MPH, 15-17 MPH, 33-35 MPH and 65-68 MPH. The roads taken for this set of tests were the same as condition #1. Each test was performed within a single 1 hour span, The RC mode was switched on/off 4 times total within the hour for each speed tested. This rendered 4 separate accumulation curves and

therefore 4 separate metabolic rate measurements. These replicate measurements are the source of the error bars, presenting standard deviation, shown in Figure 52.

6.3 Results

Results from ventilation condition #1 are shown below:

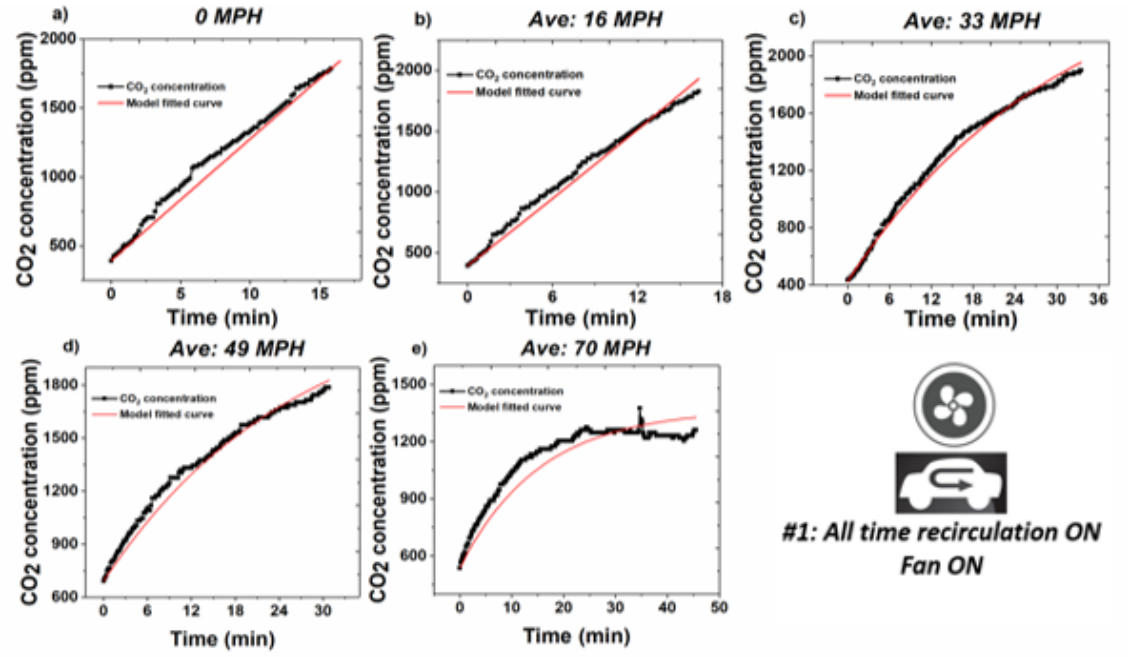

Figure 49. CO_2 Accumulation Data from Recirculation Mode Across 0-70 MPH.

The data from Figure 49 were analyzed using equation (1) with a reference k_{gen} value generated from the Korr ReeVue^{TM}'s REE value. The resulting λ_{Acc} versus vehicle speed dataset was used to build the following regression, shown below in Figure 50 and used as the training set for Figure 51.

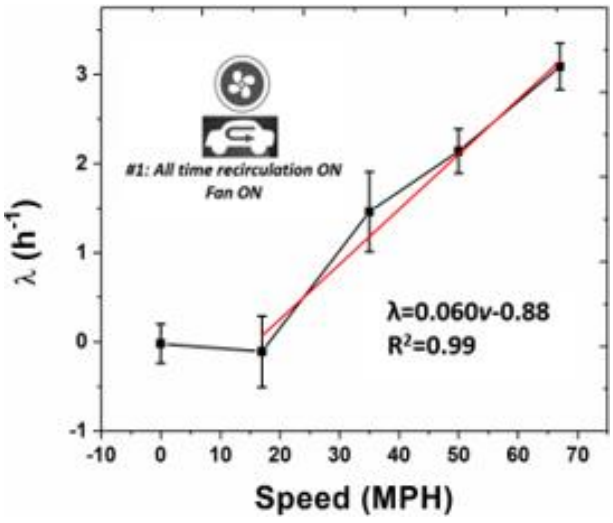

Figure 50. Relationship Between Effective Air Exchange Rate (λ) and Driving Speed. Red line indicates linear regression curve above 17 MPH.

Real-time CO_2 profiles are shown in Figure 51. The model was applied for a λ_{Acc} of 0.05 hours^{-1}, which is a non-null but negligible value for speeds lower than 18 MPH. The assessment of this condition was based on the experimental observation that at parked and at low speeds air exchange rate between the vehicle cabin and the environment was negligible. For speeds greater than 18 MPH, the λ_{Acc} was calculated from the regression equation shown in Figure 50 and used in equation (1) to determine the k_{gen} for each CO_2 growth period test cycle obtained during the periods of 36-48 minutes driving at a certain speed.

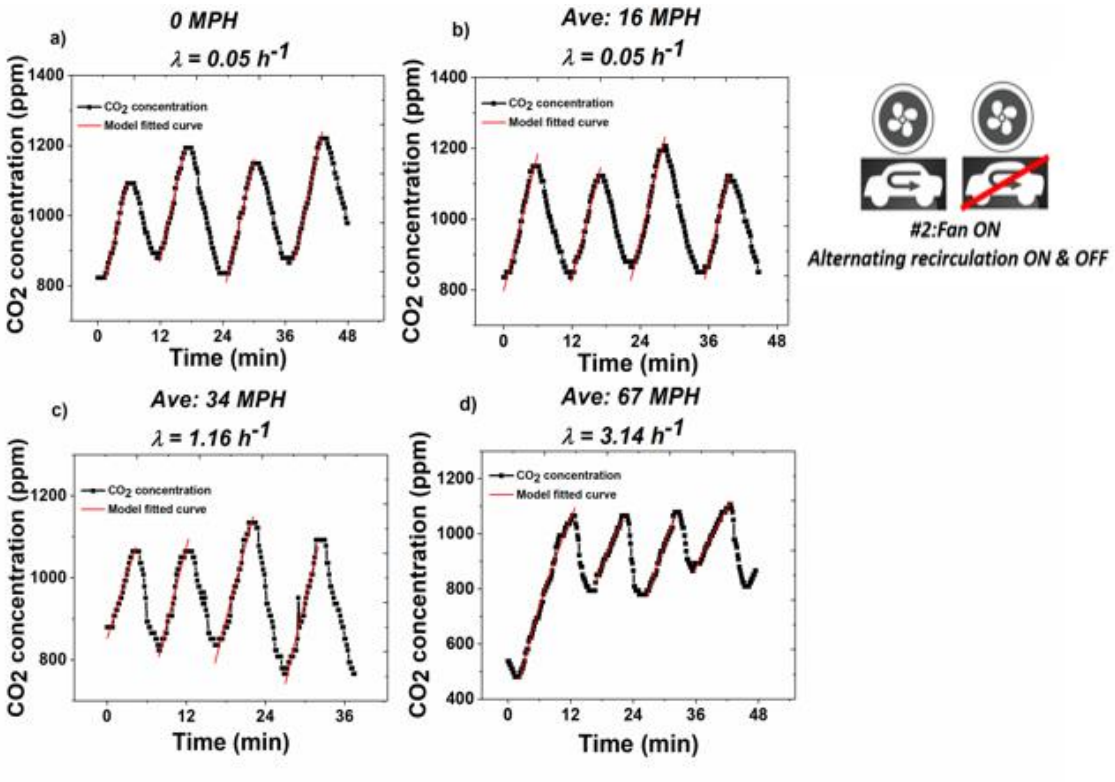

Figure 51. Real Time Data from Contactless REE Measurements from in a Vehicle a) 0 MPH; b) 16 MPH; c) 37 MPH; d) 64 MPH.

Energy expenditure measured during driving tests were compared with those determined with conventional instrumentation. The subject's energy expenditure while sitting in a computer and working was measured by indirect calorimetry using 2 different instruments: the desktop Korr ReeVue™ (www.korr.com, Salt Lake City, UT) and the Breezing Pro™ (https://breezing.com/, Tempe, AZ) , obtaining an average of (1550±150) kcal/day for 10 measurements utilizing both indirect calorimetry instruments (5 readings each). This represents only ~4% difference in comparison with the Smart Pad's calculated EE value. It should be noted that the participant did not perform any intense activity on the days of tests, since strenuous exercise increase a person's instantaneous energy expenditure (McArdle, 2010). The results demonstrated that this model could be

used to determine EE of drivers, as the difference between mean values determined with each method was lower than the relative error for each of them. However, it is of course important to note that the subject did not perform the reference instrument EE assessments simultaneously while driving, due to safety concerns regarding vehicle operation.

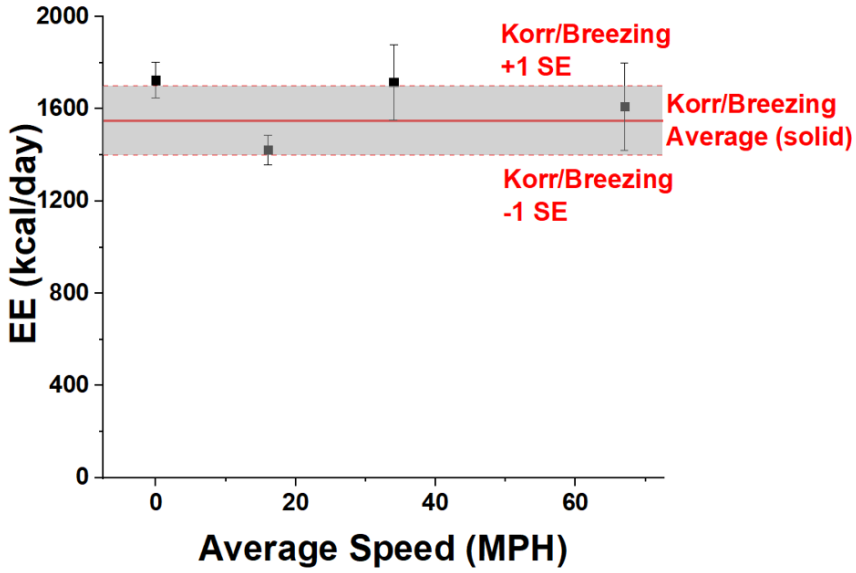

Figure 52: Contactless REE Measurement Accuracy within a Moving Vehicle. Energy Expenditure (EE) estimates generated from experimental data shown in Fig 15 (shown as black points with error bars) and corresponding reference instrument (Korr ReeVue™ and Breezing Pro™) measurements shown as horizontal redline (average) ±1 standard error (taken from repeat measurements)

6.3 Simulation of CO_2 Accumulation Patterns Within a Vehicle Cabin

The simulation presented in this work has been developed to extend the experimental findings introduced in this work's assessment to several other conditions that could not be tested. The model estimated the car cabin volume to be 3.1 m^3, a

baseline CO_2 concentration of 400 ppm, a λ_{Acc} of 1 $hours^{-1}$ (unless indicated otherwise), a linear relationship between λ_{Acc} and vehicle speed (validated by experimental findings presented in Figure 52), a linear relationship between CO_2 generation and the number of occupants within the vehicles, and an occupant energy expenditure EE = 1700 kcal/day (unless indicated otherwise).

To expand upon the experimental results shown in the previous sections of this work, a computational simulation was developed using MATLAB® to generate model CO_2 growth profiles under various conditions that were not investigated experimentally in this study. Figure 53 simulates CO_2 concentration growth profiles inside a car cabin (RC mode on) with different number of occupants under various speeds. A horizontal line has been drawn at both 1000 and 2500 ppm with a label to indicate the corresponding time at which a vehicle with a single occupant reaches the aforementioned CO_2 concentration, used as a reference from recent cognitive performance studies (Allen et al., 2016; Norbäck et al., 2013; Satish et al., 2012; Zhang et al., 2015). The simulation predicts that CO_2 levels within the car cabin reaches 1000 ppm for a single occupant in less than 15 minutes with RC mode on. CO_2 accumulation is significantly higher for car cabins where there is more than 1 occupant; this is clearly evidenced in the simulation's output where CO_2 levels exceeding 2500 ppm are reached in under 15 minutes when the vehicle is occupied with at least 3 occupants, regardless of vehicle speed.

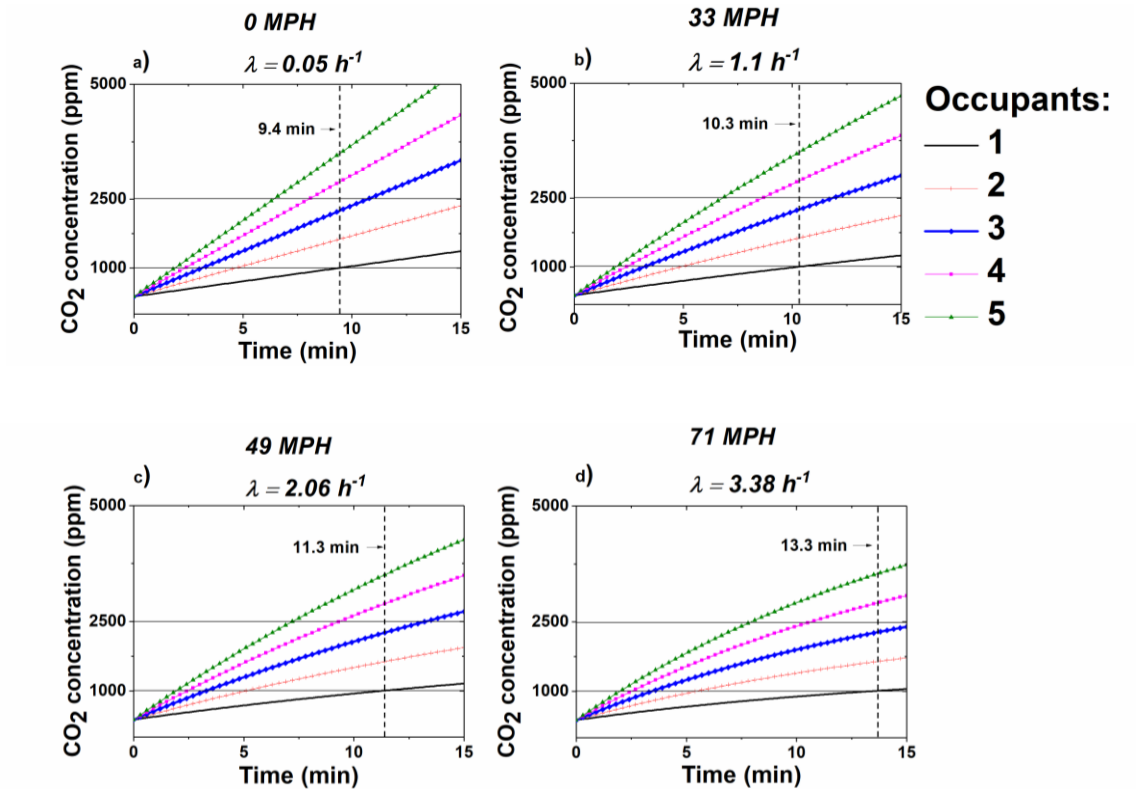

Figure 53. CO_2 Concentration Profiles for Various Occupants/Driving Speeds. a) 0 MPH; b) 33 MPH; c) 49 MPH; d) 71 MPH.

Figure 53 shows how a CO_2 profile can be affected by changing the effective air exchange rate from 1 to a higher value, up to 22 hours^{-1}, e.g. by alternating the RC mode on and off, and/or opening windows. The effect of different fan levels (with corresponding λ_{Acc} values extrapolated from experimental data) were simulated using the aforementioned model. To keep the CO_2 concentration below a desired level, it is necessary to increase λ_{Acc}. At higher fan levels the CO_2 concentration decreases faster to safer levels.

Figure 54b demonstrates the effect of occupant metabolic rate on CO_2 accumulation within a vehicle. This parameter has a substantial influence on the CO_2

concentration growth profile. A driver with a relatively high EE of 2500 kcal/day will reach a CO_2 concentration of 1000 ppm in just 6.8 minutes, as compared with virtually twice as long (13.7 min) for a driver spending only 1300 kcal/day. The high-EE driver can reach a CO_2 concentration of 2500 ppm in less than half an hour.

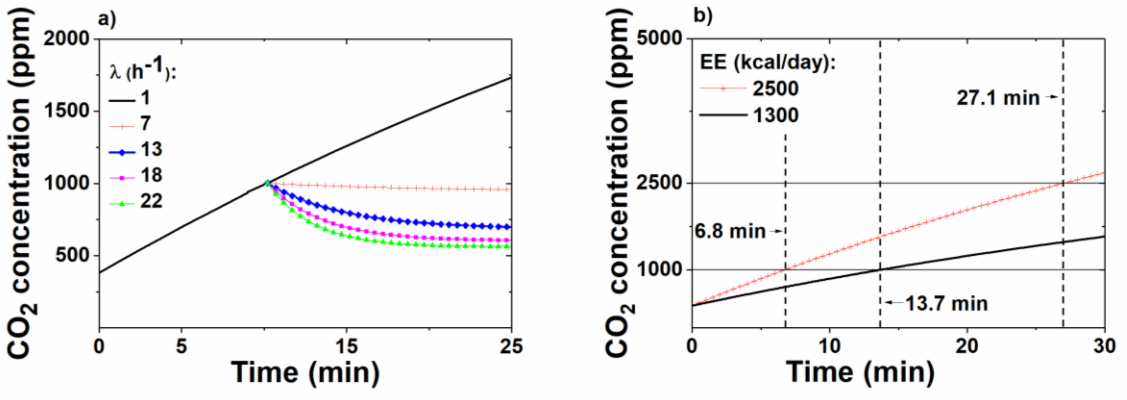

Figure 54. Effects of EE and Air Exchange on CO_2 Accumulation Patterns. a) Model CO_2 concentration profile showing effect of air exchange rate on CO_2 level; b) Modeled CO_2 concentration profile showing effect of metabolic rate on growth rate

CHAPTER 7

7 SMART PAD AND INTEGRATION WITH MULTIPLE IOT DEVICES

7.1 Abstract

The research performed in this study strives to implement the Smart Pad system with wearable devices and complementary urine testing to initially test the feasibility of implementation of a multitude of research-level (i.e. not yet clinically validated) methods simultaneously in a “smart system”. The system comprises measures of balance, breathing, heart rate, metabolic rate, joint flexibility, hydration, and physical performance functions in addition to lab testing related to biological aging and mechanical cell strength. A proof-of-concept test is illustrated for two adult individuals disparate ages: a 22-year-old and a 73-year-old matched in height and weight. The system has been tested in a pilot study, demonstrating functionality and age-related clinical relevance. Balance measurements indicated changes in sway area of 45.45% and 25.44%, respectively for before/after biking. The 22-year-old and the 73-year-old saw heart rate variabilities of 0.11 and 0.02 seconds at resting conditions, and metabolic rate changes of 277% and 222%, respectively, in comparison between the biking and seated conditions. A smart camera was used to assess biking speed and the 22- and 73-year-old subjects biked at 60 rpm and 28.5 rpm, respectively. The study probed feasibility of 1) multi-metric assessment under free living conditions, and 2) tracking of the various metrics over time.

7.2 Smart Pad Measurements

The integrative sensor system described in as assembled in a single location to simultaneously collect raw sensor data in a time-stamped fashion. After data collection,

the data was synchronized for further analysis. Study participants of different ages (ranging from 22-75 year-old) were provided with sensors (shown in Figure 55) for simultaneous assessment of physical and chemical parameters while performing a sequence of predetermined tasks under three conditions (shown in Figure 55): 1. Resting (sitting in a chair), 2. Activity (walking and running in a treadmill/ fixed biking), 3. Supine (sleeping).

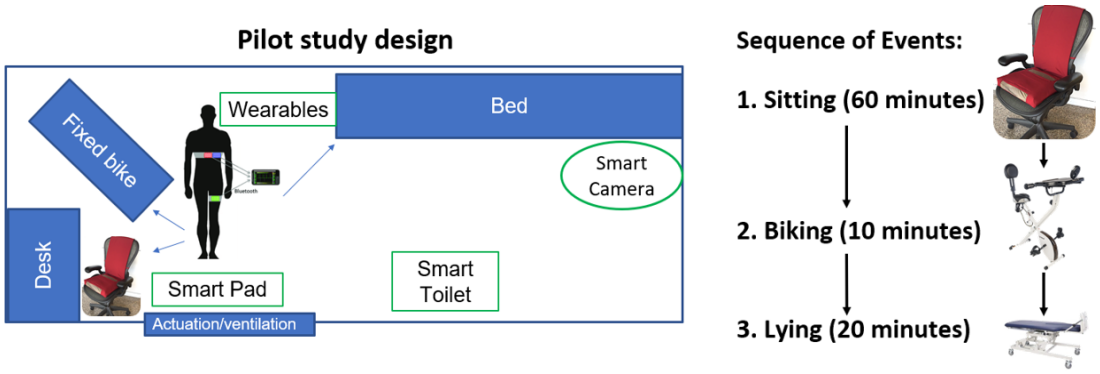

Figure 55. Aging Pilot Study Design and Sequence of Events

Smart Pad raw measurements were used to assess metabolic rate data as well as environmental data related to comfort (temperature and relative humidity). Metabolic rate generally decreases with age in humans, and with all other factors held constant, is a primary driver of age related weight gain (Piers et al., 1998). Figure 56A-B shows the metabolic rate assessment from the Smart Pad for the older and younger subject. Figure 56C shows a summary of the metabolic rate values for the study subjects at sitting, biking and lying positions. It can be observed that the metabolic rates were significantly different between the young and aged subjects with similar BMI. Sudden drops in metabolic rate can lead to sudden weight gain in any individual if caloric intake is kept constant (due to an increased positive overall caloric balance). Therefore, if these sudden

changes in metabolic rate can be detected (in the frame of a few weeks/months), then the subject could potentially be immediately alerted and better able to manage their caloric needs via caloric tracking. On the contrary, if metabolic rate increases without a change in lifestyle (e.g., exercise), it may be a warning of increase of catabolic processes such as worsening of pulmonary obstructions (Agha & El Wahsh, 2013; Hugli et al., 1996), cancer proliferation (T. Y. V. Nguyen et al., 2016), and hormonal imbalances (Meunier et al., 2005; Mullur et al., 2014; Salomon et al., 1992). Figure 56D shows a custom-made reproduction from (McArdle, 2010) and serves to delineate the changes in metabolic rate due to age. In Figure 56D, the orange line represents metabolic rate for males as a function of age and the pink line represents the metabolic rate for females as a function of age. The differences of metabolic rate observed in Figure 56C are supported by the information provided in Figure 56D.

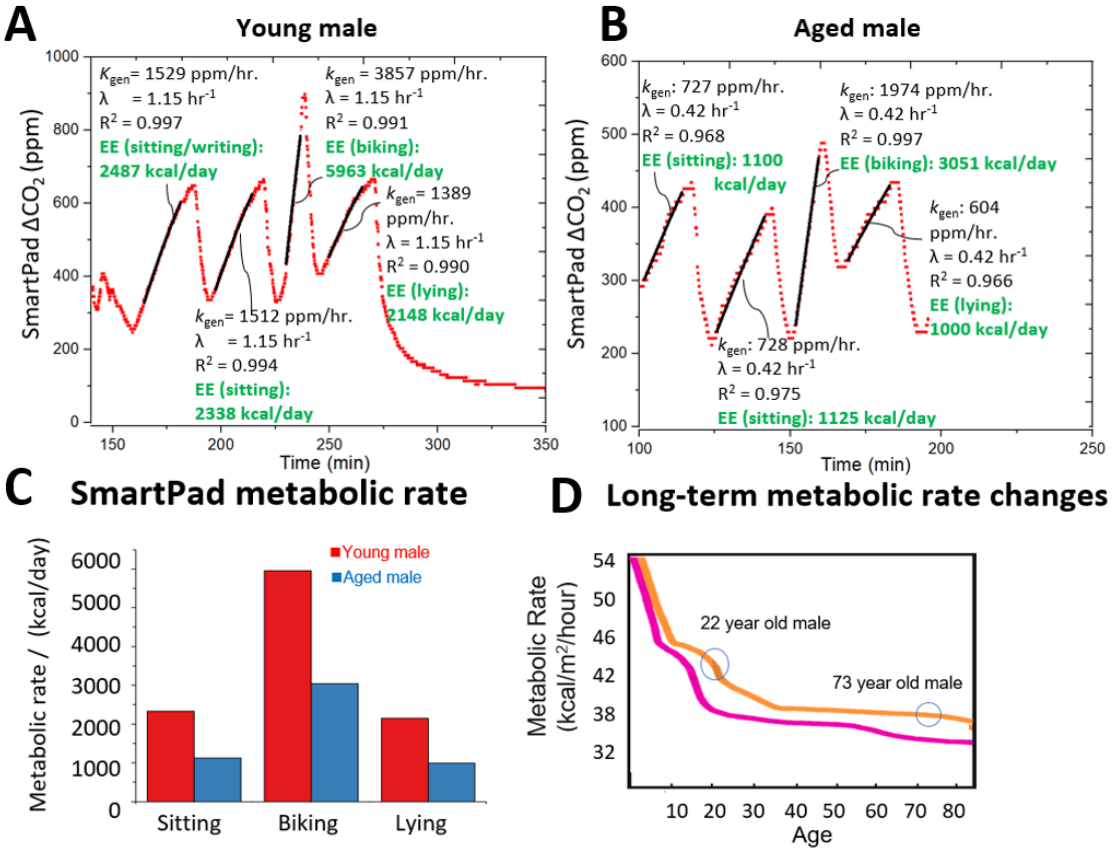

Figure 56. Tracking Age Related Metabolic Changes using Smart Pad. Smart Pad sensor raw and fitted data for the young (A) and aged (B) subjects. (C) Metabolic rate results corresponding to data in (A-B). (D) Data reconstructed from (McArdle, 2010): The curves represent population average metabolic rate for males (orange) and female (pink) as a function of age.

7.2 Smart Camera and Combined Metrics

Figure 57 shows the results assessed with the smart camera obtained for the young and aged subjects of our study within the smart room. The results were simultaneously assessed with the aforementioned sensors, including the Smart Pad. The subjects were video recorded during their biking activity. The smart camera software

written in Python generated a realistic 3D model that encoded the various position of each subject's angle, knee, and hip joints among other joints. The positions were then mathematically transformed using algorithms to generate pitch (knee angle) vs. time data. These data sets were then analyzed using Fast Fourier Transforms (FFTs) to determine the frequency distribution pattern of the biking frequency (RPM) for each subject. Knowing the biking frequency and the bike resistance, the biking power was calculated and correlated to the Smart Pad's measured metabolic rate to assess each subject's physical fitness level. It is worth noting that the physical fitness assessment of the study subjects could be exclusively performed by fusing the data from the smart sensors integrated in the Smart Pad and the Smart Camera. The younger subject showed higher physical fitness than the older subject given that the younger subject was able to perform same amount of power with less energy expenditure and oxygen consumption rate.

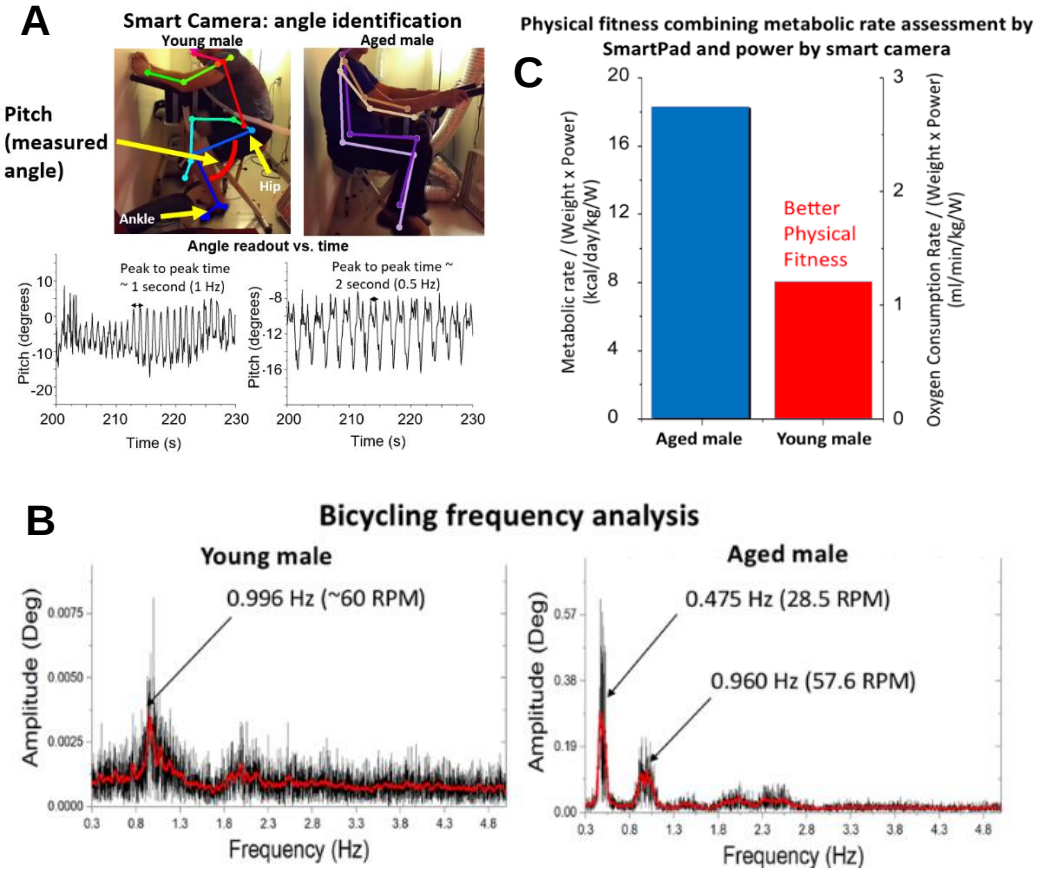

Figure 57. Smart Pad Integration with Contactless Human Tracking Software. (A) Smart camera images showing the joint angle identification, as well as the measurements of the pitch angle over time during biking for the two study subjects. (B) Fast Fourier Transform analysis of the data shown in (A), indicating the most frequent biking revolution-per-minute (RPM) for each subject. (C) Physical fitness assessment based on metabolic rate and oxygen consumption rate normalized by the subject's corresponding body weight and power production (from RPM and load measurement of bike).

Figure 57 shows that the Smart Pad system can be used to assess physical fitness for a test subject based on their power production, which can be calculated from bike load and RPM.

7.3 Fifteen Month Follow-up for BMI Matched Young and Old Subjects

Fifteen months later a follow up assessment was performed on the same set of test subjects with a similar physical fitness assessment performed. In neither physical fitness assessment was biking RPM or intensity a control variable, leading to drastically differences in energy efficiency. In the first assessment, both subjects cycled at a higher intensity, which has been observed to increase mechanical efficiency keeping other variables constant (Jabbour & Majed, 2019). In the latter experiment, pilot data was collected for a novel contactless low intensity exercise test for the purposes of cardiovascular diagnostics (Kharabsheh et al., 2006). Result are shown below in Figure 58.

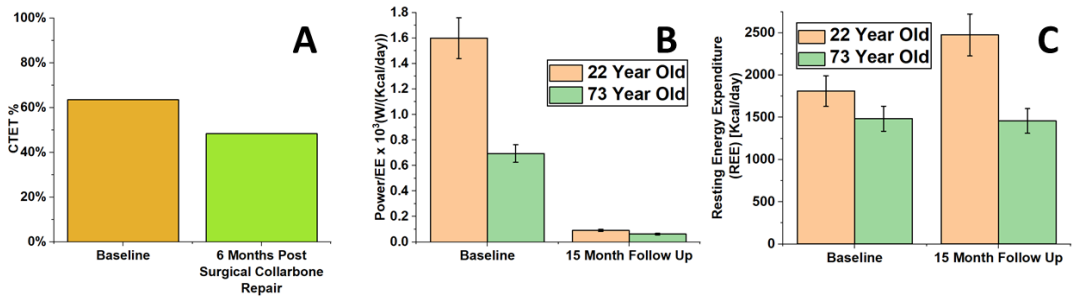

Figure 58. Changes in Physical Fitness and Metabolism Due to Aging and Injury.

Figure 58A shows changes in contactless thermodynamic efficiency (CTET) for the 22 year old subject before and after the subject had undergone a collarbone surgery after a serious injury. His thermodynamic efficiency was measured as the ratio of the power output on a cycle ergometer to the energy expenditure of the person x 100%, with 100% being the maximum possible thermodynamic efficiency for any abstract body, per the first law of thermodynamics (Ward-Smith, 1985). A slight decrease in thermodynamic efficiency was observed before the injury and 6 months after his

collarbone surgery, suggesting his cardiovascular fitness decreased over time, a logical result of sedentary behavior that is necessary after a significant surgical intervention.

Figure 58B shows changes in physical fitness for both subjects over time. As mentioned previously, both subjects biked at a higher intensity during the first assessment. While biking at lower intensity, both subjects were less efficient (i.e. less power output in comparison with energy expenditure), a result observed as well in other works (Jabbour & Majed, 2019). Figure 58C shows the difference in REE between both subjects 15 months after the initial metabolic assessment described earlier in this chapter. The older male's REE did not see any significant change in that timeframe, a somewhat surprising result given the Mifflin St. Joer equation suggests age varies linearly with REE (Mifflin St Jeor, 1990). On the other hand, the younger male (24 years old at the time) did see a large increase in his REE, a somewhat surprising result given REE tends to be at a maximum near the early 20s in most males and decreases linearly with age, according to the Mifflin St. Joer equation (Mifflin St Jeor, 1990). However, this may simply speak to the large day to day variance in REE and also possibly changes in the subject's muscle mass, bodyweight, stress, sleep, or a litany of other factors.

CHAPTER 8

8 SUMMARY AND FUTURE WORK

8.1 Further Engineering Requirements for a Viable Product

As currently designed, the Smart Pad system is a fully engineered medical device prototype with all necessary inputs and outputs for full functionality. REE measurement model and fundamental measurements performance of device have been validated for accuracy and reproducibility to current FDA standards for Type II medical devices with existing predicates for REE measurement. There is a current gap in a need for validation of the iOS application which has been developed as part of this dissertation project, however, this can be applied with relative ease to collected data from Chapters 3 and 4. There is also a gap in need for assessment of α in equation 10 or λ_{Acc} in equation 1. This can potentially be achieved via α assessment following the first installation of the Smart Pad in a room using a portable indirect calorimeter as a reference method to assess λ_{Acc} and k_{gen} multicollinearity. There is the additional possibility of an absence of significant multicollinearity between λ_{Acc} and k_{gen} as identified in equation 8, which may be true for some environments. In this case (α=0), λ_0 from CO_2 decay should likely suffice as an accurate predictor of λ_{Acc}. Additionally, there is a need for some type of ventilation blocking mechanism or integration of the actuator system with building controls. Either an external hardware product could be engineered, which fits over an existing ventilation source to a room, or a simple plastic cover could be purchased and utilized for blocking ventilation.

8.2 U.S. Regulatory (FDA/CLIA/IBC) Clearance Pathway

U.S. regulatory approval is key to development of any trustworthy medical device or diagnostic technique. There are multiple approval pathways for the Smart Pad depending on application type. For use of the Smart Pad as a standalone medical device with no actuator system, FDA clearance may be approachable through the 510(k) pathways since the system would not present any clear safety characteristics (assuming no modifications to building ventilation). However, in this instance, it is likely best to assess feasibility of regulatory approval via strong evidence for substantial equivalence of accuracy for REE measurement predicate devices, which is notably low for multiple U.S. 510(k) cleared predicate devices due to need for indirect measurement of energy consumption (Cooper et al., 2009). Fortunately, the measurement accuracy of the Smart Pad device in this work, when using the N=56 REE measurement dataset (a truly "clean" dataset with no outliers removed and distinct training/test set data) with no reference instrument calibration, was comparable to 4 FDA 510(k) cleared medical devices that are frequently used for metabolic assessment. A formal comparison with only FDA soured accuracy data is shown below in Table 19:

Table 19. Smart Pad Comparison with FDA 510(k) Cleared Indirect Calorimeters

Indirect Calorimeter Device (U.S. FDA legally adjudicated device as "safe and effective" "for prescription use" w/ 510(k) active). Only including 510(k)'s from past 25 years.	Single Breath Gas, VCO_2 or VO_2 [ml/min], Measurement Accuracy	Regulatory Considerations (no indirect calorimeter is FDA (515(c)) approved)	Sensing Mechanism for Gas Analysis
CareFusion (Becton Dickenson (BD)) MasterScreen CPX™	±50 ml/min (VCO_2) (FDA, 2007, 2014)	510(k) Cleared (FDA, 2007, 2014)	Thermal Conductive
CareFusion (Becton Dickenson (BD)) Oxycon Pro™	±50 ml/min (VCO_2) (FDA, 2000, 2014)	510(k) Cleared (FDA, 2000, 2014)	IR Absorption
CareFusion (Becton Dickenson (BD)) Vyntus CPX™	±50 ml/min (VCO_2) (FDA, 2014)	510(k) Cleared (FDA, 2014)	IR Absorption
Microlife Medical Home Solutions MedGem™	Y=0.83X (R=0.81) (VO_2) (FDA, 2002, 2003)	510(k) Cleared (FDA, 2002, 2003)	Florescent Quenching
Smart Pad (with λ_{Acc} calibration)	±24 ml/min (VCO_2) (Sprowls, Victor, Mora, et al., 2021)	Substantially equivalent accuracy to 5 predicate devices	IR Absorption
Smart Pad (without λ_{Acc} calibration using Equation 9)	±45 ml/min (VCO_2) (Sprowls, Victor, Mora, et al., 2021)	Substantially equivalent accuracy to 4 predicate devices	IR Absorption
Smart Pad (without λ_{Acc} calibration using Equation 9)	Y=1.05X (R=0.82) (VCO_2) (Sprowls, Victor, Mora, et al., 2021)	Outperforms MedGem™	IR Absorption

The Smart Pad device is totally unique given the new contactless VCO_2 measurement principle, there is a possibility that the De Novo pathway is necessary, given the strong possibility that the contactless VCO_2 measurement technique may raise fundamental questions of measurement efficacy, as defined by FDA standards which are based on measurements of physical quantities. In this case, U.S. regulatory approval would be more difficult, time-consuming, and costly to achieve (~$30,000 being the quoted amount for a De Novo classification (FDA, 2021)). However, one should be aware that the De Novo process may grant indirect protection and a form of extended patent protection for the entire class of new medical device granted through a De Novo (i.e. “contactless carbon dioxide production monitor”, which does not yet exist but could be founded through a De Novo). This is not intended by the FDA legislation, but, is a known consequence of 2011 changes to the code of federal regulations that must be considered for a novel medical device (Sherkow & Aboy, 2020), as, another manufacturer could potentially prevent the 510(k) clearance of a similar device via implementation of this patent extension strategy through a De Novo classification. This could potentially be achieved via implementation of a patented control technique (i.e. an occupancy sensor) in the De Novo submission. Through either route, the FDA should be contacted directly for specific comment on feasibility for regulatory clearance through a 513(g) submission, although, notably, this costs nearly the full price of a 510(k) (FDA, 2021). An additional consideration is that the FDA already does have a history of providing regulatory clearance for a contactless medical device (FDA, 2009) through the 510(k) route and by comparison performance characteristics to a contact based medical device with the same intended use. As such, the Smart Pad currently has the

advantageous position of having the optionality to either begin a new device class through a De Novo submission or submitting a 510(k) to an existing device class, each with their own nuanced considerations.

Another possible avenue for application of this technology is using a fully integrated actuator and applying the technology as a smart home/building system for ventilation energy efficiency, air quality optimization, and occupant metabolic rate measurement. In this case, the international building code (IBC) is a relevant standard followed by many U.S. counties and in many other nations across the world. With regards to building code, there is a strong need to provide evidence of fundamental safety in terms of mechanical risk to a building's ceiling and fire hazard risk. To address these, a lightweight (<10lbs) and fire resistance actuator door system was developed for quick and easy installation onto any ventilation inlet. Additionally, it is possible to develop lightweight ventilation-blocking accessories to remove intermittent ventilation from any small/medium sized rooms. Another avenue is to simply block the HVAC inlet and outlet duct to a small room by accessing the suspended ceiling and covering both parts of the duct with a metal collar and nonpermeable plastic fabric. Yet another solution is to integrate the system with a smart actuator system, controlled by the buildings ventilation control switchboard (and can be actuated automatically based on sensor data by multiple developed smart building products). Clearly, there are many ways to approach the HVAC modification need that is required for a true smart system and the convenience of each technique may vary from room to room depending on size/building/HVAC system. In this application, one promising approach would be to use the Smart Pad smart system as a U.S. regulatory (CLIA) approved laboratory developed test (LDT). In this application, it

would be necessary to install the Smart Pad system by any HVAC configuration within an office, and subsequently calibrate and validate the system's REE measure using a FDA cleared predicate device (i.e. portable metabolic analyzer). This may offer a possible work-around to providing useful medical diagnostics without the necessity of tremendous resource cost for FDA approval through the premarket approval pathway.

8.3 Future Scientific and Physiological Research Focused Work

Besides application as a respected FDA 510(k) cleared medical device for prescription or consumer use, the Smart Pad and techniques developed through this thesis work also provide immense potential to develop new fundamental scientific knowledge. One substantial research application of the device is in a better fundamental understanding of the accuracy and physiological effects of using contact-based metabolic analyzers. From personal experience and discussions with experienced researchers in the field, the first 5 minutes of data from a contact-based indirect calorimeter will not be in agreeance with data collected after the subject has reached steady state (Simonson & DeFronzo, 1990). That being said, this common occurrence has never been studied in great detail. A scientific work evaluating the agreeance of VCO_2 measurements from randomized and sequential contactless and contact based indirect calorimetry has never been completed. The expected results of such a study could bring great knowledge and attention to this observed, but, not rigorously studied phenomena with regards to contact-based indirect calorimeters.

Another research application of the device is for assessment of physiological stress (G. Seematter et al., 2000) where there is no well-established biomarker. Cortisol is commonly referred to as the principal stress biomarker, however, strong fundamental

concerns exists with regards to the body's hormonal pathways and how that might affect Cortisol concentrations within blood and saliva (Hellhammer et al., 2009). Metabolic rate has a strong case to be the most comprehensive stress biomarker since all physiological responses must fundamentally result in changes in metabolism given all thermodynamic processes require energy. As such, one might expect a stressed person to see an elevated heart rate, breathing rate, and physical activity patterns, all of which would correlate with increased metabolic activity. With this all in mind, current indirect calorimeter medical devices cannot accurately assess cognitive or physiological stress without concern, given, the devices are incredibly distracting to wear and therefore will always raise fundamental questions of accuracy with regards to measurement of a person in their free-living state. Fortunately, the Smart Pad device can resolve this research gap given it does not obstruct in any way a person's free living state. As such, a study design could be developed which assesses the validity of metabolism as the fundamental biomarker for physiological stress. The investigation might compare the cortisol and metabolic response of individuals under differing conditions known to induce stress. Any significant difference between the biomarkers would be worthy of scientific publication and agreeance as well would partially validate the accuracy of both biomarkers (cortisol and metabolic rate). A similar study was published (Gall et al., 2021), but, fundamental questions of accuracy must be raised in that publication based on the novel findings of this work.

Yet another research application of the device is to study the variability of metabolism in differing physiological groups. The variance of metabolism could be studied on the scale of hours, months, or years the physiological groups of interest might be (but are not limited to) persons differing in age, health status, biological sex, disease

status, or bodyweight. The application for this specific research protocol is left open ended since it might be best suited for a massive dataset, statistical analysis approach. Since the Smart Pad can be used to collect contactless data accurately, it would be logical to reason a singular person could generate 4-16 hours of metabolic data each day by installing the system in their bedroom or work office. If integrated with other non-invasive physiological sensors (Sprowls, Serhan, et al., 2021), parallel assessments of multiple physiological parameters could generate a large wealth of inter-related health data (e.g. sleep cycle and sleep metabolism, for example) enabling newfound knowledge of human physiological as it relates to human metabolism.

8.4 Conclusions

The device developed as a result of this dissertation research project, the Smart Pad, shows immense potential for improving the both the clinical and research capabilities of energy expenditure assessment. Validation studies performed in multiple environments and across 25 total subjects suggests comparable accuracy to multiple FDA cleared devices including the Korr Reevue™, MGC Ultima CPX™, and the Breezing™ portable indirect calorimeter for measurement of REE using only contactless measurements. Contactless REE measurements were performed in a moving vehicle, medical office, private office, and enclosed curtained area of a larger lab space successfully, once air exchange rate was calibrated for using a reference instrument. Exercise measurements were also shown to be recorded at good accuracy for VCO_2, a key breath gas which can be used to estimate $VO_{2,\ max}$ the gold standard measurement for cardiovascular fitness assessment. A new model was developed for REE measurement which does not rely on air exchange assessment from reference instrument calibration or

CO_2 decay analysis and was validated on 5 subjects over 56 total measurements. Air exchange measurements were performed in the first time within an occupied environment using a FDA 510(k) cleared reference instrument for CO_2 source strength measurement.

BIBLIOGRAPHY

Agha, M. A., & El Wahsh, R. A. (2013). Basal metabolic rate in bronchial asthma and chronic obstructive pulmonary disease patients. *Egyptian Journal of Chest Diseases and Tuberculosis, 62*(1), 39-44. doi:https://doi.org/10.1016/j.ejcdt.2013.01.007

Ainslie, P., et al. (2003). Estimating human energy expenditure: a review of techniques with particular reference to doubly labelled water. *Sports, Med, 33*(9), 0112-1642. doi:10.2165/00007256-200333090-00004

Alfonzo-González, G., et al. (2006). Greater than predicted decrease in resting energy expenditure with age: cross-sectional and longitudinal evidence. *European Journal of Clinical Nutrition, 60*(1), 18-24. doi:10.1038/sj.ejcn.1602262

Allen, J. G., et al. (2016). Associations of Cognitive Function Scores with Carbon Dioxide, Ventilation, and Volatile Organic Compound Exposures in Office Workers: A Controlled Exposure Study of Green and Conventional Office Environments. *Environmental Health Perspectives, 124*(6), 805-812. doi:doi:10.1289/ehp.1510037

Altman, D. G., & Bland, J. M. (2005). Standard deviations and standard errors. *The BMJ (British Medical Journal), 331*(7521), 903. doi:10.1136/bmj.331.7521.903

ASTM D 6245. (2007). Standard Guide for Using Indoor Carbon Dioxide Concentrations to Evaluate Indoor Air Quality and Ventilation: American Soceity for Testing and Materials (ASTM). https://compass.astm.org/EDIT/html_annot.cgi?D6245+18

Auerswald, S., et al. (2020). Experimental Investigation of the Air Exchange Effectiveness of Push-Pull Ventilation Devices. *Energies, 13*(21). doi:10.3390/en13215817

Bakó-Biró, Z., et al. (2012). Ventilation rates in schools and pupils' performance. *Building and Environment, 48*, 215-223. doi:https://doi.org/10.1016/j.buildenv.2011.08.018

Batterman, S. (2017). Review and Extension of CO_2-Based Methods to Determine Ventilation Rates with Application to School Classrooms. *International journal of environmental research and public health, 14*(2), 145. doi:10.3390/ijerph14020145

Benedict, C., et al. (2011). Acute sleep deprivation reduces energy expenditure in healthy men. *The American Journal of Clinical Nutrition, 93*(6), 1229-1236. doi:10.3945/ajcn.110.006460

Black, A. E., & Cole, T. J. (2000). Within- and between-subject variation in energy expenditure measured by the doubly-labelled water technique: implications for validating reported dietary energy intake. *European Journal of Clinical Nutrition, 54*(5), 386-394. doi:10.1038/sj.ejcn.1600970

Bluyssen, P. M., et al. (1996). European Indoor Air Quality Audit Project in 56 Office Buildings. *Indoor Air, 6*(4), 221-238. doi:https://doi.org/10.1111/j.1600-0668.1996.00002.x

Bray, G. A. (2004). Medical consequences of obesity. *Journal Of Clinical Endocrinology & Metabolism, 89*(6), 2583-2589.

Calcagno, M., et al. (2019). The Thermic Effect of Food: A Review. *Journal of the American College of Nutrition, 38*(6), 547-551. doi:10.1080/07315724.2018.1552544

Campos, P., et al. (2006). The epidemiology of overweight and obesity: public health crisis or moral panic? *International Journal Of Epidemiology, 35*(1), 55-60.

Cancello, R., et al. (2018). Analysis of Predictive Equations for Estimating Resting Energy Expenditure in a Large Cohort of Morbidly Obese Patients. *Frontiers in Endocrinology, 9*(367). doi:10.3389/fendo.2018.00367

CDC. (2021). Defining Adult Overweight and Obesity: Centers for Disease Control and Prevention (CDC). https://www.cdc.gov/obesity/adult/defining.html#:~:text=If%20your%20BMI%20is%20less,falls%20within%20the%20obese%20range

Cheong, K. W., & Chong, K. Y. (2001). Development and application of an indoor air quality audit to an air-conditioned building in Singapore. *Building and Environment, 36*(2), 181-188. doi:https://doi.org/10.1016/S0360-1323(99)00064-5

Chowdhury, E. A., et al. (2017). Assessment of laboratory and daily energy expenditure estimates from consumer multi-sensor physical activity monitors. *PloS one, 12*(2), e0171720. doi:10.1371/journal.pone.0171720

Claude-Alain, R., & Foradini, F. (2002). Simple and Cheap Air Change Rate Measurement Using CO2 Concentration Decays. *International Journal of Ventilation, 1*(1), 39-44. doi:10.1080/14733315.2002.11683620

Cooper, J. A., et al. (2009). Assessing validity and reliability of resting metabolic rate in six gas analysis systems. *Journal of the American Dietetic Association, 109*(1), 128-132. doi:10.1016/j.jada.2008.10.004

Criscione, L., et al. (2013). Calogenetic Balance, an educational program for lifelong weight control on measured resting metabolic rate and intake of favorite foods, promotes adherence and success rate. *European Congress on Obesity, Liverpool, UK*.

Cui, S., et al. (2015). CO2 tracer gas concentration decay method for measuring air change rate. *Building and Environment, 84*, 162-169. doi:https://doi.org/10.1016/j.buildenv.2014.11.007

Dascalaki, E. G., et al. (2008). Air quality in hospital operating rooms. *Building and Environment, 43*(11), 1945-1952. doi:https://doi.org/10.1016/j.buildenv.2007.11.015

de Jonge, L., et al. (2012). Effect of Diet Composition and Weight Loss on Resting Energy Expenditure in the POUNDS LOST Study. *Obesity, 20*(12), 2384-2389. doi:10.1038/oby.2012.127

de Jonge, L., et al. (2012). Poor Sleep Quality and Sleep Apnea Are Associated with Higher Resting Energy Expenditure in Obese Individuals with Short Sleep Duration. *The Journal of Clinical Endocrinology & Metabolism, 97*(8), 2881-2889. doi:10.1210/jc.2011-2858

Deng, Y., & Scott, B. J. (2019). Comparison of Resting Metabolic Rates: Calculated using predictive equation and measured using Portable Indirect Calorimeter. *Global Journal of Obesity, Diabetes and Metabolic Syndrome*, 010-016. doi:10.17352/2455-8583.000036

Deng, Y., et al. (2020). An Unobstructive Sensing Method for Indoor Air Quality Optimization and Metabolic Assessment within Vehicles. *Sensors, 20*(24). doi:10.3390/s20247202

Donahoo, W. T., et al. (2004). Variability in energy expenditure and its components. *Curr Opin Clin Nutr Metab, Care*(1363-1950 (Print)).

Dulloo, A., & Schutz, Y. (2015). Adaptive Thermogenesis in Resistance to Obesity Therapies: Issues in Quantifying Thrifty Energy Expenditure Phenotypes in Humans. *Curr Obes Rep., Jun;4*(2), 230-240. doi: 210.1007/s13679-13015-10156-13679.

Dulloo, A. G., & Jacquet, J. (1998). Adaptive reduction in basal metabolic rate in response to food deprivation in humans: a role for feedback signals from fat stores. *Am J Clin Nutr, 68*(3), 599-606. doi:10.1093/ajcn/68.3.599

Elliot, D. L., et al. (1987). Sustained decrement in resting metabolic-rate following weight loss. *Clinical Research, 35*(3), A365-A365.

Elliot, D. L., et al. (1989). Sustained depression of the resting metabolic-rate after massive weight loss. *American Journal Of Clinical Nutrition, 49*(1), 93-96.

Esparza, J., et al. (2000). Daily energy expenditure in Mexican and USA Pima Indians: low physical activity as a possible cause of obesity. *International Journal Of Obesity, 24*(1), 55-59.

FDA. (2000). Oxycon$_{TM}$ Pro 510(k) Premarket Notification (K992214): U.S. Food and Drug Administration. URL: https://www.accessdata.fda.gov/cdrh_docs/pdf/K992214.pdf

FDA. (2002). MedGem^{TM} 510(k) Premarket Notification (K021605): U.S. Food and Drug Administration. URL: https://www.accessdata.fda.gov/cdrh_docs/pdf2/K021605.pdf

FDA. (2003). ReeVue Indirect Calorimeter, Model#8100 510(k) Premarket Notification. In Korr Medical Technologies Incorporated (Ed.): U.S. Food and Drug Administration. URL: https://www.accessdata.fda.gov/scripts/cdrh/cfdocs/cfPMN/pmn.cfm?ID=K021490

FDA. (2006). Medgraphics Ultima System 510(k) Premarket Notification: U.S. Food and Drug Administration. URL: https://www.accessdata.fda.gov/scripts/cdrh/cfdocs/cfpmn/pmn.cfm?ID=K061731

FDA. (2007). MasterScreen CPX^{TM} 510(k) Premarket Notification (K072323). U.S. Food and Drug Administration. URL: https://www.accessdata.fda.gov/cdrh_docs/pdf7/K072323.pdf

FDA. (2009). Kai Sensors Non-Contact Respiratory Rate Spot Check Model 100 ("Kai RSpot 100") (K090273): U.S. Food and Drug Administration.

FDA. (2014). Vyntus^{TM}/SentrySuite^{TM} product line 510(k) Premarket Notification (K133925): U.S. Food and Drug Administration. URL: https://www.accessdata.fda.gov/cdrh_docs/pdf13/K133925.pdf

FDA. (2021). Medical Device User Fee Amendments (MDUFA): U.S. Food and Drug Administration. https://www.fda.gov/industry/fda-user-fee-programs/medical-device-user-fee-amendments-mdufa

Fleg, J. L., & Lakatta, E. G. (1988). Role of muscle loss in the age-associated reduction in VO2 max. *Journal of Applied Physiology, 65*(3), 1147-1151. doi:10.1152/jappl.1988.65.3.1147

Fock, K. M., & Khoo, J. (2013). Diet and exercise in management of obesity and overweight. *Journal of Gastroenterology and Hepatology, 28*(S4), 59-63. doi:https://doi.org/10.1111/jgh.12407

Forzani, E., et al. (2018). Method for assessing metabolic rate and maintaining indoor air quality and efficient ventilation energy use with passive environmental sensors. *CPT filed Patent*.

Frankenfield, D. C. (2013). Bias and accuracy of resting metabolic rate equations in non-obese and obese adults. *Clinical Nutrition, 32*(6), 976-982. doi:https://doi.org/10.1016/j.clnu.2013.03.022

Gall, E. T., et al. (2021). Impact of Cognitive Tasks on CO2 and Isoprene Emissions from Humans. *Environmental Science & Technology, 55*(1), 139-148. doi:10.1021/acs.est.0c03850

GE. (2021). Telaire 7001 CO_2 Sensor Specifications: GE Sensing. URL: https://www.onsetcomp.com/products/sensors/tel-7001/

Gong, J., et al. (2015). Impact of Disease Activity on Resting Energy Expenditure and Body Composition in Adult Crohn's Disease. *Journal of Parenteral and Enteral Nutrition, 39*(6), 713-718. doi:10.1177/0148607114528360

Gorostiaga, E. M., et al. (1989). Decrease in Respiratory Quotient During Exercise Following L-Carnitine Supplementation. *International Journal Of Sports Medicine, 10*(03), 169-174. doi:10.1055/s-2007-1024895

Grunwald, G. K., et al. (2003). Comparison of Methods for Achieving 24-Hour Energy Balance in a Whole-Room Indirect Calorimeter. *Obesity Research, 11*(6), 752-759. doi:https://doi.org/10.1038/oby.2003.105

Hasson, R. E., et al. (2011). Accuracy of four resting metabolic rate prediction equations: Effects of sex, body mass index, age, and race/ethnicity. *Journal of Science and Medicine in Sport, 14*(4), 344-351. doi:https://doi.org/10.1016/j.jsams.2011.02.010

Haverinen-Shaughnessy, U., et al. (2011). Association between substandard classroom ventilation rates and students' academic achievement. *Indoor Air, 21*(2), 121-131. doi:https://doi.org/10.1111/j.1600-0668.2010.00686.x

Hellhammer, D. H., et al. (2009). Salivary cortisol as a biomarker in stress research. *Psychoneuroendocrinology, 34*(2), 163-171. doi:https://doi.org/10.1016/j.psyneuen.2008.10.026

Hill, J. O., et al. (2012). Energy balance and obesity. *Circulation, 126*(1), 126-132. doi:10.1161/CIRCULATIONAHA.111.087213

Horner, N. K., et al. (2001). Indirect calorimetry protocol development for measuring resting metabolic rate as a component of total energy expenditure in free-living postmenopausal women. *J. Nutr, 131*(8), 0022-3166.

Hugli, O., et al. (1996). The daily energy expenditure in stable chronic obstructive pulmonary disease. *American Journal of Respiratory and Critical Care Medicine, 153*(1), 294-300. doi:10.1164/ajrccm.153.1.8542132

Issekutz, B., & Rodahl, K. (1961). Respiratory quotient during exercise. *Journal of Applied Physiology, 16*(4), 606-610. doi:10.1152/jappl.1961.16.4.606

Jabbour, G., & Majed, L. (2019). Mechanical Efficiency at Different Exercise Intensities Among Adolescent Boys With Different Body Fat Levels. *Frontiers in Physiology, 10*, 265. doi:10.3389/fphys.2019.00265

Jacobson, T. A., et al. (2019). Direct human health risks of increased atmospheric carbon dioxide. *Nature Sustainability, 2*(8), 691-701. doi:10.1038/s41893-019-0323-1

Jebb, S. A., et al. (1996). Changes in macronutrient balance during over- and underfeeding assessed by 12-d continuous whole-body calorimetry. *Am, J. Clin Nutr, 64*(3). doi:10.1093/ajcn/64.3.259

Kharabsheh, S. M., et al. (2006). Overview of exercise stress testing. *Annals of Saudi medicine, 26*(1), 1-6. doi:10.5144/0256-4947.2006.1

Lührmann, P. M., et al. (2009). Longitudinal changes in energy expenditure in an elderly German population: a 12-year follow-up. *European Journal of Clinical Nutrition, 63*(8), 986-992. doi:10.1038/ejcn.2009.1

Lyden, K., et al. (2014). Estimating energy expenditure using heat flux measured at a single body site. *Medicine and science in sports and exercise, 46*(11), 2159-2167. doi:10.1249/MSS.0000000000000346

Magoffin, A., et al. (2008). Longitudinal Analysis of Resting Energy Expenditure in Patients with Cystic Fibrosis. *The Journal of Pediatrics, 152*(5), 703-708. doi:https://doi.org/10.1016/j.jpeds.2007.10.021

Manore, M. M., et al. (2009). Sport Nutrition for Health and Performance. *Human Kinetics (Ed.), Second Edition*.

Marra, M., et al. (2004). Fasting Respiratory Quotient as a Predictor of Long-Term Weight Changes in Non-Obese Women. *Annals of Nutrition and Metabolism, 48*(3), 189-192. doi:10.1159/000079556

Matarese, L. E. (1997). Indirect calorimetry: technical aspects. *J Am Diet Assoc, 97*(10 Suppl 2), S154-160. doi:10.1016/s0002-8223(97)00754-2

McArdle, W. D. K., F. I.; Katch, V. L. (2010). *Exercise physiology: nutrition, energy, and human performance.*: Lippincott Williams & Wilkins.

McClave, S. A., et al. (2016). Guidelines for the Provision and Assessment of Nutrition Support Therapy in the Adult Critically Ill Patient: Society of Critical Care Medicine (SCCM) and American Society for Parenteral and Enteral Nutrition (A.S.P.E.N.). *Jpen J. Parenter Enteral Nutr*(1941-2444 (Electronic)).

McDoniel, S. O., et al. (2008). Employing RMR Technology in a 90-Day Weight Control Program. *Obesity Facts, 1*(6), 298-304. doi:10.1159/000178026

Meunier, N., et al. (2005). Basal metabolic rate and thyroid hormones of late-middle-aged and older human subjects: the ZENITH study. *European Journal of Clinical Nutrition, 59*(2), S53-S57. doi:10.1038/sj.ejcn.1602299

Mifflin, M. D., et al. (1990). A new predictive equation for resting energy expenditure in healthy individuals. *The American Journal of Clinical Nutrition, 51*(2), 241-247. doi:10.1093/ajcn/51.2.241

Mifflin St Jeor, H. L. A. S., B. J, Daugherty S. A, Koh Y. O. (1990). A new predictive equation for resting energy expenditure in healthy individuals. *Am J Clin Nutr., 51*.

Mullur, R., et al. (2014). Thyroid hormone regulation of metabolism. *Physiological reviews, 94*(2), 355-382. doi:10.1152/physrev.00030.2013

Nguyen, T., et al. (2003). Chamber for indirect calorimetry with accurate measurement and time discrimination of metabolic plateaus of over 20 min. *Med Biol Eng, Comput, 41*(5).

Nguyen, T. Y. V., et al. (2016). Comparison of Resting Energy Expenditure Between Cancer Subjects and Healthy Controls: A Meta-Analysis. *Nutrition and Cancer, 68*(3), 374-387. doi:10.1080/01635581.2016.1153667

NIH. (1998). Clinical Guidelines on the Identification, Evaluation, and Treatment of Overweight and Obesity in Adults--The Evidence Report. National Institutes of Health. *Obesity Research, 6 Suppl 2*, 51s-209s.

Norbäck, D., et al. (2013). Carbon dioxide (CO2) demand-controlled ventilation in university computer classrooms and possible effects on headache, fatigue and perceived indoor environment: an intervention study. *International Archives of Occupational and Environmental Health, 86*(2), 199-209. doi:10.1007/s00420-012-0756-6

Novoselac, A., & Srebric, J. (2003). Comparison of Air Exchange Efficiency and Contaminant Removal Effectiveness as IAQ Indices *ASHRAE Transactions*. https://www.caee.utexas.edu/prof/novoselac/Publications/Novoselac_ASHRAE_Transactions_2003.pdf

OSHA. (2020). Fit Testing Procedures (Mandatory). In O. S. a. H. Administration (Ed.): U.S. Department of Labor. https://www.osha.gov/pls/oshaweb/owadisp.show_document?p_id=9780&p_table=STANDARDS

Piers, L. S., et al. (1998). Is there evidence for an age-related reduction in metabolic rate? *Journal of Applied Physiology, 85*(6), 2196-2204. doi:10.1152/jappl.1998.85.6.2196

Purcell, S. A., et al. (2019). Accuracy of Resting Energy Expenditure Predictive Equations in Patients With Cancer. *Nutrition in Clinical Practice, 34*(6), 922-934. doi:https://doi.org/10.1002/ncp.10374

Ramalho, O., et al. (2013). Air Stuffiness and Air Exchange Rate in French Schools and Day-Care Centres. *International Journal of Ventilation, 12*(2), 175-180. doi:10.1080/14733315.2013.11684013

Ravussin, E., et al. (1986). Determinants of 24-hour energy expenditure in man. Methods and results using a respiratory chamber. *J Clin Invest, 78*(6), 1568-1578. doi:10.1172/jci112749

Redlich, C. A., et al. (1997). Sick-building syndrome. *The Lancet, 349*(9057), 1013-1016. doi:https://doi.org/10.1016/S0140-6736(96)07220-0

Reed, G. W., & Hill, J. O. (1996). Measuring the thermic effect of food. *The American Journal of Clinical Nutrition, 63*(2), 164-169. doi:10.1093/ajcn/63.2.164

Rising, R., et al. (2015). Evaluation of a new whole room indirect calorimeter specific for measurement of resting metabolic rate. *Nutrition & Metabolism, 12*(1), 46. doi:10.1186/s12986-015-0043-0

Roza, A. M., & Shizgal, H. M. (1984). The Harris Benedict equation reevaluated: resting energy requirements and the body cell mass. *Am J Clin Nutr, 40*(1), 168-182. doi:10.1093/ajcn/40.1.168

Ruiz, I., et al. (2018). Assessing Metabolic Rate & Indoor Air Quality with Passive Environmental Sensors. *Journal of Breath Research, Apr 4;12*(3), 036012.

Rumpler, W. V., et al. (1990). Repeatability of 24-h energy expenditure measurements in humans by indirect calorimetry. *The American Journal of Clinical Nutrition, 51*(2), 147-152. doi:10.1093/ajcn/51.2.147

Salomon, F., et al. (1992). Basal metabolic rate in adults with growth hormone deficiency and in patients with acromegaly: relationship with lean body mass, plasma insulin level and leucocyte sodium pump activity. *Clinical Science, 83*(3). doi:10.1042/cs0830325

Satish, U., et al. (2012). Is CO2 an Indoor Pollutant? Direct Effects of Low-to-Moderate CO2 Concentrations on Human Decision-Making Performance. *Environmental Health Perspectives, 120*(12), 1671-1677. doi:10.1289/ehp.1104789

Sawai, A., et al. (2007). Influence of Mental Stress on Cardiovascular Function as Evaluated by Changes in Energy Expenditure. *Hypertension Research, 30*(11), 1019-1027. doi:10.1291/hypres.30.1019

Schoeller, D. A., & van Santen, E. (1982). Measurement of energy expenditure in humans by doubly labeled water method. *Journal of Applied Physiology, 53*(4), 955-959. doi:10.1152/jappl.1982.53.4.955

Scott, H. R., et al. (2001). Longitudinal study of resting energy expenditure, body cell mass and the inflammatory response in male patients with non-small cell lung cancer. *Lung Cancer, 32*(3), 307-312. doi:https://doi.org/10.1016/S0169-5002(00)00244-0

Seagle, H., et al. (2009). Position of the American Dietetic Association: Weight Management. *Journal of the American Dietetic Association, 109*(2), 330-346.

Seematter, G., et al. (2002). Metabolic Effects of Mental Stress during Over- and Underfeeding in Healthy Women. *Obesity Research, 10*(1), 49-55. doi:10.1038/oby.2002.7

Seematter, G., et al. (2000). Effects of mental stress on insulin-mediated glucose metabolism and energy expenditure in lean and obese women. *American Journal of Physiology-Endocrinology and Metabolism, 279*(4), E799-E805. doi:10.1152/ajpendo.2000.279.4.E799

Sharma, S., & Kavuru, M. (2010). Sleep and metabolism: an overview. LID - 10.1155/2010/270832 [doi] LID - 270832 [pii]. *Int, J. Endocrinol*(1687-8345 (Electronic)).

Sherkow, J. S., & Aboy, M. (2020). The FDA De Novo medical device pathway, patents and anticompetition. *Nature Biotechnology, 38*(9), 1028-1029. doi:10.1038/s41587-020-0653-6

Shlisky, J. D., et al. (2012). Partial Sleep Deprivation and Energy Balance in Adults: An Emerging Issue for Consideration by Dietetics Practitioners. *Journal of the Academy of Nutrition and Dietetics, 112*(11), 1785-1797. doi:https://doi.org/10.1016/j.jand.2012.07.032

Siervo, M., et al. (2014). Accuracy of predictive equations for the measurement of resting energy expenditure in older subjects. *Clinical Nutrition, 33*(4), 613-619. doi:https://doi.org/10.1016/j.clnu.2013.09.009

Simonson, D. C., & DeFronzo, R. A. (1990). Indirect calorimetry: methodological and interpretative problems. *American Journal of Physiology-Endocrinology and Metabolism, 258*(3), E399-E412. doi:10.1152/ajpendo.1990.258.3.E399

Speakman, J., & Selman, C. (2003). Physical activity and resting metabolic rate. *Proceedings of the Nutrition Society, 62*, 621–634.

Sprowls, M., et al. (2020). An Unobstructive Sensing Method for Indoor Air Quality Optimization and Metabolic Assessment within Vehicles. *Sensors, 20*(24). doi:10.3390/s20247202

Sprowls, M., et al. (2021). Integrated Sensing Systems for Monitoring Interrelated Physiological Parameters in Young and Aged Adults: A Pilot Study. *International Journal of Prognostics and Health Management (Accepted)*.

Sprowls, M., et al. (2021). A Smart Medical Device for Contactless Energy Expenditure Measurement. *Biosensors and Bioelectronics (Submitted)*.

Sprowls, M., et al. (2021). A system for contact free energy expenditure assessment under free-living conditions: Monitoring metabolism for weight loss using carbon dioxide emission. *Journal of Breath Research, 15*(2). doi:10.1088/1752-7163/abd52f

Storer, T. W., et al. (1990). Accurate prediction of VO2max in cycle ergometry. *Medicine and science in sports and exercise, 22*(5), 704-712. doi:10.1249/00005768-199010000-00024

Stump, C. S., et al. (2017). Study of the Effect of Mobile Indirect Calorimeter on Weight Management. *Glob J Obes Diabetes Metab Syndr, 4*(2), 044-050. DOI: http://doi.org/010.17352/12455-18583.000022.

Sun, M., et al. (2001). A longitudinal study of resting energy expenditure relative to body composition during puberty in African American and white children. *The American Journal of Clinical Nutrition, 73*(2), 308-315. doi:10.1093/ajcn/73.2.308

Sun, M., et al. (1994). Modification of a whole room indirect calorimeter for measurement of rapid changes in energy expenditure. *Journal of Applied Physiology, 76*(6), 2686-2691. doi:10.1152/jappl.1994.76.6.2686

Tans, P., & Keeling, R. (2020). Trends in atmospheric carbon dioxide: NOAA ESRL Global Monitoring Division. URL: https://www.esrl.noaa.gov/gmd/ccgg/trends/gl_trend.html

Thiese, M. S., et al. (2016). P value interpretations and considerations. *Journal of thoracic disease, 8*(9), E928-E931. doi:10.21037/jtd.2016.08.16

Turanjanin, V., et al. (2014). Indoor CO2 measurements in Serbian schools and ventilation rate calculation. *Energy, 77*, 290-296. doi:https://doi.org/10.1016/j.energy.2014.10.028

Ward-Smith, A. J. (1985). A mathematical theory of running, based on the first law of thermodynamics, and its application to the performance of world-class athletes. *Journal of Biomechanics, 18*(5), 337-349. doi:https://doi.org/10.1016/0021-9290(85)90289-1

Weir, J. B. (1949). New methods for calculating metabolic rate with special reference to protein metabolism. *J Physiol*(0022-3751 (Print)). doi:D - CLML: 5018:220c:7:9 OTO - NLM

World Health Organization. WHO. (2020). Obesity and Overweight: Key Facts. Retrieved from http://www.who.int/mediacentre/factsheets/fs311/en/

Yang, W., et al. (2009). Indoor air quality investigation according to age of the school buildings in Korea. *Journal of Environmental Management, 90*(1), 348-354. doi:https://doi.org/10.1016/j.jenvman.2007.10.003

Zhang, X., et al. (2015). Effects of Exposure to Carbon Dioxide and Human Bioeffluents on Cognitive Performance. *Procedia Engineering, 121*, 138-142. doi:10.1016/j.proeng.2015.08.1040

APPENDIX A

PUBLICATION AUTHORSHIP RESULTING FROM PHD STUDIES

[1] **Sprowls, M.**, Victor, S. Destaillats, H., Wheatley-Guy, C., Tao, N.J., Johnson, B., Kulick, D., and Forzani, E. *A system for contact free energy expenditure assessment under free-living conditions: monitoring metabolism for weight loss using carbon dioxide emission.* Journal of Breath Research 2021, 15 026004. https://doi.org/10.1088/1752-7163/abd52f

[2] **Sprowls, M.**, Serhan, M., Chao, E.-F., L. Lin, V. Jammula, C. Frames, I. Kucherenko, Y. Li, M. Khine, Y. Yang, T. Lockhart, J. Claussen, L. Dong, J. Chen, J. Ren, C. Gomes, D. Kim, T. Wu, B. Narasimhan, J. Margrett, and E. Forzani, Integrated sensing systems for monitoring inter-related physiological parameters in older adults. International Journal of Prognostics and Health Management, 2020. Accepted.

[3] **Sprowls, M.**, Victor, S., Mora, S.J., Pyznar, G., Destaillats, H., Wheatley-Guy, C., Johnson, B. Kulick, D., Forzani, E. *A Smart Home Medical Device for Contactless Energy Expenditure Measurement*. Biosensors and Bioelectronics (submitted), 2021.

[4] **Sprowls**, **M.**, Y. Deng, Kulick, D. Tao, N., Destaillats, H. and Forzani, E. An Unobstructive Sensing Method for Indoor Air Quality Optimization and Metabolic Assessment within Vehicles. Sensors 2020, 20(24), 7202; https://doi.org/10.3390/s20247202.

[4] Ruiz, I., **Sprowls**, **M.** Y. Deng, D. Kulick, H. Destaillats, and E.S. Forzani, *Assessing Metabolic Rate & Indoor Air Quality with Passive Environmental Sensors.* Journal of Breath Research, 2018. Apr 4;12(3): p. 036012. DOI: https://doi.org/10.1088/1752-7163/aaaec9

[5] Liu, N.-Y., P. Cay-Durgun, **Sprowls**, **M.**, T. Lai, L.F. Thomas, M.L. Lind, and E.S. Forzani, *A handheld, colorimetric optoelectronic dynamics analyzer (CODA) for measuring total ammonia of biological samples*, in *IEEE Journal of Translational Engineering in Health and Medicine* 2018. DOI: 10.1109/JTEHM.2018.2840678

[6] Serhan, M., D. Jackemeyer, M. Long, **Sprowls**, **M.,** I. Diez Perez, W. Maret, F. Chen, N.J. Tao, and E. Forzani, *Total iron measurement in human serum with a smartphone.* IEEE Journal of Translational Engineering in Health & Medicine, 2020. DOI: 10.1109/JTEHM.2020.3005308

[8] M. Serhan, D. Jackemeyer, K. Abi-Karam, Kasyap Chakravadhanula, **Sprowls**, **M.**, Cay-Durgun, P., and Forzani, E. "Point of care detection of iron in whole blood through a vertical flow colorimetric sensor," Analyst, 2020. DOI: 10.1039/D0AN02351E

[9] Mora, S.J., **Sprowls, M.**, Tipparaju, V. Wheatley-Guy, C., Kulick, D., Johnson, B., Xian, X. Forzani, E. The validation of a novel portable indirect calorimeter for the use in the in-office and telemedicine settings. Clinical Nutrition ESPEN (submitted), 2021.